Synthesis, characterization and application of polyacrylamide grafted bioflocculants

(TMT^{-1}-g-PAM 2 and TST^{-1}-g-PAM 3)

University of Zululand

Masters Dissertation

by

Siyanda Senzo Ngema

Student number: 201100298

Faculty of Science and Agriculture

Biochemistry and Microbiology Department

University of Zululand

Private bag x1001

KwaDlangezwa

3886

Supervisor: Prof AK Basson

Co-supervisor(s): Dr TS Maliehe & Prof JJ Simonis

Declaration

The research project presented in this dissertation was conducted in the Department of Biochemistry and Microbiology of the University of Zululand (UZ) under the supervision of Prof A.K. Basson, Dr T.S. Maliehe and Prof J.J. Simonis.

I, Siyanda Senzo Ngema declare that this work, apart from the supervisory guidance received, is the product of my own original work and effort.

……..

Mr SS Ngema

……

Prof AK Basson

……

Prof JJ Simonis

……

Dr TS Maliehe

Acknowledgements

I thank God for being with me throughout the course of the study and my supervisor Prof A.K. Basson and co-supervisors Prof J.J. Simonis and Dr T.S. Maliehe for their immense support. I am also deeply grateful to my family, colleagues (including the honours students 2017–2018) and friends for their help and encouragement during my studies.

I would like to acknowledge the National Research Foundation (NRF) through the University of Zululand for their financial support. My thanks are also extended to the University of KwaZulu-Natal for allowing me to use their equipment for zeta potential and cytotoxicity studies.

Abbreviations

%	Percent
$(NH_4)_2SO_4$	Ammonium sulphate
°C	Celsius
µg	Microgram
µl	Microliter
µml	Micro millilitre
16S-rRNA	16S-ribosomal ribonucleic acid
AM	Acrylamide
AMD	Acid mine drainage
ANOVA	One-way analysis of variance
$BaCl_2$	Barium chloride
BOD	Biological oxygen demand
C	Carbon
Ca	Calcium
$CaCl_2$	Calcium chloride
Cl	Chlorine
COD	Chemical oxygen demand
FA	Flocculating activity
$FeCl_3$	Iron chloride
FTIR	Fourier transform infrared spectroscope
g	Gram
HEK 293	Human embryonic kidney cells
Hg	Mercury
IMC	Inter Ministerial Committee on Acid Mine Drainage
JHB	Johannesburg
K	Potassium
KBr	Potassium bromide
KCl	Potassium chloride
l	Litre
LiCl	Lithium chloride
MBC	Minimal bactericidal concentration

$MgCl_2$	Magnesium chloride
mg	Milligram
MIC	Minimal inhibitory concentration
min.	Minute
ml	Millilitre
MTT	3-(4,5-dimethylthiazol-2-)-2,5-diphenyl tetrazolium bromide
mV	Millivolts
N	Nitrogen
NaCl	Sodium chloride
nm	Nanometer
O	Oxygen
OD	Optical density
P	Phosphorus
PAM	Polyacrylamide
Pb	Lead
PCP	Personal care products
r.p.m.	Revolutions per minute
RSA	Republic of South Arica
S	Sulfur
SD	Standard deviation
SEM	Scanning electron microscope
TGA	Thermo gravimetric analyzer
TMT	Bioflocculant from *Bacillus pumilus* JX860616
TMT^{-1}-g-PAM 2	Polyacrylamide grafted bioflocculant from *Bacillus pumilus* JX860616
TST	Bioflocculant from a consortium of *Bacillus pumilus* JX860616 and *Bacillus subtilis* CSM5
TST^{-1}-g-PAM 3	Polyacrylamide grafted bioflocculant from a consortium of *Bacillus pumilus* JX860616 and *Bacillus subtilis* CSM5
UK	United Kingdom
UNICEF	United Nations International Children's Emergency Fund
UNIZULU	University of Zululand
USA	United States of America

UV	Ultraviolet
v	Volume
W	Watt
w	Weight
WHO	World Health Organisation
Wt.	Weight
WWF	World Wide Fund for Nature
XRD	X-ray diffractometer

Research output

1. **Submitted manuscript**

Ngema, S.S., Basson, A.K., Maliehe, T.S. and Simonis, J.J. (2018) Synthesis, characterization and application of polyacrylamide grafted bioflocculant (TMT^{-1}-g-PAM 2). *Physics and Chemistry of the Earth.*

2. **Conference presentations**

2.1 Poster presentation

Ngema, S.S., Basson, A.K., Maliehe, T.S. and Simonis, J.J. (2018) Synthesis, characterization and application of polyacrylamide grafted bioflocculant (TMT^{-1}-g-PAM 2). Bio Africa Convention. 27-29 August 2018. Inkosi Albert Luthuli Convention Centre, Durban, RSA.

2.2 Oral presentation

Ngema, S.S., Basson, A.K. and Maliehe, T.S. (2018) Synthesis, characterization and application of polyacrylamide grafted bioflocculant (TMT^{-1}-g-PAM 2). 19^{th} WaterNet/WARFSA/GWP-Southern Africa Symposium. 31^{st} October – 2^{nd} November 2018. Avani Victoria Falls Resort, Livingstone, Zambia.

Table of Contents

Declaration i
Acknowledgements ii
Abbreviations iii
Research output vi
Table of Contents vii
List of Figures x
List of Tables xii
Abstract xiii
Chapter 1 1
1.1 Introduction 1
1.2 Rationale of the study 2
1.3 Study area 3
1.4 Aim 3
1.5 Objectives 3
1.6 Hypothesis 3
Chapter 2: Literature survey 4
2.1 Water scarcity 4
2.1.1 Water pollution 4
2.2 Flocculation 6
2.3 Bioflocculation 7
2.4 Graft copolymerization 9
2.4.1 Graft copolymers 9
2.4.2 Advantages of graft copolymers 9
2.4.3 The mechanism of flocculation used by grafted bioflocculants/graft copolymers 11
2.4.4 Factors controlling graft copolymerization 12
2.5 Sources of bioflocculant producers 17
2.5.1 *Bacillus subtilis* 18
2.5.2 *Bacillus pumilus* 18
2.6 Composition of bioflocculants TMT^{-1} and TST^{-1} 19
Chapter 3: Materials and method 20
3.1 Chemicals purchased from E. Merck, South Africa 20
3.2 Wastewater 20
3.3 Bacteria used for bioflocculants production 21

3.4 Production media for TMT^{-1} and TST^{-1} 21
3.5 Extraction and purification of bioflocculants TST^{-1} and TMT^{-1} 21
3.6 Synthesis of the graft copolymer using the "microwave initiated" method 22
3.7 Purification of graft copolymer by solvent extraction method 23
3.8 Characterization 23
3.8.1 Intrinsic viscosity 23
3.8.2 Elemental analysis 23
3.8.3 Scanning electron microscopy 23
3.8.4 Fourier transform infrared spectroscopy 24
3.8.5 X-ray diffractometry analysis 24
3.8.6 Thermogravimetric analysis 24
3.8.7 Biosafety assay of TMT^{-1}-g-PAM 2 and TST^{-1}-g-PAM 3 24
3.8.8 Antimicrobial activity of the grafted flocculants (TST^{-1}-g-PAM and TMT^{-1}-g-PAM) 25
3.8.8.1 Reviving the bacteria 25
3.8.8.2 Minimum inhibitory concentration (MIC) 26
3.8.9 Biodegradation studies 26
3.9 Evaluation of flocculation properties of the grafted bioflocculants 27
3.9.1 Dosage and cation type 27
3.9.2 Thermal and pH stabilities of the grafted bioflocculants 28
3.9.3 Saline stabilities of the grafted bioflocculants 28
3.10 Proposed flocculation mechanism 29
3.11 Application of grafted bioflocculants in wastewater treatment 29
3.12 Software and statistical analysis 30
Chapter 4: Results and discussion 31
4.1 Introduction 31
4.2 Results and discussion for TMT^{-1}-g-PAM 2 and TST^{-1}-g-PAM 3 31
4.2.1 Extracted bioflocculant 31
4.2.2 TMT^{-1}-g-PAM and TST^{-1}-g-PAM synthesis by microwave irradiation 31
4.2.3 Characterization 34
4.2.4 Flocculation properties 48
4.2.5 Application of the grafted bioflocculants in domestic and industrial wastewater treatment 63
Chapter 5 67
5.1 Conclusion 67

5.2 Recommendations 67
References 68
Appendix 85

List of Figures

Chapter 2

Figure 2.1: General structure of a graft copolymer……9

Figure 2.2: Structural configuration of linear polymer and graft copolymer……11

Figure 2.3: Polymer bridging between particles……12

Figure 2.4: Influence of monomer concentration on grafting percentage (when other factors are kept constant)……14

Figure 2.5: Influence of radiation time on grafting percentage (when other factors are kept constant)……17

Chapter 4

Figure 4.2.1: Schematic presentation of the mechanism for TMT^{-1}-g-PAM 2 or TST^{-1}-g-PAM 3……32

Figure 4.2.2: SEM micrographs of (a) acrylamide (b) bioflocculant TMT^{-1} (c) TMT^{-1}-g-PAM 2……36

Figure 4.2.3: SEM micrographs of (a) acrylamide (b) bioflocculant TST^{-1} (c) TST^{-1}-g-PAM 3……37

Figure 4.2.4: FTIR spectra of TMT^{-1} and TMT^{-1}-g-PAM 2……38

Figure 4.2.5: FTIR spectra of TST^{-1} and TST^{-1}-g-PAM 3……39

Figure 4.2.6: X-ray diffractograms of TMT^{-1} and TMT^{-1}-g-PAM 2……40

Figure 4.2.7: X-ray diffractograms of TST^{-1} and TST^{-1}-g-PAM 3……40

Figure 4.2.8: Thermo-gravimetric analysis of TMT^{-1} and TMT^{-1}-g-PAM 2……42

Figure 4.2.9: Thermo-gravimetric analysis of TST^{-1} and TST^{-1}-g-PAM 3……43

Figure 4.2.10: *In-vitro* cytotoxicity of different concentrations of TMT^{-1} and TMT^{-1}-g-PAM 2……44

Figure 4.2.11: *In-vitro* cytotoxicity of different concentrations of TST^{-1} and TST^{-1}-g-PAM 3……45

Figure 4.2.12: A comparative study of the effect of dosage (mg/ml) on TMT^{-1}-g-PAM 2 and other flocculants' flocculating activities……50

Figure 4.2.13: A comparative study of the effect of dosage (mg/ml) on TST^{-1}-g-PAM 3 and other flocculants' flocculating activities……50

Figure 4.2.14: Influence of cations on flocculating activity of TMT^{-1}-g-PAM 2……52

Figure 4.2.15: Effect of cations on flocculating activity of TST^{-1}-g-PAM 3……53
Figure 4.2.16: Flocculating activity of TMT^{-1}-g-PAM 2 in the absence of cations……54
Figure 4.2.17: Flocculating activity of TST^{-1}-g-PAM 3 in the absence of cations……55
Figure 4.2.18: Comparative analysis of the influence of pH on flocculating activity of TMT^{-1}-g-PAM 2 and other flocculants……57
Figure 4.2.19: Comparative analysis of the influence of pH on flocculating activity of TST^{-1}-g-PAM 3 and other flocculants……57
Figure 4.2.20: Influence of temperature on the flocculating activity of TMT^{-1}-g-PAM 2 and comparison to other flocculants……58
Figure 4.2.21: Influence of temperature on the flocculating activity of TST^{-1}-g-PAM 3 and comparison to other flocculants……59
Figure 4.2.22: Effect of salinity on flocculation by TMT^{-1}-g-PAM 2 and comparison to other flocculants (TMT^{-1}, $FeCl_3$ and PAM)……60
Figure 4.2.23: Effect of salinity on flocculation by TST^{-1}-g-PAM 3 and comparison to other flocculants (TST^{-1}, $FeCl_3$ and PAM)……61

List of Tables

Chapter 3

Table 3.1: Characteristics of a domestic wastewater……20

Table 3.2: Properties of Tendele coal mine wastewater……21

Table 3.3: Bacteria strains that were utilized in this study to evaluate antibacterial activity of graft copolymers……25

Chapter 4

Table 4.2.1: Synthetic details of TMT^{-1}-g-PAM using microwave irradiation……33

Table 4.2.2: Synthetic details of TST^{-1}-g-PAM using microwave irradiation……34

Table 4.2.3: Elemental analysis results for TMT^{-1}-g-PAM 2……35

Table 4.2.4: Elemental analysis results for TST^{-1}-g-PAM 3……36

Table 4.2.5: Minimum inhibitory concentration of TMT^{-1}-g-PAM 2 on certain bacterial strains……46

Table 4.2.6: Minimum inhibitory concentration of TST^{-1}-g-PAM 3 on certain bacterial strains……46

Table 4.2.7: Biodegradation studies of TMT^{-1}-g-PAM 2……47

Table 4.2.8: Biodegradation studies of TST^{-1}-g-PAM 3……48

Table 4.2.9: Zeta potential of samples……62

Table 4.2.10: Zeta potential of samples……62

Table 4.2.11: Removal efficiency (RE) and flocculating activity (FA) of TMT^{-1}-g-PAM 2 in domestic wastewater……64

Table 4.2.12: Removal efficiency (RE) and flocculating activity (FA) of TST^{-1}-g-PAM 3 in domestic wastewater……64

Table 4.2.13: Removal efficiency (RE) and flocculating activity (FA) of TMT^{-1}-g-PAM 2 in coal mine wastewater……66

Table 4.2.14: Removal efficiency (RE) and flocculating activity (FA) of TST^{-1}-g-PAM 3 in coal mine wastewater……66

Abstract

Water pollution is one of the major problems in the world. It contributes to water scarcity. Grafted bioflocculants have been found to have excellent wastewater remediation capabilities. Therefore, they have become one of the main research focal points in recent times as flocculants. The high efficacy is owed to their unique characteristics, which include having a branched structure and a high molecular weight. Therefore, the aim of this research was to synthesise, characterize and apply polyacrylamide grafted bioflocculants to wastewater treatment. Bioflocculants (TMT^{-1} and TST^{-1}) produced by *Bacillus pumilus* JX860616 and a consortium of *Bacillus pumilus* JX860616 and *Bacillus subtilis* CSM5, respectively, were grafted with acrylamide chains using a microwave initiated method. To optimize the synthesis of the grafted bioflocculants, irradiation time and acrylamide concentration were varied. Optimum grades (TMT^{-1}-g-PAM 2 and TST^{-1}-g-PAM 3) were then characterized by intrinsic viscosity, elemental analysis, scanning electron microscopy (SEM), Fourier transform infrared (FTIR) spectroscopy, X-ray diffractometry (XRD) and thermo-gravimetric analysis (TGA). Furthermore, these optimum grades' biosafety (on human embryonic kidney 293 cells, HEK 293) were assessed by 3-(4,5-dimethylthiazol-2-)-2,5-diphenyl tetrazolium bromide (MTT) assay. The grafted bioflocculants were also screened for antibacterial activity, using micro-dilution assay. Their biodegradation was investigated by a composting method. The effects of dosage size, cations, pH, temperature and salinity on the flocculating activities of the grafted bioflocculants were also evaluated, spectrophotometrically. The flocculation mechanism was determined by evaluating zeta potentials using Zetasizer Nano. Spectrophotometric cell tests were utilized to assess COD, BOD, N, P and S removal on domestic and coal mine wastewater by the grafted bioflocculants. The optimum grade (TMT^{-1}-g-PAM 2) was obtained when a concentration of 2.5 g of acrylamide was used for grafting on TMT^{-1} at irradiation time of 3 min.; while TST^{-1}-g-PAM 3 was synthesized by using 7.5 g of acrylamide at irradiation time of 3 min. Changes observed in intrinsic viscosity, elemental analysis, SEM, FTIR, XRD and TGA confirmed that grafting was successful. HEK 293 cells displayed high viability (75% in TMT^{-1}-g-PAM 2 and 85% in TST^{-1}-g-PAM 3) when exposed to high concentrations (i.e. 200 µg/ml) of the grafted bioflocculants. Both grafted bioflocculants did not show any antibacterial activity against the tested species. The grafted bioflocculants were biodegradable. The flocculants' dosage size of 0.2 mg/ml possessed flocculating activities of

81% for TMT^{-1}-g-PAM 2 and 90% for TST^{-1}-g-PAM 3. Furthermore, the grafted bioflocculants showed stability over a wide pH range (3–11), displaying flocculating activities above 75%. They also demonstrated thermal stability, both giving flocculating activity of 81% at 100 °C. Moreover, they were able to flocculate saline water (35 g/l NaCl), giving flocculating activity of 63% (TMT^{-1}-g-PAM 2) and 64% (TST^{-1}-g-PAM 3). There was a decrease in zeta potentials with the presence of cations (Ca^{2+}; TMT^{-1}-g-PAM 2 and Ba^{2+}; TST^{-1}-g-PAM 3), implying that flocculation could be due to double layer compression by cations, chemical reactions and bridging mechanisms. The removal of COD, BOD, N and P, in domestic wastewater, by the graft copolymer TMT^{-1}-g-PAM 2 reached 98%, 54%, 53%, and 57% respectively. Whereas, the removal of those parameters by TST^{-1}-g-PAM 3 was as follows: 98%; COD, 73%; BOD, 74%; N and 17%; P. In the case of coal mine wastewater, the removal efficiency by TMT^{-1}-g-PAM 2 was: 98%; COD, 93%; BOD, 59%; N and 83%; S. For TST^{-1}-g-PAM 3, the removal efficiency from coal mine wastewater achieved the following results: 95%; COD, 62%; BOD, 89%; N and 57%; S. Considering the unique properties – such as many functional groups, high stability, biosafety and removal efficiencies of water pollutants – both flocculants attract a potential industrial applicability.

Chapter 1

1.1 Introduction

Water pollution is one of the major problems in the world, especially in the developing countries (WHO, 2017). For example, in these countries, 90% of polluted water is discharged (untreated) into the receiving water bodies (Corcoran *et al*., 2010). Pollutants may include heavy metals, nutrients, microorganisms and organic matter (Willey *et al*., 2011). Therefore, pollutants degrade water quality and pose a danger to human health and the ecosystem (WHO, 2017).

Many pollutants exist as colloidal particles. This means that they are very small (1 nm – 1 µm in diameter) (Spellman, 2014). They remain continually suspended because of their electrostatic charge (often negative) which causes them to repel each other (Lee *et al*., 2014). Therefore, for these types of pollutants to settle, flocculation needs to be employed. Flocculation is the physical process of slowly mixing the coagulated water in order to increase particle collision, which leads to destabilized colloids colliding and binding together to form large flocs (Spellman, 2014). The flocs can then be removed by sedimentation, flotation or filtration processes (Edward, 2011).

In wastewater treatment industries, flocculation is the most preferred technology for primary wastewater treatment. This is due to its simplicity, effectiveness and affordability (Lee *et al*., 2014). This technology is made possible by using flocculants. Flocculants are grouped according to their chemical composition. The two main groups available are natural occurring flocculants and chemical (inorganic and synthetic organic) flocculants (Salehizadeh and Shojaosadati, 2001). Natural flocculants are biodegradable and have shear stability. However, they have limited efficiency at low doses (Bolto and Gregory, 2007). On the other hand, synthetic organic flocculants, which are mostly used in industries, are highly efficient at very low doses. They are also inexpensive. But, they are non-biodegradable and have a weak shear resistance (Nayak *et al*., 2002). Thus, there is a steady demand for flocculants that are cost-effective, ecofriendly and innocuous to humans. Grafted bioflocculants have thus emerged as potential materials in biotechnological processes. They are synthesized through graft copolymerization (Lee *et al*., 2012).

Graft copolymerization is the physico-chemical modification of the properties of natural occurring and synthetic flocculants (Mishra *et al*., 2014). Thus, by combining the best properties of both chemical and natural occurring flocculants through graft copolymerization, a superior flocculant, which is synergistically efficient at low doses, shear resistant, inexpensive, ecofriendly and has controlled biodegradability, can be obtained.

In this study, grafted bioflocculants (TMT^{-1}-g-PAM 2 and TST^{-1}-g-PAM 3) were synthesized by grafting polyacrylamide chains to bioflocculants TMT^{-1} and TST^{-1}. The grafted bioflocculants were characterized, and their flocculation efficacies assessed on domestic and coal mine wastewater.

1.2 Rationale of the study

Water pollution greatly contributes to water scarcity worldwide. Wastewater treatment and purification industries commonly use flocculation technology to address this problem. The conventional chemical flocculants – usually employed during the flocculation process – are highly effective, inexpensive and have a long shelf life. But they have been reported to be shear labile, carcinogenic and neurotoxic to humans. Furthermore, they cause environmental pollution, due to their non-biodegradability. Hence, their usage has been limited in most developed countries (Nayak *et al*., 2002; Reddy, 2017).

Bioflocculants, on the other hand, are biologically degradable and therefore do not cause environmental pollution. They are also shear stable and non-toxic to the ecosystems. However, they have moderate flocculation performance and short shelf life. These drawbacks prevent industrial application of bioflocculants (Bolto and Gregory, 2007).

Lately, graft copolymerization technique has become popular. It produces graft copolymers/grafted bioflocculants which have the best properties of both chemical flocculants and natural bioflocculants. Thus, grafted bioflocculants tend to have high flocculation efficiency and shear-resistance, long shelf life and innocuousness to humans and the environment (Mishra *et al*., 2014).

Therefore, this study aimed to synthesize polyacrylamide grafted bioflocculants (TMT^{-1}-g-PAM 2 and TST^{-1}-g-PAM 3) possessing improved flocculation efficiency, long shelf life, shear-stability and non-cytotoxic effects.

1.3 Study area

The study was carried out in the Department of Biochemistry and Microbiology at the University of Zululand (UNIZULU) main campus. UNIZULU is located at Kwadlangezwa in the north of KwaZulu-Natal, South Africa.

1.4 Aim

The aim of this study was to synthesize polyacrylamide grafted bioflocculants (TMT^{-1}-g-PAM 2 and TST^{-1}-g-PAM 3), characterize them and apply them to wastewater.

1.5 Objectives

1. To produce, extract and purify bioflocculants from single and mixed bacterial species
2. To synthesize and characterize the grafted bioflocculants
3. To evaluate the flocculation characteristics of the grafted bioflocculants
4. To apply the grafted bioflocculants in wastewater treatment

1.6 Hypothesis

Grafted bioflocculants have higher flocculation efficiency than both chemical flocculants and natural bioflocculants.

Chapter 2: Literature survey

2.1 Water scarcity

Water scarcity is a dilemma besetting both the developed and the developing countries (Reddy, 2017). It is documented that 4 billion people are living in water scarce conditions (Mekonnen and Hoekstra, 2016). Furthermore, UNICEF and WHO have reported that 663 million individuals do not have access to potable water (UNICEF and WHO, 2015). This problem is bound to worsen in future due to rapid population growth, which is forecasted to reach over 10 billion people in 2050 (Hanna *et al*., 2016).

2.1.1 Water pollution

Water pollution is a major factor contributing to water scarcity (Reddy, 2017). Water pollution is defined as the presence of agents (pollutants) that make water to be unfit for beneficial use (Schweitzer and Noblet, 2017). For instance, water heavily polluted with heavy metals, such as mercury (Hg) and lead (Pb), is not suitable for human consumption as it may lead to cancer (Tchounwou *et al*., 2012).

Pollutants have industrial and domestic sources (Rezania, 2016). In South Africa, one of the most important industrial sources of pollutants is coal mining. The significance of this industry stems from the fact that 90% of South Africa's electricity is produced from coal (Eskom, 2018). Yet, the detrimental effects of coal mining on humans and the environment are well documented (WWF, 2011).

One of the ways in which coal mining can destroy the ecosystem is through generating acid mine drainage (AMD). AMD is the effluent that usually seeps from mines or mine wastes to the surrounding environment (Groenewald, 2012). It is formed when strata (containing sulphide) are exposed to oxygen and water (WWF, 2011). The exposure then causes the strata to be oxidized, resulting in the formation of sulphuric acid and iron. Consequently, other metals are leached from the strata that produced the AMD (IMC, 2010). Thus, in addition to iron, this effluent often contains high concentrations of other heavy metals such as aluminium, manganese and others (Masindi *et al*., 2018). High levels of metal cations tend to cause nucleic acid conformational changes that may trigger cell cycle modification, carcinogenesis and cell death in living organisms (Tchounwou *et al*., 2012).

Whether AMD develops or its severity is determined by some factors (Bell *et al*., 2002). If the sulphide-bearing materials are abundant within the coal-carrying minerals, the AMD may be severe. In other cases, there might be sufficient carbonate-containing rocks in the mining area, which can neutralize acidity (WWF, 2011).

Besides the industrial sources of water pollution, there are domestic sources as well. Domestic wastewater may contain a number of pollutants arising from personal care products (PCPs) and excreta (Reddy, 2017). PCPs consist of items such as shampoos, lotions, toothpastes, bath soaps, dental care products and deodorants. The majority of such items contain synthetic polymers called microplastics, which are used as scrubbing agents (Gouin *et al*., 2011). After their intended external use, the PCPs are washed off and pollute the aquatic environment. In the United States, about 8 billion microplastics are released per day into water (Rochman *et al*., 2015). In the Gauteng province (South Africa), water was reported to be heavily contaminated by microplastics (Naidoo, 2018). These synthetic polymers are hazardous to the aquatic ecosystem. Because of their small size (< 5 mm), microplastics can accumulate in the cells and tissues of the living organisms. Human ingestion can cause changes in chromosomes that may result in gaining weight, infertility and cancer (Sharma and Chatterjee, 2017).

Excreta refer to waste material discharged from the body, particularly urine and faeces (Sommer *et al*., 2013). Water polluted with human and animal faeces is linked with various bacterial, viral and protozoan diseases (Willey *et al*., 2011). Bacteria such as *Escherichia coli* 0157: H7, *Salmonella enterica*, *Shigella sonnei* and *Vibrio cholerae* may cause acute diarrheal diseases. Similarly, certain viruses – rotaviruses, Norwalk viruses and others – also result in diarrhoea. Hepatitis A virus generates liver disease. Parasitic protozoa (e.g. *Entamoeba histolytica*) lead to amoebic dysentery (Bonadonna *et al*., 2002).

2.1.1.1 Measuring water quality

There are certain parameters that are used to assess the quality of water. They include pH, biological oxygen demand, chemical oxygen demand, nitrogen, phosphate, sulphate and metals (Larsdotter, 2006). A wastewater that has a pH value below 7 may indicate that it is contaminated with bacteria; whereas, pH extremes (pH < 5 or pH > 10) may signal the

presence of industrial pollutants and non-existence of life in a particular effluent. According to Akpor and Muchie (2011), the pH range that is known to support life is usually between 6 and 9.

The extent of organic material pollution in a water body can be measured by observing its chemical oxygen demand (COD) and biochemical oxygen demand (BOD) (Willey *et al*., 2011). BOD represents the amount of dissolved oxygen that is required by organisms to oxidize the organic matter in water. COD measures the amount of oxygen needed in order to chemically oxidize the organic material in effluent (Akpor and Muchie, 2011). Thus, high COD and BOD values indicate water pollution.

Water pollution is also indicated by a high nitrogen concentration in a water body. Nitrogen exists in different forms. The main kinds are organic nitrogen, ammonia, nitrate and nitrite (Maliehe, 2017, 9). High levels of these nitrogen forms (>10 mg/l) can have adverse influence on the ecosystem (Akpor and Muchie, 2011). They may generate eutrophication. This is the excessive supplementation of nutrients in aquatic environment (Willey *et al*., 2011). It leads to algal and cyanobacterial overgrowth. Toxic algae may then accumulate in the food chain and may generate shell fish poisoning, hepatic damage, diarrhoea and amnesia, in humans (WHO, 2006). Other causes of eutrophication are excessive concentrations of phosphorous and sulphate in a wastewater (Willey *et al*., 2011).

2.2 Flocculation

Pollutants can be categorized into suspended, colloidal or solutions (Spellman, 2014). According to Brady and Senese (2004) a solution consists of particles which are dissolved in a solvent. Unlike a solution, suspensions and colloids are insoluble. Moreover, a suspension has solid particles that are large enough (usually greater than 1 µm in diameter) to settle on their own. Colloids, on the other hand, are very small (1 nm-1 µm) in diameter. They remain continuously suspended because they have electrostatic charge (often negative) which causes them to repel each other (Lee *et al*., 2014). Therefore, for colloids to settle, flocculation is necessary. This is the process of shaking water at low speed in order to increase the likelihood of particle collision. This leads to particles (that are unstable)

colliding and binding with each other to form large flocs or flakes (Spellman, 2014). The flocs can be removed by sedimentation, flotation or filtration processes (Edward, 2011).

Flocculation relies on flocculants. These are substances which are utilised, in different industries, to separate solids (such as colloids and cells) from liquid by flocculation process (Hu *et al*., 2006). They are usually classed into three groups, namely: (i) inorganic flocculants, for example polyaluminium chloride and aluminium sulfate; (ii) organic synthetic flocculants which include polyethylene amine and the derivatives of polyacrylamide; and (iii) natural flocculants that entail sodium alginate and bioflocculants (Kurane *et al*., 1994). Flocculants are commonly employed in different industrial processes which include downstream processing, water purification and treatment, dredging, textile, mining, cosmetology, pharmacology and food and fermentation processes (Nakata and Kurane, 1999; Salehizadeh and Shojaosadati, 2001).

The reasons why chemical (inorganic and organic synthetic) flocculants are widely used in industrial processes are due to their cost-effectiveness and high flocculating efficiency (Li *et al*., 2008). However, they have been implicated in health and environmental problems. For example, polyaluminium salts have been implicated in Alzheimer's disease (Arezoo, 2002). Polyacrylamides are linked with neurotoxicity and carcinogenicity in mankind (Dearfield e*t al*., 1988). Moreover, acrylamide monomers are non-biodegradable, leading to environmental pollution (Zheng *et al*., 2008).

2.3 Bioflocculation

Bioflocculation is the natural process that uses bioflocculants to flocculate particle suspensions (Cong-Liang *et al.,* 2012). Microbial bioflocculants are extracellular polymers that are produced by microorganisms during growth (Buthelezi *et al*., 2010; Nie *et al*., 2011). They are generally secreted by both prokaryotic and eukaryotic microorganisms (Flemming and Wingender, 2010). Bioflocculants are mainly composed of proteins, polysaccharides, lipids, humic substances and nucleic acids. However, the dominant components are proteins and carbohydrates. They also have the derivatives of polysaccharides and proteins, for example, glycoproteins, lipoproteins and lipopolysaccharides (Marvasi *et al*., 2010; Sheng *et al*., 2010).

The carbohydrates in the bioflocculants are neutral carbohydrates (usually hexose) and uronic acids (which include galacturonic, mannuronic and glucuronic acid). These uronic acids or subtitutes such as acetate ester, succinates, pyruvate ketals and inorganic phosphates and sulphates, determines whether the bioflocculant is anionic, cationic or neutral (More *et al*., 2014).

The proteins present in the bioflocculants are structural proteins and enzymes. According to Flemming and Wingender (2010), these extracellular enzymes can degrade the microbial bioflocculant components during starvation. The components of a microbial bioflocculant enable it to carry out its functions. That includes aiding bacteria to adhere to surfaces, being a protective barrier for cells, cell-cell recognition, aggregation of bacterial cells, water retention to decrease drying out of the cells, and formation of floc and biofilm (Wingender *et al*., 1999).

Bioflocculants have received much scientific attention due to the following advantages: they are biodegradable, produce no secondary pollution, and their degraded intermediates are safe for humans and the environment (Buthelezi *et al*., 2010; Mabinya *et al*., 2012). Furthermore, bioflocculants produce less sludge (Okaiyeto *et al*., 2016). As a result, over the past decades many studies have been conducted on bioflocculant production using varied types of microorganisms, including bacteria, fungi, actinomycetes and algae (More *et al*., 2014).

The large-scale production and industrial application of bioflocculants are limited by a few disadvantages. Bioflocculants have shorter shelf life, compared to chemical flocculants, due to high biodegradability. This biodegradability leads to the formation of flocs that have a tendency to lose stability and strength with time (Lee *et al*., 2014). According to Singh *et al*. (2000) degradation can occur via hydrolysis, because most bioflocculants possess some hydrolysable groups. Furthermore, other anionic bioflocculants have moderate flocculation efficiency and thus high dosages are required to achieve efficient flocculation (Lee *et al*., 2014). Therefore, research is now focused on combining the best characteristics of both chemical flocculants and natural bioflocculants through graft copolymerization.

2.4 Graft copolymerization

Graft copolymerization is a commonly used method of polymer modification where vinyl monomers are linked (covalently) onto the polymer chain, resulting in the formation of graft copolymers (Bhattacharya and Misra, 2004). It is a very effective method for transforming structure and characteristics of biological polymers (Sen *et al*., 2009). It allows for modification of polymers, such that the bulk characteristics are not changed, while new modified properties are acquired from the polymer that is grafted (Bhattacharyna and Misra, 2004).

2.4.1 Graft copolymers

Graft copolymers have a polymer backbone with lateral covalently bonded side chains (Stannett, 1981). The side chains have a chemical nature that is different to the backbone (Kalia and Sabaa, 2013). The general structure of a graft copolymer is displayed in Figure 2.1, where the monomer (X_2) is bonded on the polymeric backbone having building unit (X_1). Monomer (X_2) can be grafted on the polymeric backbone as a unitary system or as a binary mixture with other monomer(s) (Kalia and Sabaa, 2013).

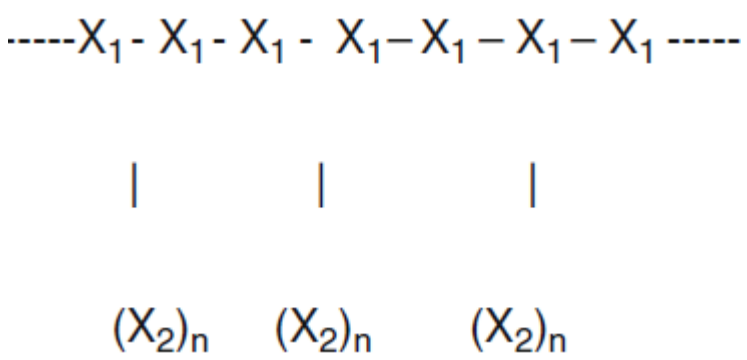

Figure 2.1: General structure of a graft copolymer (Kalia and Sabaa, 2013)

2.4.2 Advantages of graft copolymers

Graft copolymers contain physical properties that differ from linear polymers due to their branched nature (Figure 2.2, p. 11) (Kalia and Sabaa, 2013). The branching allows for ease of approachability of contaminants in wastewater, thus enabling graft copolymers to be more efficient in flocculation at low dosages (Singh *et al*., 2006). Some studies have shown

graft copolymers to have superior flocculation efficiency when compared to chemical flocculants and naturally occurring flocculants (Lee *et al*., 2014).

The grafting of long chains of a vinyl monomer to a biopolymeric backbone leads to an increase in molecular weight of the biopolymer (Pal *et al*., 2011; Yahya *et al*., 2015). Sen and Pal (2009) found that the polyacrylamide grafted carboxymethyl starch had a relatively higher molecular weight than the pure carboxymethyl starch. In another study, grafting of polyacrylamide chains onto casein improved its molecular weight (Sinha *et al*., 2013). High molecular weight means that more adsorption sites are available for colloids to bind to the polymer. This enhances the bridging flocculation mechanism by a polymeric flocculant (Wang *et al*., 2011).

Graft copolymers have reduced biodegradability due to the modification of the original structure of the natural polymer as well as the increased synthetic polymer content in the product (Lee *et al*., 2014). These structural changes decrease the susceptibility of graft copolymers to enzymatic degradation. According to Singh *et al*. (2000), the inert polymer content (for example, polyacrylamide) increases with grafting, making the resultant graft copolymer to be less vulnerable to biological attack. The decreased biodegradability results in a longer shelf-life for the grafted bioflocculants when compared with natural bioflocculants (Lee *et al*., 2014).

It can also be seen that, when shear degradable chemical flocculants are grafted onto the stiff polysaccharide, the produced graft copolymer are shear stable (Singh *et al*., 2000). Thus the chemical combination of bioflocculants and synthetic flocculants, through graft copolymerization, produces grafted flocculants with desirable characteristics of both synthetic flocculants and natural bioflocculants (Sen *et al*., 2009).

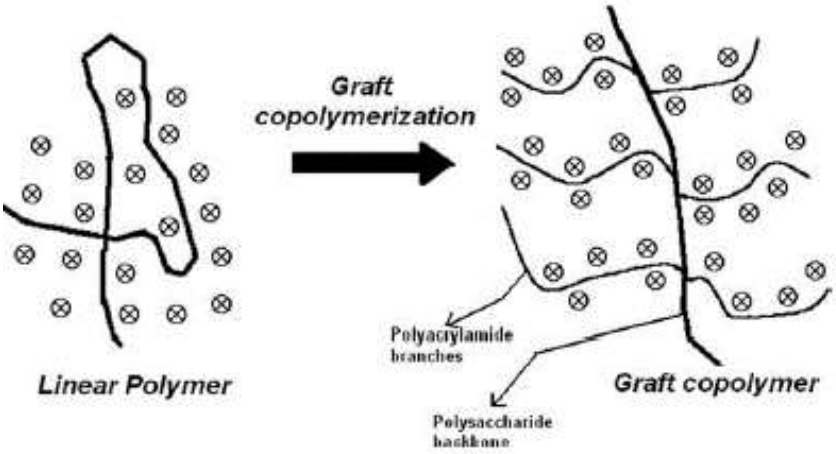

Figure 2.2: Structural configuration of linear polymer and graft copolymer (Sen *et al*., 2009)

2.4.3 The mechanism of flocculation used by grafted bioflocculants/graft copolymers

According to Pal *et al*. (2011) grafted bioflocculants use a flocculation mechanism that combines charge neutralization and bridging by polymer. In the beginning of flocculation, charge neutralization dominates and forms microflocs (Lee *et al*., 2014). Then, through the bridging mechanism, the microflocs form larger flocs, which eventually cause sedimentation (Yang *et al*., 2013).

2.4.3.1 Charge neutralization

Charge neutralization operates when the flocculants and the suspended particles have opposite surface charges (Lee *et al*., 2014). It functions by reducing surface charge of particles, which then enables the formation of van der Waals attraction forces amongst the colloidal particles. The forces of attraction then result in microflocs formation (More *et al*., 2014).

2.4.3.2 Polymer bridging

The polymer bridging mechanism works when the flocculants and colloidal particles have neutral or the same surface charges (More *et al*., 2014). Long chain polymers, having high molecular weight and low charge density, adsorb colloidal particles in such a way that long loops and tails extend past the electrical double layer in a solution. Thus, the dangling polymer parts adsorb to other particles, therefore causing bridging among particles (Figure 2.3) (Lee *et al*., 2012).

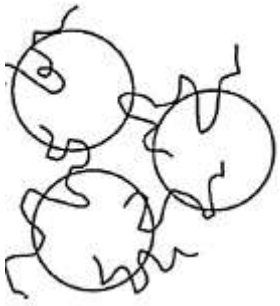

Figure 2.3: Polymer bridging between particles (Sharma *et al*., 2006)

2.4.4 Factors controlling graft copolymerization

Graft copolymerization is affected by a number of factors. These include the following: nature of the backbone, monomer, solvent, initiator and temperature (Bhattacharya and Misra, 2004).

2.4.4.1 Nature of the polymeric backbone

The physical and chemical composition of polymeric backbone influences the graft copolymerization. For example, if the polymeric backbone contains lignin, then lignin may need to be removed since it is very good at scavenging free radicals (Tyuganova *et al*., 1985). Moreover, according to Bhattacharya and Misra (2004) when ethyl acrylate was grafted to sisal (with lignin content of 8%) the percentage of grafting increased because NaOH was utilised to remove lignin. However, having lignin may enhance the percentage of grafting if the backbone is first ozonized and then Fe^{2+}-H_2O_2 (initiator) used during graft copolymerization process. In such a case, lignin is oxidized, resulting in the formation of carboxylic group in lignin, which supports free radical production (Kokta *et al*., 1981).

The majority of graft copolymers which have been successfully synthesized have involved grafting polyacrylamide on plant based carbohydrates (Lee *et al*., 2014). Some of the examples include the following: Sen and Pal (2009) used maize starch to synthesize polyacrylamide grafted carboxymethyl starch (CMS-g-PAM), for use as matrix for drug delivery; Yahya *et al*. (2015) succesfully grafted polyacrylamide chains onto cellulose that was extracted from pandan leaves. Thus, there is a need to also explore microbial carbohydrates which may have unique characteristics.

2.4.4.2 Effect of monomers

The degree of reactivity of monomers influences the percentage of grafting (Bhattacharya and Misra, 2004). For example, the higher reactivity of ethyl acrylate to free radicals, compared to vinyl acetate, resulted in a higher percentage of grafting of ethyl acrylate on wool. This is because less ethyl acrylate is lost in a side reaction, resulting in higher percentage of grafting than when vinyl acetate is used.

In a study by Bhattacharya *et al*. (1998) the order of grafting on cellulose acetate was shown to be acrylamide > methylacrylamide > N,N dimethylacrylamide. It was concluded that methylacrylamide's methyl group possibly made the monomer to be less mobile, thus reducing the degree of graft copolymerization. The lower grafting percentage when N,N dimethylacrylamide is used (as a monomer) was ascribed to the two methyl groups; which prevented dimethylacrylamide from approaching the cellulose acetate.

Among vinyl and acrylic monomers, acrylamide is commonly preferred for grafting (Yahya *et al*., 2015). This is because it has the relatively higher propagation to termination (K_p/K_t) rate constants. Consequently, acrylamide polymerizes easily to form polymers with a very high molecular weight (10^6–10^7) (Tripathy and De, 2006). Therefore, in this study acrylamide was used as a monomer for grafting onto the microbial bioflocculants (TMT^{-1} and TST^{-1}).

Grafting is also affected by the concentration of monomers (Sen *et al*., 2010). As can be seen in Figure 2.4, the grafting percentage rises, as the concentration of monomer increases, up to a certain point and then drops when there is a further increase in the monomer concentration (Sun *et al*., 2003). This is due to an increase in monomer concentration, beyond a certain point, which increases the formation of homopolymers rather than grafting (Dey *et al*., 2017).

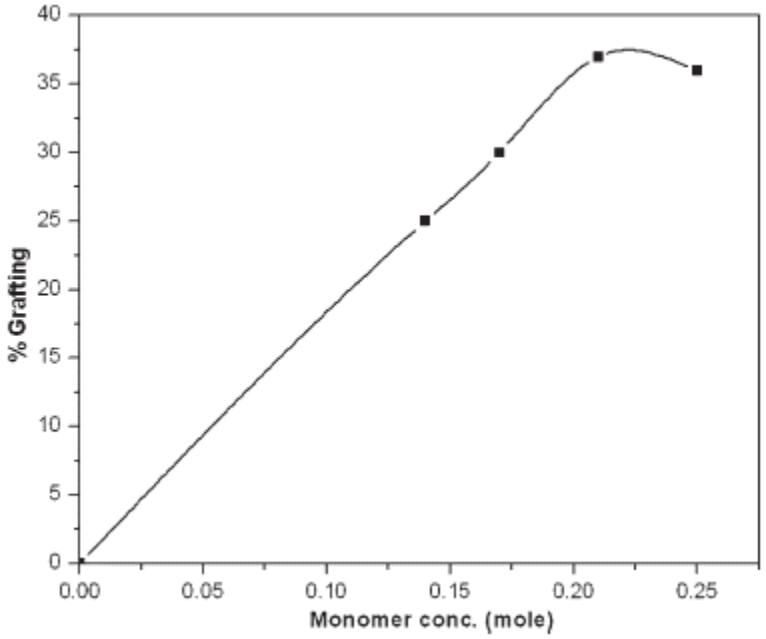

Figure 2.4: Influence of monomer concentration on grafting percentage (when other factors are kept constant) (Sen *et al*., 2010)

2.4.4.3 Effect of solvents

Grafting reaction require solvent(s) in order to occur. The solubility of a monomer in a solvent enhances grafting. Moreover, the grafting is also enhanced by a solvent which is able to loosen the networks of the polymeric backbone (Battacharya and Misra, 2004). This ensures that the monomer can easily diffuse into the polymeric backbone. For example, alcohols were used as solvent for the grafting of styrene on to cellulosic structure. The grafting was possible because the alcohols are able to swell the cellulosic structure effectively and also dissolve the monomer styrene (Dilli and Garnett, 1967).

Grafting efficiency is also affected by the competition, between monomer and solvent, for free radicals created in the polymeric backbone (Bhattacharya and Misra, 2004). For example, consider the following reactions taken from Bhattacharya and Misra (2004):
(1) $C^{\cdot} + X \rightarrow CX^{\cdot}$ and (2) $C^{\cdot} + CH_3OH \rightarrow CH + {}^{\cdot}CH_2OH$ where $C^{\cdot}$ stands for polymeric backbone with free radical; X represents monomer. Reaction 1 gives the required graft copolymer. On the other hand, in reaction 2 the radical of polymeric backbone takes the H^+ from the alcohol and forms ${}^{\cdot}CH_2OH$ rather than a graft copolymer.

When pure alcohols are used as solvents for grafting of styrene on the cellulosic structure, reaction 1 speeds up, resulting in a high grafting efficiency. In contrast, when pure alcohols are utilized for grafting of acrylamide on the cellulosic structure, reaction 2 predominates, which favours homopolymer formation and low grafting efficiency. Thus pure alcohols are not suited for usage as solvents in graft copolymerization of acrylamide to polymeric backbone (Bhattacharya and Misra, 2004).

Hydrogen ion abstraction (shown in reaction 2) and chain transfer play a role in decreasing grafting efficiency. Water has minimal side chain reaction involving chain transfer, because it has zero chain transfer constant. This makes water a very good medium for grafting. Therefore, water has been successfully used for grafting polysaccharides and proteinous materials (Kojima *et al*., 1983; Bhattacharya and Misra, 2004).

2.4.4.4 Effect of temperature

In general, increasing the temperature results in an increase in grafting percentage until a certain limit is reached (Bhattacharya and Misra, 2004). This phenomenon can be due to the increase in monomeric diffusion rate as temperature increases (Dilli and Garnett, 1967). This was observed when Samal *et al*. (1987) grafted methylmethacrylate on silk. The grafting percentage increased as temperature increased, because methylmethacrylate diffused faster into the silk as the temperature increased.

2.4.4.5 Effect of initiator

Except for radiation based grafting, all graft copolymerization methods need an initiator (Singh *et al*., 2012). Examples of initiators include $K_2S_2O_8$ and $Fe^{2+}H_2O_2$. They are chemicals that are used to produce free radicals on a biopolymer. The biopolymer radicals then react with a vinyl monomer, forming a graft copolymer. Initiators are commonly employed in a grafting procedure termed: microwave assisted grafting. Where, the initiator and microwave irradiation are used together to generate free radicals on a polymeric backbone. The nature, concentration and solubility of an initiator affect grafting efficiency (Bhattacharya and Misra, 2004).

2.4.4.5.1 The nature of the initiator

The nature of the initiator is important because it affects grafting. For example, when grafting on cellulose, $K_2S_2O_8$ is not suited for use as an initiator, because it breaks down the cellulose (Bhattacharya and Misra, 2004).

2.4.4.5.2 The concentration of the initiator

The grafting efficiency increases with increase in initiator concentration, up to a certain limit after which, a further rise in concentration does not increase grafting efficiency (Patil and Fanta, 1993). According to Sanli and Pulet (1993), above certain concentration limits, extra radicals take part in stopping the growth of polymer chain, causing a decrease in grafting yield.

2.4.4.5.3 The solubility of the initiator

The grafting efficiency is affected by the solubility of the initiator on the graft copolymerization media. In an ideal situation, the initiator must be soluble so that it can start the grafting process (Bhattacharya and Misra, 2004).

2.4.4.6 The effect of time

Figure 2.5 shows temporal influence on grafting yield. As time increases, grafting yield also increases up to a certain time limit. This phenomenon was seen in a study done by Sen *et al*. (2010) involving the grafting of acrylamide monomers on to sodium alginate. They observed that as microwave irradiation time increased, the grafting yield increased as well. This continued up to a certain time limit, beyond which any further rise in time resulted in a decrease in percentage grafting. The decrease in grafting yield was attributed to the polymeric backbone damage due to an overexposure to irradiation.

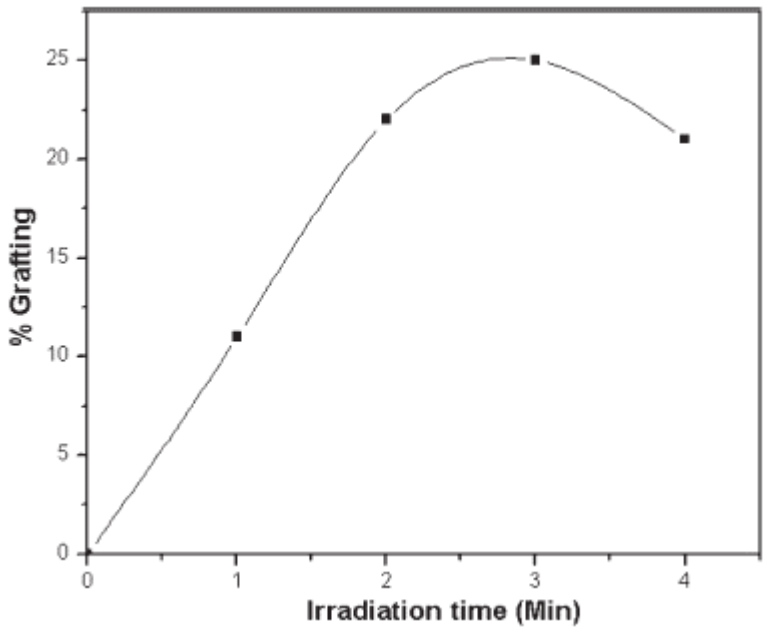

Figure 2.5: Influence of radiation time on grafting percentage (when other factors are kept constant) (Sen *et al*., 2010)

2.5 Sources of bioflocculant producers

Soil, activated sludge, river and deep sea water samples are excellent sources for obtaining new bioflocculant producing microorganisms (Bala *et al*., 2010; Salehizadeh and Shojaosadati, 2001). Moreover, soil and activated sludge samples have mostly been utilized for isolation of bioflocculant-producing microorganisms. However, the marine environment, such as the deep sea, has high pressure, low temperature and nutrition. Furthermore, the sea generally contains high salinity (Li *et al*., 2008).

Because of the above-mentioned extreme conditions, marine samples have numerous diverse secondary metabolites producing microorganisms. These microorganisms have morphological, physiological and metabolic adaptations that are significantly different from microorganisms found on land (Okaiyeto *et al*., 2016). Therefore, it is expected that marine microorganisms produce bioflocculants with distinct properties which are different from those produced by terrestrial microorganisms. It is anticipated that bioflocculants from marine microorganisms can have special adaptations to low temperature and high salinity conditions, normally found in wastewater treatment process. Therefore, these bioflocculants can be effective in wastewater treatment (Li *et al*., 2008).

2.5.1 *Bacillus subtilis*

Bacillus subtilis and *Bacillus pumilus* are members of the genus *Bacillus* (Willey *et al*., 2011). This genus is made up of a large number of different bacteria, which are all Gram-positive, rod-shaped, endospore-forming, catalase positive, motile and aerobic (Madigan *et al*., 2012).

Bacillus subtilis is a mesophilic bacterium that is usually found in soil, water and on plants (Perez *et al*., 2000). It is normally non-pathogenic to humans (Batzing, 2002). This bacterium is important industrially due to its excellent fermentation enhancing characteristics. It is able to produce large amounts of industrially useful enzymes such as amylase and proteases (Morikawa, 2006). Furthermore, it is capable of withstanding harsh conditions that may arise during the fermentation process, because of its ability to synthesize endospores and catalase. The catalase catalyzes the breaking down of H_2O_2, thereby enabling the bacterium to resist oxidative stress (Handtke *et al*., 2014).

2.5.2 *Bacillus pumilus*

Bacillus pumilus has cellular features that are similar to *B. subtilis* and other species of the genus *Bacillus*. They are Gram-positive, aerobic, rod-shaped, mesophilic and spore-forming bacteria with natural habitats that include soil and water (Kempf *et al*., 2005).

Harsh conditions (such as salt, heat and oxidative stress) can occur during industrial fermentation process (Handtke *et al*., 2014). *Bacillus pumilus* is able to resist these unfavourable conditions because of its ability to form endospores (Nicholson *et al*., 2000). The enzyme catalase helps the bacterium to resist oxidative stress, because it catalyzes the breakdown of hydrogen peroxide (Handtke *et al*., 2014).

The good fermentation properties of *B. pumilus* have enabled this bacterium to be utilized in the production of industrially useful products such as keratinase, vanillin and xylanase (Converti *et al*., 2010; Rajput and Gupta, 2014; Thomas *et al*., 2014).

2.6 Composition of bioflocculants TMT^{-1} and TST^{-1}

According to Maliehe *et al.* (2016) bioflocculant TMT^{-1} (which is produced by *B. pumilus* JX860616) is made up of 93% polysaccharides (w/w) and 6% proteins (w/w). Furthermore, it is negatively charged with a zeta potential of -11.6 mV. On the other hand, bioflocculant TST^{-1} (which is produced by a consortium of *B. pumilus* JX860616 and *Bacillus subtilis* CSM5) consists of 80% carbohydrates (w/w) and 15% proteins (w/w). It is also a negatively charged bioflocculant with a zeta potential of -11.2 mV. In this study, these bioflocculants were used for the synthesis of polyacrylamide grafted bioflocculants.

Chapter 3: Materials and method

3.1 Chemicals purchased from E. Merck, South Africa

Acrylamide, formamide, acetic acid, hydroquinone, NaCl, K_2HPO_4, $MgSO_4.7H_2O$, glucose, $(NH_4)_2SO_4$, KH_2PO_4, ethanol, chloroform, butanol, HCl, NaOH and kaolin clay were all obtained from E. Merck Limited, South Africa. They were utilized without being purified further.

3.2 Wastewater

Domestic wastewater was collected from Vulindlela Wastewater Treatment Plant (KwaDlangezwa, KwaZulu-Natal Province, RSA). The surrounding community has livestock and agricultural farms. Thus, the plant receives mostly domestic effluent. The effluent used in this study was obtained in the aeration tanks of the plant. Some of the chemical characteristics of this raw water are shown in Table 3.1.

Table 3.1: Characteristics of a domestic wastewater from Vulindlela Wastewater Treatment Plant

Parameter	Value	Units
COD	1600	mg/l
BOD	183	mg/l
P	20.7	mg/l
N	13.1	mg/l
Optical density	2.8	
pH	6.4	

Industrial effluent was procured from Tendele Coal Mine (Mtubatuba, KwaZulu-Natal Province, RSA). Some of the chemical characteristics of this effluent are shown in Table 3.2.

Table 3.2: Properties of Tendele Coal Mine wastewater

Parameter	Value	Units
COD	1557	mg/l
BOD	73	mg/l
N	2.9	mg/l
S	0.3	mg/l
Optical density	2.2	
pH	8.1	

3.3 Bacteria used for bioflocculants production

Bacillus pumilus JX860616 was used for bioflocculant TMT^{-1} production. Furthermore, a consortium of *B. pumilus* JX860616 and *B. subtilis* CSM5 for TST^{-1} production was prepared. The bacteria were previously isolated from Sodwana Bay, in Kwazulu-Natal, Republic of South Africa and identified using 16S rRNA gene sequencing with BLAST Analysis. The bacteria were stored in 20% glycerol at -80 °C, in order to preserve them, at UNIZULU culture collection (Maliehe, 2017, 37).

3.4 Production media for TMT^{-1} and TST^{-1}

The production medium that is optimum for the production of bioflocculant TMT^{-1} was previously done by Maliehe *et al*. (2016) and it consisted of NaCl (0.1 g), K_2HPO_4 (5.0 g), $MgSO_4.7H_2O$ (0.2 g), glucose (20 g), $(NH_4)_2SO_4$ (1.2 g) and KH_2PO_4 (2.0 g) in 1000 ml of filtered seawater. Furthermore, the optimum production medium for TST^{-1} was also found to be similar to the one for TMT^{-1} production (Maliehe, 2017, 152).

3.5 Extraction and purification of bioflocculants TST^{-1} and TMT^{-1}

The extraction and purification of each bioflocculant was carried out using the methodology described by Chang *et al*. (1998) with few modifications. One thousand millilitres of production medium was inoculated with 20 ml of inoculum (containing *Bacillus pumilus* JX860616 in case of TMT^{-1} production; and a consortium of *B. pumilus* JX860616 and *B. subtilis* CSM5 for TST^{-1} production). The inoculated production medium was then incubated using a Labcon shaking incubator (FSIM-SP, JHB, RSA) at 165 r.p.m. for 72 h. Afterwards, the

fermented medium was put in a centrifuge set at a speed of 5000 x g, temperature of 4 °C, and a time of 30 min. Deionized water (1000 ml) was transferred to the supernatant and centrifuged (5000 × g, 30 min., 4 °C) in order to get rid of the insoluble materials. Ethanol (2000 ml) was poured into the supernatant, mixed thoroughly and then left to precipitate overnight at a temperature of 4 °C. The precipitate was dried using a vacuum-drier. The resulting crude bioflocculant was dissolved in 100 ml of deionized water. Chloroform and butanol was mixed in one volume in a ratio of 5:2 (v/v). This mixture was then poured into the solution of crude bioflocculant, mixed and left to settle for 12 h at room temperature. Finally, the precipitate was vacuum-dried in order to obtain a pure bioflocculant.

3.6 Synthesis of the graft copolymer using the "microwave initiated" method

Microwave irradiation was employed to produce free radical sites on the bioflocculant (Sen *et al*., 2009). The bioflocculant (0.5 g) was dissolved in 20 ml of distilled water. Acrylamide (2.5–7.5 g) was dissolved in 10 ml of distilled water; and then added to the bioflocculant solution. They were mixed thoroughly and then transferred to the reaction beaker which was then placed on the turntable of the microwave oven (25 l LG Microwave oven Model: MG-577 B). Microwave irradiation at 900 W was performed for the desired amount of time ranging from 1 to 4 min. Periodically, the microwave irradiation was stopped, and the reaction mixture was cooled by placing the reaction beaker in cold water. This was done in order to keep the reaction temperature below 70 °C so as to avoid thermal damage to the bioflocculant. Once the microwave irradiations for the intended time period was completed, the reaction mixture was cooled and then left to stand. After 24 h, the reactions were ended by adding saturated solution of hydroquinone, and then the gel-like mass left in the reaction beaker was added to 250 ml acetone. The resulting precipitates of grafted polymers were collected by a spatula and put in hot air oven (60 °C, 6 h) to dry. The percentage grafting of each of the synthesized graft copolymers was evaluated as:

$$\text{Grafting (\%)} = \left(\frac{\text{Wt. of graft copolymer} - \text{Wt. of pure bioflocculant}}{\text{Wt. of pure bioflocculant}}\right) * 100$$

Figure 4.2.1 (p. 32) shows the suggested mechanism of graft copolymer synthesis when microwave initiated method is used. Tables 4.2.1 and 4.2.2 (pp. 33–34) display different parameters that were employed for the synthesis of the graft copolymers TMT^{-1}-g-PAM 2 and TST^{-1}-g-PAM 3.

3.7 Purification of graft copolymer by solvent extraction method

Any obstructed polyacrylamide formed by competing homopolymer formation reaction was removed by solvent extraction using formamide and acetic acid mixture in a ratio of 1:1 (v/v) (Fanta, 1973).

3.8 Characterization

3.8.1 Intrinsic viscosity

Absolute viscosities of polymer solutions were measured using a Brookfield viscometer (DV2TRVTJO, USA) at 25 °C. In each experiment, 0.1 g of a polymer was dissolved in 100 ml of distilled water and viscosity measurements were then performed (Mishra *et al*., 2006). Relative viscosity (η_r) was obtained using the formula $\eta_r = \eta/\eta_o$ where η is the absolute viscosity of a polymer and η_o is the absolute viscosity of a pure solvent. The relation $\eta_{sp=}\,\eta_r - 1$ was utilized to calculate specific viscosity (η_{sp}) (Sen and Pal, 2009). Then intrinsic viscosity of each polymer was calculated using Solomon-Ciuda equation which states that intrinsic viscosity = $(2\eta_{sp} - 2\ln\eta_r)^{0.5}/C$, where C is a concentration of a polymer in mg/ml (Rheosense, 2016).

3.8.2 Elemental analysis

The elemental analysis of acrylamide, TMT^{-1}, TST^{-1}, TST^{-1}-g-PAM 3 and TMT^{-1}-g-PAM 2 was conducted using an elemental analyser (Oxford instrument x-max, UK). Each compound was analysed for 5 elements, which included the following: carbon, hydrogen, nitrogen, oxygen, and sulfur (Mishra and Sen, 2011).

3.8.3 Scanning electron microscopy

The morphological surface structures of the acrylamide, TMT^{-1}, TST^{-1}, TMT^{-1}-g-PAM 2 and TST^{-1}-g-PAM 3 were ascertained using a SEM (SIGMA VP-03-67, UK) (Karthiga and Natarajan, 2015). The compounds were evaluated by fixing a few drops of its powder on the iron stub

of the scanning electron microscope and coated with gold to investigate surface morphology.

3.8.4 Fourier transform infrared spectroscopy

The Fourier transform-infrared (FTIR) spectrophotometer (Perkin Elmer UATR TWO, 2000, Germany) was used in order to determine functional groups of TMT^{-1}, TST^{-1}, TMT^{-1}-g-PAM 2 and TST^{-1}-g-PAM 3 (Sen and Pal, 2009). Each polymer powder was investigated by firstly grinding it with KBr at 25 °C, and then pressing it into a pellet to be analysed by FTIR at a wavenumber ranging from 4000 to 400 cm^{-1}.

3.8.5 X-ray diffractometry analysis

XRD analysis of TMT^{-1}, TST^{-1}, TMT^{-1}-g-PAM 2 and TST^{-1}-g-PAM 3 was completed using a X-ray diffractometer (Ultima-I II, Rigaku, Japan) utilizing a copper target slit 10 mm and a scattering angle varying from 5-60° (2θ) (Giri *et al*., 2015).

3.8.6 Thermogravimetric analysis

The thermogravimetric analysis (TGA) of TMT^{-1}, TST^{-1}, TMT^{-1}-g-PAM 2 and TST^{-1}-g-PAM 3 were carried out with a TGA instrument (Model: DTG-60; Shimadzu, Japan). Ten milligrams of every polymer was analysed in each experiment. The study was performed in an inert atmosphere (nitrogen) from 25 °C to 800 °C. The heating rate was uniform in all cases at 5 °C/min (Okaiyeto *et al*., 2016).

3.8.7 Biosafety assay of TMT^{-1}-g-PAM 2 and TST^{-1}-g-PAM 3

The cell cytotoxicity was measured according to the method by Mosman (1983). Human embryonic kidney 293 cells (HEK 293) were all grown to confluence in 25 cm^3 flasks. They were then trypsinised and plated into 48 well plates. Cells were incubated overnight at 37 °C. Old medium was supplemented with the fresh medium (MEM + Glutmax + antibiotics). Grafted bioflocculants were then added and incubated for 4 h. Thereafter, the medium was removed and replaced by complete medium (MEM + Glutmax + antibiotics +10% fetal bovine serum). After 48 h, the cells were subjected to 200 µl of 3-(4,5-dimethylthiazol-2-yl)-2,5-diphenyl tetrazolium bromide) (MTT) with a concentration of 5 mg/ml in phosphate buffered saline (PBS) and 200 µl medium was added to each well and incubated at 37 ˚C for

4 h. Thereafter, the medium with MTT was aspirated from the wells and the formed formazan crystals were solubilized in 200 µl of dimethyl sulfoxide (DMSO).

Finally, the optical density of the solutions was read at 570 nm using a micro-plate reader. The cell viability was expressed as percentage with control using the equation: cell viability (%) = (F_1/F_0) x 100, where F_1 and F_0 are the final and initial values obtained after and before treatment with the grafted bioflocculants, respectively.

3.8.8 Antimicrobial activity of the grafted flocculants (TST^{-1}-g-PAM and TMT^{-1}-g-PAM)

The bacteria that were chosen for the screening of the antibacterial activity of the flocculants are shown in Table 3.3. These bacteria strains are known to cause infections of the gastrointestinal tract (Maliehe *et al*., 2015).

Table 3.3: Bacteria strains utilized in this study to evaluate antibacterial activity of graft copolymers

Bacteria	Strain number	Gram stain
Bacillus cereus	ATCC 10102	+
Staphylococcus aureus	ATCC 25925	+
Escherichia coli	ATCC 25922	-
Klebsiella pneumoniae	ATCC 4352	-

3.8.8.1 Reviving the bacteria

The bacteria were transferred into sterilised nutrient broth. The nutrient broth was then placed overnight at 37 °C in an incubator. Afterward, 1 ml of each bacterial culture was pipetted into different test tubes consisting of sterile nutrient broth (9 ml). The tubes were then again placed into an incubator at 37 °C overnight. Afterward, absorbance of the bacteria was read from the spectrophotometer (600 nm) in order to determine their turbidity. The turbidity was then adjusted to be similar to 0.5 McFarland's standard. Thus, the expected density of cells in the bacteria suspension was approximately 1.5 x 10^6 CFU/ml and the absorbance between 0.08 to 0.1 (Qaralleh *et al.,* 2012).

3.8.8.2 Minimum inhibitory concentration (MIC)

Successive dilutions were performed on a 96-well microplate in order to determine MIC of the grafted bioflocculants (Ellof, 1998; Qaralleh *et al*., 2012). Fifty microliter of a sterilised Mueller-Hinton broth was poured into each of the 96 wells. Thereafter, 50 µl of the grafted bioflocculants (50 mg/ml, in distilled water) was transferred into each of the wells that are in the first rows and thoroughly mixed. A serial dilution procedure was used to transfer 50 µl of the grafted bioflocculant mixtures from all the wells in row A, into the wells down the columns. Fifty microliter was then discarded from the last well of each column, to produce a volume in every well of 50 µl. In addition, 50 µl of the chosen bacteria strains was introduced into the corresponding wells. Autoclaved distilled water was employed as a negative control whereas 20 µg/ml of ciprofloxacin served as a positive control.

The plates were enclosed and put into the incubator overnight at 37 °C. Forty microliter was poured from the solution of 0.2 mg/ml *P*-iodonitrotetrazolium violet (INT), into each well and then placed in an incubator for 30 min. at 37 °C. MIC was then recorded as the least concentration of the grafted bioflocculants that was able to inhibit bacterial growth. A reddish colour formation indicated bacterial activity (i.e. reduction of INT to formazan). A clear colour indicated the absence of bacterial activity.

3.8.9 Biodegradation studies

A modified composting method by Kalea *et al*. (2007) was used to study the biodegradation of both the natural bioflocculants and the grafted bioflocculants. Each of these flocculants was mixed with the soil and effluent that were collected from Vulindlela Domestic Wastewater Treatment Plant, KwaDlangezwa, RSA. The effluent was collected from an aeration basin and the soil was obtained from the sludge drying beds.

For each test, 4 g of soil was transferred into a diamond shaped weighing boat (80x60x14 mm) and mixed with 0.5 g of either pure bioflocculant or the grafted bioflocculant. The effluent was poured into the weighing boat up to a level just underneath the surface of the soil. Effluent was sprinkled every day to stop the samples from drying out. The samples were left uncovered at room temperature.

After every week of a 5 weeks period, samples were dried using hot oven (37 °C) and then weighed. This was done in order to monitor biodegradation progress. For the control, all the above-mentioned steps were followed but instead of using a mixture of soil and flocculants, only 4.5 g of soil was transferred into a diamond shaped weighing boat.

To calculate the weight of the flocculant remaining after biodegradation (Wr) the following formula was used: Wr = Wm – Ws. Wherein, Wm is a weight of a mixture of soil and flocculant, and Ws is a weight of soil.

3.9 Evaluation of flocculation properties of the grafted bioflocculants

Flocculation properties of the grafted bioflocculants (TMT^{-1}-g-PAM 2 and TST^{-1}-g-PAM 3) were studied by assessing the influence of different parameters on their flocculating activities. Parameters such as dosage size, cations, pH, temperatures and salinity were utilised. The influence of these parameters, on TMT^{-1}-g-PAM 2 and TST^{-1}-g-PAM 3, was then compared to their influence on other flocculants such as the natural bioflocculants (TMT^{-1} and TST^{-1}) and the commercial flocculants ($FeCl_3$ and PAM).

3.9.1 Dosage and cation type

The jar test procedure, on kaolin clay solution (4 g/l), was used for comparative analysis of the influence of dosage size on the flocculating activities of the grafted bioflocculants and other flocculants - TMT^{-1}, TST^{-1}, $FeCl_3$ and PAM. For each test, 2 ml of a flocculant (having a concentration ranging from 0.1 to 2 mg/ml) and 3 ml of 1% $BaCl_2$ were added to 100 ml of kaolin clay suspension in a 250 ml Erlenmeyer flask. The mixture was then vigorously stirred, by a Labcon shaking incubator (FSIM-SP, JHB, RSA), for 1 min. at 180 r.p.m., flocculated for 3 min. at 45 r.p.m.; and thereafter, settled for 5 min. in a graduated measuring cylinder. After a settling period, the supernatant was collected for optical density measurement using a spectrophotometer (Spectroquant Pharo 100 M, EU), at a wavelength of 550 nm (Lee *et al.,* 2001). For the control, a same method was followed but the bioflocculant solution was substituted with distilled water. The flocculating activity (FA) was calculated by the following formula:

FA (%) = $(\frac{A - B}{A})^{*} 100$

Where A is the optical density of the control and B represents the optical density of a sample.

The jar test experiment was used to assess the effect of various cations on flocculation. $BaCl_2$ previously used, was replaced by the following cations: KCl, NaCl, LiCl, $CaCl_2$, $MgCl_2$ and $FeCl_3$ (1% w/v) (Cosa and Okoh, 2014). A negative control was obtained with the same procedure without a cation.

3.9.2 Thermal and pH stabilities of the grafted bioflocculants

A comparative analysis of the influence of pH on flocculating activities of the grafted bioflocculants and other flocculants (TMT^{-1}, TST^{-1}, $FeCl_3$ and PAM) was carried out according to Wang *et al*. (2010). The pH of kaolin clay suspension (4 g/l) was adjusted in a range of pH 3–11 with 0.1 ml HCl and 0.1 ml NaOH addition. The flocculating activities were determined again, using the jar test procedure.

Thermal stabilities of the flocculants were assessed at different temperature ranges (50 to 100 °C). This was done by heating 2 ml of each flocculants' solutions (having an optimum concentration/dosage previously determined in section 3.9.1) at different temperatures for 60 min. Thereafter, the flocculating activities were evaluated by the jar test procedure (Okaiyeto *et al*., 2013).

3.9.3 Saline stabilities of the grafted bioflocculants

The influence of salinity on the flocculating activities of the grafted bioflocculants was assessed using a method proposed by Li *et al*. (2008). The salinity of kaolin clay suspension (4 g/l) was varied in a range of 5–35 g/l by NaCl. The flocculating activities of the grafted bioflocculants were then evaluated, using the jar test procedure. The results were compared to those of the flocculants TMT^{-1}, TST^{-1}, $FeCl_3$ and PAM under similar saline conditions.

3.10 Proposed flocculation mechanism

The flocculation mechanism of the grafted bioflocculants was proposed after the zeta (ζ) potentials were evaluated by a Zetasizer Nano (Malvern, UK). The ζ potentials of TMT^{-1}-g-PAM 2, kaolin clay suspension and kaolin clay suspension flocculated by TMT^{-1}-g-PAM 2 in the presence of $CaCl_2$ were measured at a pH of 7 and at room temperature (Aljuboori *et al*., 2015). The ζ potentials of TST^{-1}-g-PAM 3 were measured under similar conditions but in the presence of $BaCl_2$ instead of $CaCl_2$.

3.11 Application of grafted bioflocculants in wastewater treatment

The flocculation efficiency of the flocculants was tested on domestic and industrial wastewater (Tables 3.1 and 3.2, pp. 20–21). The jar test experiment was utilized to determine the removal efficiencies of the grafted bioflocculants in comparison with other flocculants (TMT^{-1}, TST^{-1}, $FeCl_3$ and PAM). For each experiment, 3 ml of 1% (w/v) $BaCl_2$ and 2 ml of an optimum dose of a flocculant were added to 100 ml of wastewater, stirred at an agitation speed of 50 r.p.m. for 10 min., and then allowed to settle for 30 min. (Okaiyeto *et al*., 2014). The supernatant was collected and the COD, BOD, N, P and S contents were determined using respective spectrophotometric cell tests (14541, 100687, 100613, 114729 and 114779) (Merck, Germany) and following manufactures' guidelines. The removal efficiency (RE) was calculated using the equation:

$$\text{RE (\%)} = \left(\frac{E - D}{E}\right) * 100$$

Where E is the initial quantity and D is the quantity after flocculation.

In order to determine the flocculating activity (FA) of each flocculant in domestic and industrial wastewater, the jar test procedure as described in section 3.9.1 was followed. However, kaolin clay suspension was replaced by either the domestic or the mine wastewater. In addition, the optimum flocculants dosage sizes, that were determined in section 3.9.1, were used in each experiment.

3.12 Software and statistical analysis

All the experiments were completed in triplicates and the error bars in the figures, in chapter 4, show the standard deviations of the data. Data were subjected to one-way analysis of variance (ANOVA) using Graph Pad prism™ 6.1. A significant level of $p < 0.05$ was used. Values with different letters on the same column or graph are significantly ($p < 0.05$) different.

Chapter 4: Results and discussion

4.1 Introduction

Chapter 4 contains the results and observations obtained from this study.

4.2 Results and discussion for TMT^{-1}-g-PAM 2 and TST^{-1}-g-PAM 3

The results and discussion for the synthesis, characterization and application of the polyacrylamide grafted bioflocculants (TMT^{-1}-g-PAM 2 and TST^{-1}-g-PAM 3) are exhibited in this section.

4.2.1 Extracted bioflocculant

Yield and productivity are good indicators of how bacteria use culture media to grow and produce secondary metabolites such as bioflocculants (Smith, 2009). *B. pumilus* JX860616 yielded 2.4 g/l of the bioflocculant; while a consortium of *B. pumilus* JX860616 and *B. subtilis* CSM5 produced 3.5 g/l. The high yield is probably caused by the ability of the strains to optimally survive and produce bioflocculants in optimised culture conditions and polarity of the solvents used during extraction.

4.2.2 TMT^{-1}-g-PAM and TST^{-1}-g-PAM synthesis by microwave irradiation

Figure 4.2.1 displays the probable mechanism for the synthesis of polyacrylamide grafted bioflocculants: TMT^{-1}-g-PAM and TST^{-1}-g-PAM. This mechanism is proposed to be similar to the one proposed in other studies involving graft copolymerization of biopolymers with vinyl monomers (Sen and Pal, 2009; Sen *et al*., 2009; Shahid *et al*., 2013; Singh *et al*., 2006; Sinha *et al*., 2013).

Microwave irradiations cause the polar hydroxyl and amine groups in TMT^{-1} or TST^{-1} to rotate, thereby leading to free radicals. When each water molecule, used in the grafting reaction, receives the same irradiation energy, the molecule is small enough to rotate and thus it heats up, without any of its bonds breaking. The water molecules then pass radiation energy to the acrylamide. This energy causes the double bonds in acrylamide molecule to break; thus creating acrylamide free radicals (Sen *et al*., 2009).

The free radicals on a bioflocculant (TMT^{-1} or TST^{-1}) and acrylamide enable these macromolecules to react with each other in order to form a graft copolymer - TMT^{-1}-g-PAM or TST^{-1}-g-PAM. Figure 4.2.1 reveals that this formation of a graft copolymer occurs in three steps: initiation, propagation and termination.

Graft copolymerization at O-H groups of bioflocculant (TMT^{-1} or TST^{-1})

$$B\text{-}OH + M \xrightarrow{MW} B\text{-}O\bullet + M\bullet \qquad \text{Initiation}$$

$$B\text{-}O\bullet + M \longrightarrow B\text{-}OM\bullet \qquad \text{Propagation}$$

$$B\text{-}OM\bullet + M \longrightarrow B\text{-}OMM\bullet$$

$$B\text{-}OMM\bullet_{n-1} + M \longrightarrow B\text{-}OM\bullet_{n}$$

$$B\text{-}OM\bullet_{n} + B\text{-}OM\bullet_{n} \longrightarrow \text{Graft copolymer} \qquad \text{Termination}$$

Development of homopolymer (rival side reaction)

$$M\bullet + M \longrightarrow MM\bullet$$

$$M\bullet_{n-1} + M \longrightarrow M\bullet_{n}$$

$$M\bullet_{n} + B\text{-}OH \longrightarrow B\text{-}O\bullet + M_nH \text{ (Homopolymer)}$$

Graft copolymerization at NH_2 groups of bioflocculant (TMT^{-1} or TST^{-1})

$$B\text{-}NH_2 + M \xrightarrow{MW} B\text{-}NH\bullet + M\bullet \qquad \text{Initiation}$$

$$B\text{-}NH\bullet + M \longrightarrow B\text{-}NHM\bullet \qquad \text{Propagation}$$

$$B\text{-}NHM\bullet + M \longrightarrow B\text{-}NHMM\bullet$$

$$B\text{-}NHMM\bullet_{n-1} + M \longrightarrow B\text{-}NHM\bullet_{n}$$

$$B\text{-}NHM\bullet_{n} + B\text{-}NHM\bullet_{n} \longrightarrow \text{Graft copolymer} \qquad \text{Termination}$$

Where B represents bioflocculant TMT^{-1} or TST^{-1}

M represents acrylamide

MW represents microwave irradiation

Figure 4.2.1: Schematic presentation of the proposed mechanism for TMT^{-1}-g-PAM or TST^{-1}-g-PAM synthesis by microwave irradiation

4.2.2.1 Effect of acrylamide concentration on % grafting

The optimum grades (TMT^{-1}-g-PAM 2 and TST^{-1}-g-PAM 3) were identified by their relatively higher grafting percentages and intrinsic viscosities. Table 4.2.1 shows that TMT^{-1}-g-PAM 2 was obtained at an optimum acrylamide concentration of 2.5 g and irradiation time of 3 min. Similarly, TST^{-1}-g-PAM 3 synthesis also required irradiation time of 3 min., but a different acrylamide concentration (7.5 g) (Table 4.2.2).

An increase in monomer (acrylamide) concentration above optimum conditions led to a decrease in % grafting (Tables 4.2.1 and 4.2.2). This was ascribed to an accumulation of excess acrylamide in a bioflocculant backbone in close proximity. Excess acrylamide probably resulted in homopolymer formation reaction that led to reduced % grafting (Dey *et al*., 2017). These findings are similar to those obtained by Ranjbar-Mohammadi *et al.* (2010) on grafting chitosan onto a fabric of wool.

Table 4.2.1: Synthetic details of TMT^{-1}-g-PAM using microwave irradiation

Sample	Power (W)	Amount of TMT^{-1}(g)	Amount of acrylamide (g)	Time (min.)	% Grafting	Viscosity (ml/mg) ± SD
TMT^{-1}-g-PAM 1	900	0.5	2.5	2	10	$0.16\pm0.05^{a,b}$
TMT^{-1}-g-PAM 2	**900**	**0.5**	**2.5**	**3**	**94**	**0.29 ± 0.01^{a}**
TMT^{-1}-g-PAM 3	900	0.5	2.5	4	2	0.09 ± 0.04^{b}
TMT^{-1}-g-PAM 4	900	0.5	5	3	51	$0.25\pm0.05^{a,b}$
TMT^{-1}-g-PAM 5	900	0.5	7.5	3	42	$0.18\pm0.04^{a,b}$
TMT^{-1}	-	-	-	-	-	0.03 ± 0.00^{c}
AM	-	-	-	-	-	$0.26\pm0.16^{a,b}$

Values with different letters (a, b and c) on the same column are significantly ($p < 0.05$) different

Table 4.2.2: Synthetic details of TST^{-1}-g-PAM using microwave irradiation

Sample	Power (W)	Amount of TMT^{-1}(g)	Amount of acrylamide (g)	Time (min.)	% Grafting	Viscosity (ml/mg) ± SD
TST^{-1}-g-PAM 1	900	0.5	2.5	3	62	$0.20\pm0.05^{a,b}$
TST^{-1}-g-PAM 2	900	0.5	5	3	74	$0.22\pm0.02^{a,b}$
TST^{-1}-g-PAM 3	**900**	**0.5**	**7.5**	**3**	**82**	**0.26 ± 0.05^{a}**
TST^{-1}-g-PAM 4	900	0.5	10	3	24	$0.17\pm0.03^{a,b}$
TST^{-1}-g-PAM 5	900	0.5	7.5	4	30	$0.15\pm0.06^{a,b}$
TST^{-1}-g-PAM 6	900	0.5	7.5	2	0	0.03 ± 0.03^{b}
TST^{-1}	-	-	-	-	-	0.04 ± 0.00^{b}
AM	-	-	-	-	-	0.26 ± 0.16^{a}

Values with different letters (a and b) on the same column are significantly ($p < 0.05$) different

4.2.2.2 Effect of time on % grafting

The grafting percentage increased with an increase in reaction time from 2 to 3 min. (Tables 4.2.1 and 4.2.2). This increase in grafting percentage can be attributed to the prolonged exposure time which allows more free radicals to form on the bioflocculants TMT^{-1} and TST^{-1} backbones. This, in turn, allows for more of the acrylamide to react with the bioflocculants, leading to an increase in % grafting. Beyond an optimized time (3 min.), there was a significant decrease in the % grafting. The decrease might be due to the degradation of bioflocculants backbones (Sen *et al*., 2009). The observed decrease maybe as a result of the depletion of acrylamide during the grafting progression. These results are comparable to those obtained by Sen and Pal (2009). They concluded that the optimum time for grafting polyacrylamide onto carboxymethylstarch is 3 min.

4.2.3 Characterization

4.2.3.1 Intrinsic viscosity

All the grades of TMT^{-1}-g-PAM and TST^{-1}-g-PAM had higher intrinsic viscosities than those of of their respective native bioflocculants (Tables 4.2.1 and 4.2.2). The Mark-Houwink-

Sakurada equation states: Intrinsic viscosity $\eta = KM\alpha$, where M is a molecular weight of a polymer, and K and α are constants linked to stiffness of a polymer (Sen *et al*., 2012). Thus the increase in intrinsic viscosity is a consequence of an increase in molecular weight (*M*) caused by the grafted polyacrylamide chains. Tables 4.2.1 and 4.2.2 also show that there is a relationship between percentage grafting and intrinsic viscosity; the higher the percentage grafting, the higher is the intrinsic viscosity. This is because the higher percentage grafting leads to a higher molecular weight (Sen and Pal, 2009). Sinha *et al*. (2013) also observed similar results when polyacrylamide chains were grafted onto casein.

4.2.3.2 Elemental analysis

Tables 4.2.3 and 4.2.4 display the results for the elemental analysis of acrylamide, TMT^{-1}, TST^{-1}, TMT^{-1}-g-PAM 2 and TST^{-1}-g-PAM 3. Both TMT^{-1} and TST^{-1} show the presence of small amounts of nitrogen – 0.9% and 3.5% – respectively. These small amounts are because of a small quantity of proteins that make up TMT^{-1} and TST^{-1}, 6% for TMT^{-1} and 15% for TST^{-1} (Maliehe, 2017, 53, 106). However, graft copolymerization resulted in the production of graft copolymers with a relatively high nitrogen content, 3.7% for TMT^{-1}-g-PAM 2 and 5.1% for TST^{-1}-g-PAM 3. This is due to the presence of grafted polyacrylamide chains in TMT^{-1}-g-PAM 2 and TST^{-1}-g-PAM 3. The elemental analysis results confirm that grafting was succesful. Similarily, Biswal and Singh (2004) observed an increase in nitrogen content when they grafted acrylamide chains on carboxymethyl cellulose.

Table 4.2.3: Elemental analysis results for TMT^{-1}-g-PAM 2

Molecules	% C	% O	% N	% P	% S
Acrylamide	79.7	16.6	3.5	0.0	0.0
TMT^{-1}	18.1	65.8	0.9	13.9	1.3
TMT^{-1}-g-PAM 2	34.9	55.3	3.7	5.9	0.2

Table 4.2.4: Elemental analysis results for TST^{-1}-g-PAM 3

Molecules	% C	% O	% N	% P	% S
Acrylamide	79.7	16.6	3.5	0.0	0.0
TST^{-1}	39.3	55.1	0.3	4.9	0.5
TST^{-1}-g-PAM 3	37.7	52.1	5.1	4.6	0.4

4.2.3.3 Scanning electron microscopy (SEM)

The SEM micrographs of the surface structures of acrylamide, TMT^{-1}, TST^{-1}, TMT^{-1}-g-PAM 2 and TST^{-1}-g-PAM 3 are displayed in Figures 4.2.2 and 4.2.3. Acrylamide had a fibrous structure (Figures 4.2.2a and 4.2.3a), bioflocculant TMT^{-1} showed an amorphous and porous structure (Figures 4.2.2b) and TST^{-1} (Figure 4.2.3b) revealed a crystalline structure. But the grafting of acrylamide chains onto the natural bioflocculants resulted in major morphological changes. For instance, the surface morphology of the graft copolymers TMT^{-1}-g-PAM 2 (Figure 4.2.2c) and TST^{-1}-g-PAM 3 (Figure 4.2.3c) became granular.

The aforementioned findings are analogous to those that were obtained by Yang *et al*. (2013). They found that the graft copolymer (carboxymethyl chitosan-graft-polyacrylamide) had a different surface morphology to its native biopolymer, carboxymethyl chitosan. These changes in surface morphology may affect the flocculation capabilities of the flocculant since surface morphology may be responsible for influencing flocculation performance by a flocculant (Zhang *et al*., 2007).

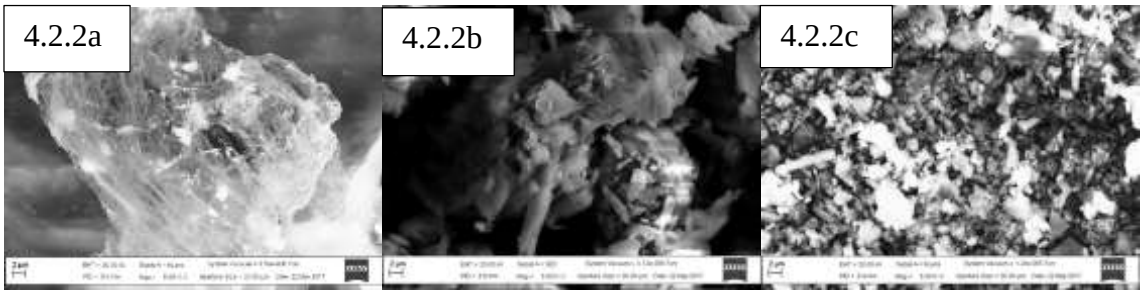

Figure 4.2.2: SEM micrographs of (a) Acrylamide (b) Bioflocculant TMT^{-1} (c) TMT^{-1}-g-PAM 2 (magnification: 5.00 KX, scale bar: 2µm, used in all micrographs)

Figure 4.2.3: SEM micrographs of (a) Acrylamide (b) Bioflocculant TST^{-1} (c) TST^{-1}-g-PAM 3 (magnification: 5.00 KX, scale bar: 2µm, used in all micrographs)

4.2.3.4 Fourier transform infrared (FTIR) spectroscopy

The FTIR spectrum, for TMT^{-1}, in Figure 4.2.4 displayed the presence of a weak and broad absorption peak at 3250 cm^{-1} caused by N-H or O-H stretching vibrations. The absorption peak at 1646 cm^{-1} was due to C=O stretching vibration of amide group and the C-O stretching vibration resulted in an absorption peak at 1057 cm^{-1} that is attributed to the methoxyl group. There was also a C-H absorption peak at 877 cm^{-1} which indicated that TMT^{-1} is a sugar derivative.

On the other hand, in TMT^{-1}-g-PAM 2, O-H and N-H stretching bands of TMT^{-1} overlap with N-H stretching bands of acrylamide and lead to broad and strong absorption peak at 3260 cm^{-1}. The amide 1 (C=O stretching) of acrylamide and the amide 1 (C=O stretching) of TMT^{-1} overlap with each other to produce a strong absorption peak at 1682 cm^{-1}. There is also appearance of new bands of N-H (1659 cm^{-1}), C-N (1390 cm^{-1}), CH_2 scissoring (1233 cm^{-1}) and twisting (1162 cm^{-1}) in TMT^{-1}-g-PAM 2. These additional bands in the grafted product confirm the successful grafting of PAM chains onto the backbone of TMT^{-1}.

Similarly, in a study by Sen and Pal (2009), graft copolymerization of polyacrylamide onto carboxymethylstarch was ascertained by the appearance of new functional groups in the grafted product. The functional groups such as hydroxyl, amines and carboxyl have been reported to improve flocculation capabilities of flocculants (Cosa *et al*., 2013).

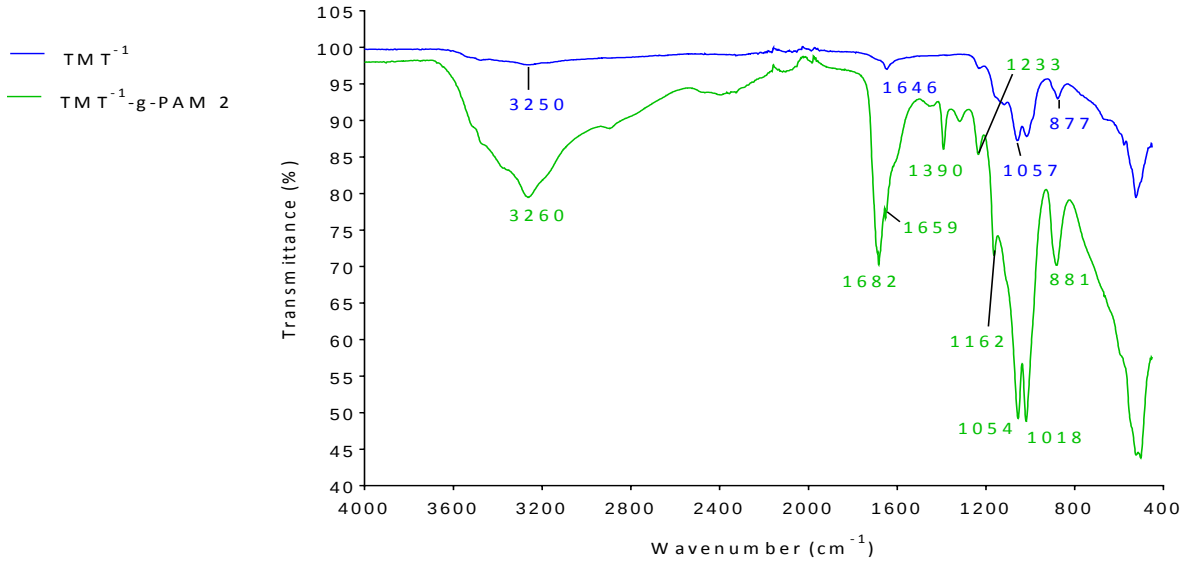

Figure 4.2.4: FTIR spectra of TMT^{-1} and TMT^{-1}-g-PAM 2

In contrast, Figure 4.2.5 reveals the FTIR spectra of TST^{-1} and TST^{-1}-g-PAM 3. TST^{-1} spectrum showed a broad stretching intense peak around 3251 cm^{-1} characteristic for hydroxyl (O-H) and amino groups (N-H). The asymmetrical stretching peak was observed at 1645 cm^{-1} and a medium symmetrical stretching peak (C-O-H) at 1154 cm^{-1}, indicating the presence of carboxyl group in the bioflocculant TST^{-1}. The presence of methoxyl group was revealed by C-O stretching bands at 1056 and 1010 cm^{-1}. The C-H absorption peak at wavenumber 874 cm^{-1} proves that TST^{-1} is a sugar derivative.

In the TST^{-1}-g-PAM 3's FTIR spectrum (Figure 4.2.5), O-H and N-H stretching bands of TST^{-1} overlap with N-H stretching bands of acrylamide to produce a broad and intense band at 3261 cm^{-1}. A weak band at 2391 cm^{-1} could be arising from CO_2 adsorption or from amine group (Okaiyeto *et al*., 2015). Stretching vibrations of CONH groups (from acrylamide chains) produce a strong absorption peak at 1681 cm^{-1}. This appearance of new bands of functional groups in TST^{-1}-g-PAM 3, which also include C-N (1390 cm^{-1}) and CH_2 (1200 cm^{-1} and 1316 cm^{-1}), means that the grafting of PAM branches on to TST^{-1} was accomplished. In the same way, Liu *et al*. (2014) confirmed the grafting of polyacrylamide chains onto cellulose by noting the appearance of new functional groups from polyacrylamide chains. The functional groups aid the flocculants to bind different colloids in a suspension, thus enhancing flocculation (Xiong *et al*., 2010).

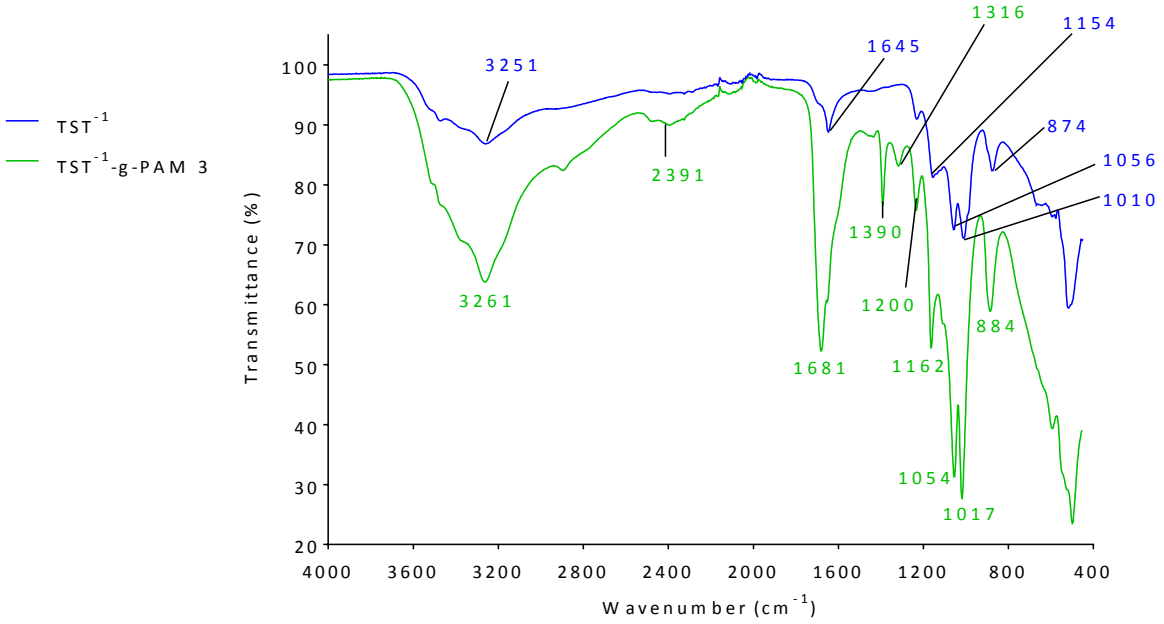

Figure 4.2.5: FTIR spectra of TST^{-1} and TST^{-1}-g-PAM 3

4.2.3.5 X-ray diffraction analysis

X-ray diffractograms of TMT^{-1} and TMT^{-1}-g-PAM 2 are exhibited in Figure 4.2.6; and those of TST^{-1} and TST^{-1}-g-PAM 3 are shown in Figure 4.2.7. TMT^{-1}, TST^{-1}, TMT^{-1}-g-PAM 2 and TST^{-1}-g-PAM 3 display partial crystallinity peaks from $2\theta = 5°$ to 60°. But the crystallinity peaks of pure bioflocculants are more intense than those of their respective polyacrylamide grafted bioflocculants.

This decrease in crystallinity of pure bioflocculants when grafted with acrylamide chains might be caused by the insertion of bulkier groups within the biopolymers; consequently decreasing the intermolecular hydrogen bonds (Mishra *et al*., 2007). A study involving the graft copolymerization of pectin with acrylamide chains found similar results (Mishra *et al*., 2007).

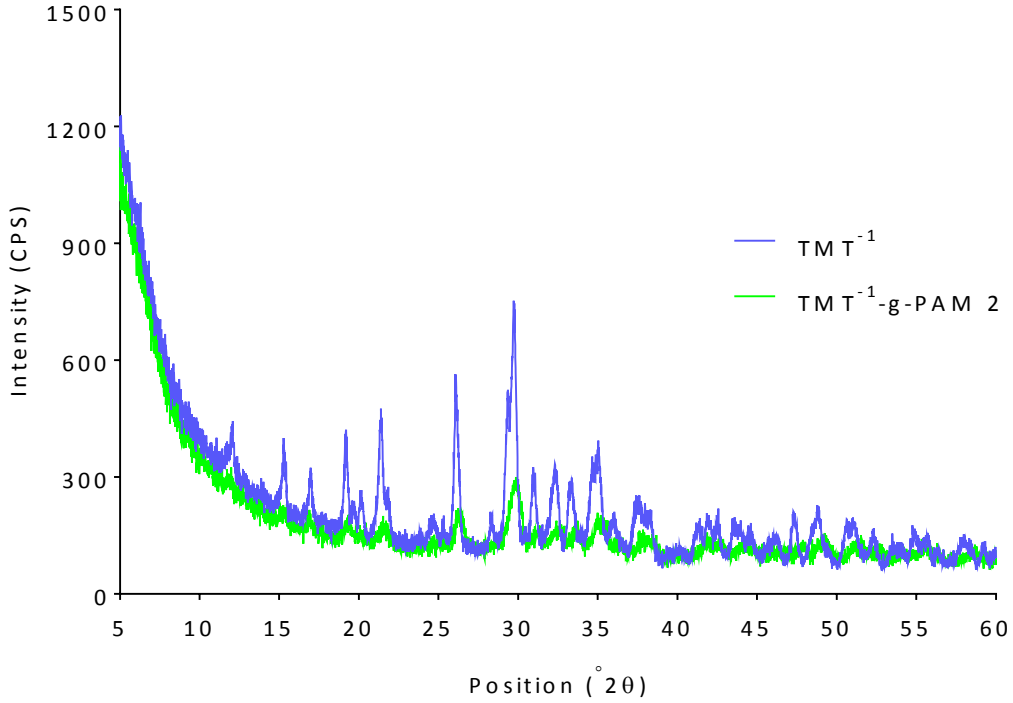

Figure 4.2.6: X-ray diffractograms of TMT^{-1} and TMT^{-1}-g-PAM 2

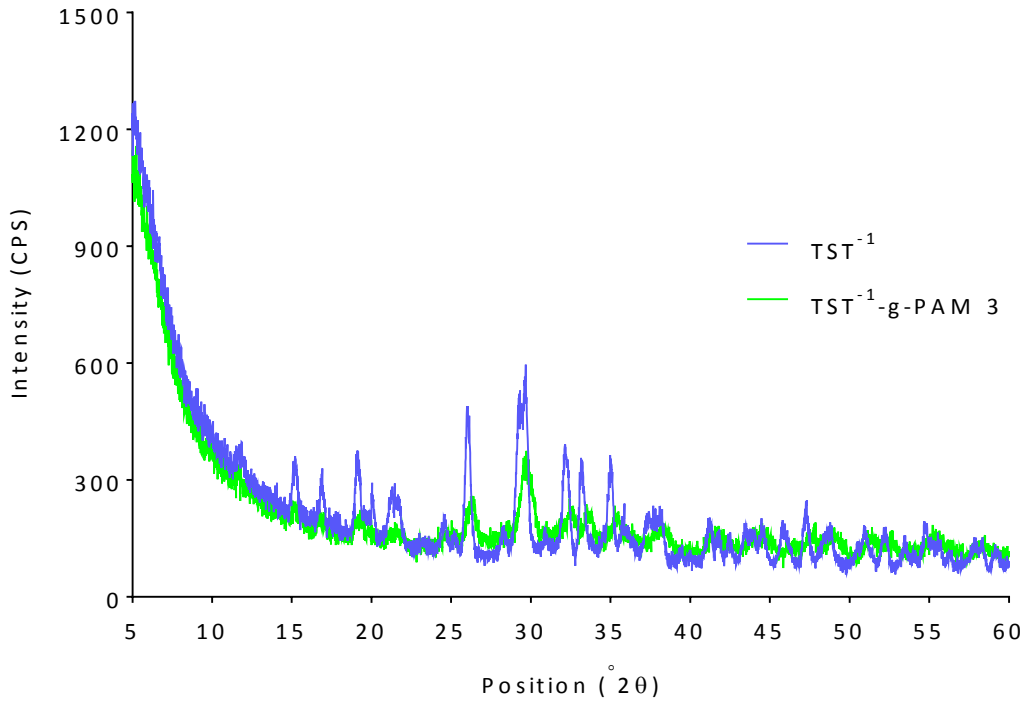

Figure 4.2.7: X-ray diffractograms of TST^{-1} and TST^{-1}-g-PAM 3

4.2.3.6 Thermo-gravimetric analysis

Thermal stabilities of TMT^{-1}, TST^{-1}, TMT^{-1}-g-PAM 2 and TST^{-1}-g-PAM 3 were studied using a thermo-gravimetric analyzer. The results for TMT^{-1} and TMT^{-1}-g-PAM 2 are presented in Figure 4.2.8. TMT^{-1} thermograph displays 3 stages of weight loss. The first stage, in a range of 30–118 °C, shows a weight loss of 3%. The loss of weight is caused by moisture content loss in TMT^{-1}. According to Maliehe *et al*. (2016) the moisture might be resulting from the presence of hydroxyl and carboxyl groups in TMT^{-1}. These groups attract water to the macromolecules. The second stage of weight loss occurs between 118–180 °C indicating thermal decomposition of the main chain of TMT^{-1}. There was a further weight loss of 15% in the third stage (180–792 °C).

TMT^{-1}-g-PAM 2 thermograph also depicts three distinct stages of weight loss (Figure 4.2.8). A weight loss of 6% in the first stage, between 30–106 °C, results from evaporation of water and other solvents from the grafted bioflocculant. A 30% weight loss in the second stage (106–631 °C) is caused by thermal degradation of the main chain of the grafted bioflocculant. In a third and last stage (644–719 °C) there was a 2% weight loss caused by polyacrylamide decomposition.

These TGA results show that TMT^{-1} is slightly more thermally stable than TMT^{-1}-g-PAM 2. This is because the thermal decomposition of the main chain of the former started at a slightly higher temperature (118 °C) than the latter (106 °C). Thus, the findings are in contrast to those observed by Mishra *et al*. (2006). In their study, they discovered that grafting of acrylamide chains to fenugreek mucilage increased its thermal stability.

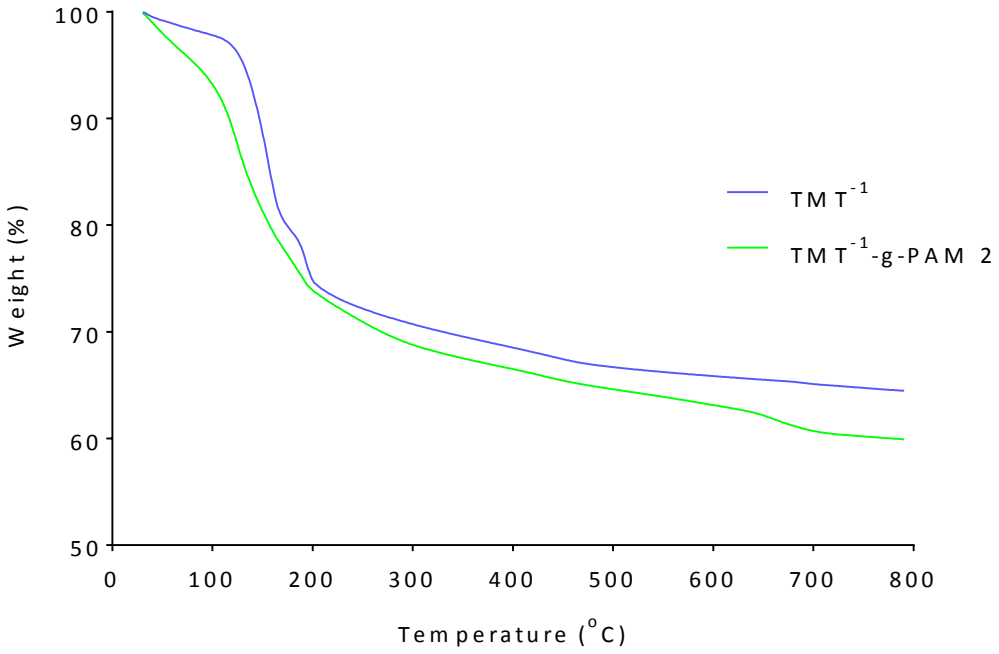

Figure 4.2.8: Thermo-gravimetric analysis of TMT^{-1} and TMT^{-1}-g-PAM 2

Thermo-gravimetric analysis of TST^{-1} and TST^{-1}-g-PAM 3 is shown in Figure 4.2.9. For TST^{-1}, weight loss happens in two stages. The first stage occurs in the range of 50–150 °C in which there was 0.5% weight loss, probably due to loss of bound water. The second stage of weight loss takes place in the range from 150–300 °C, with 29% weight loss caused by the degradation of TST^{-1} structure.

In the case of TST^{-1}-g-PAM 3, there are three stages of weight loss. The first stage, in the range of 50–115 °C, results from the loss of moisture content in the copolymer. The second stage of weight loss, from 115–370 °C, is caused by the degradation of the non-grafted component of TST^{-1}-g-PAM 3. The last stage, between 370–720 °C, is due to the thermal degradation of polyacrylamide chains in TST^{-1}-g-PAM 3.

Thermal decomposition of TST^{-1} started at a higher temperature (150 °C) than that of TST^{-1}-g-PAM 3 (115 °C) (Figure 4.2.9). Therefore, the pure bioflocculant is more thermally stable than the grafted product. These findings are different from those which were obtained by Singh *et al*. (2006), where the chitosan-graft-polyacrylamide was found to be more thermally stable than chitosan.

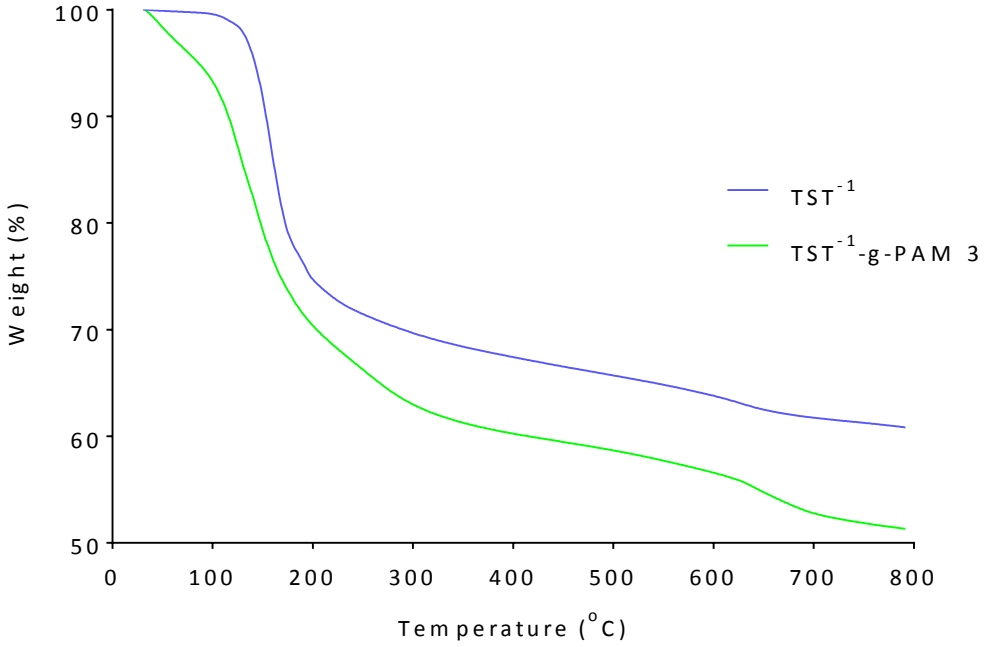

Figure 4.2.9: Thermo-gravimetric analysis of TST^{-1} and TST^{-1}-g-PAM 3

In summary, the polyacrylamide grafted bioflocculants (Figures 4.2.8 and 4.2.9) show the degradation point around 700 °C, typical of the polyacrylamide breakdown. They also reveal a slight reduction in thermal stability caused by a decrease in their crystallinity (verified by Figures 4.2.6 and 4.2.7, p. 40) (Carraher, 2003).

4.2.3.7 Biosafety assay of TMT^{-1}-g-PAM 2 and TST^{-1}-g-PAM 3

The results for the cytotoxicity studies of the polyacrylamide grafted bioflocculants are presented in Figures 4.2.10 and 4.2.11. Figures 4.2.10 and 4.2.11 reveal that HEK 293 cells had 75% and 85% cell viability when exposed to high concentrations (200µg/ml) of TMT^{-1}-g-PAM 2 and TST^{-1}-g-PAM 3, respectively.

According to Lin *et al*. (2005), these cell viability percentages mean that the polyacrylamide grafted bioflocculants have a cytotoxicity index of 1. The conclusion is therefore that these graft copolymers are non-cytotoxic in the tested concentration range. The bioflocculants TMT^{-1} and TST^{-1} were also shown to be non-cytotoxic in HEK 293 cell line, giving a 100% cell survival and therefore a cytotoxic index of 0 in the concentrations 50–200 µg/ml (Maliehe, 2017, 60, 114). These results compare with those obtained by Giri *et al*. (2015). They

depicted the graft copolymer of acrylamide and locust bean gum to be non-toxic in *in-vivo* toxicity study performed in mice.

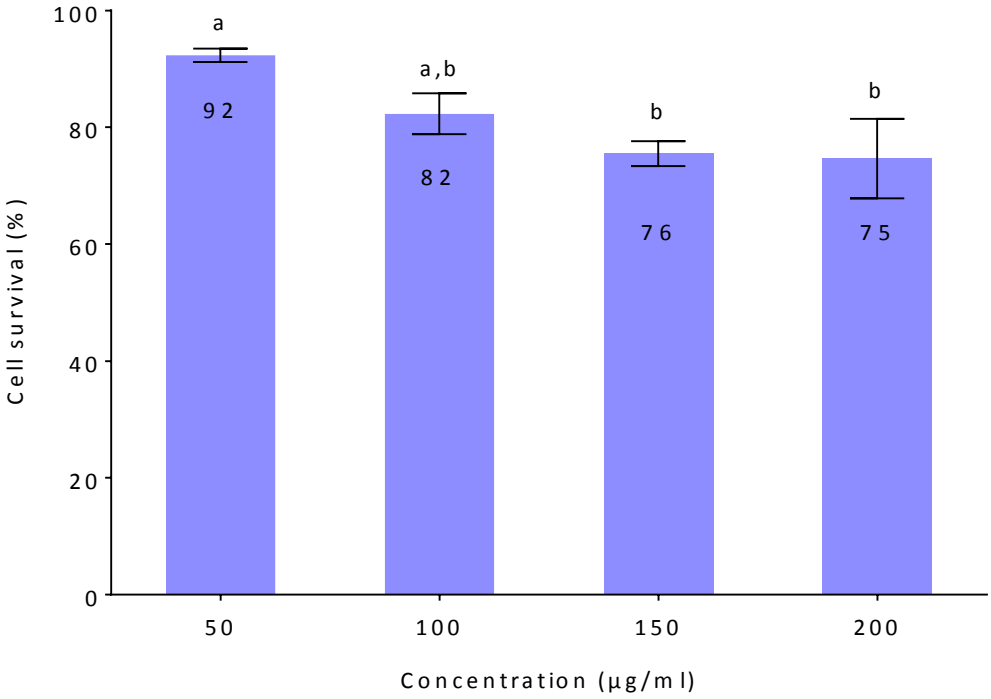

Figure 4.2.10: *In-vitro* cytotoxicity of different concentrations of TMT^{-1}-g-PAM 2 on HEK 293. Values with different letters (a and b) on the graph are significantly ($p < 0.05$) different

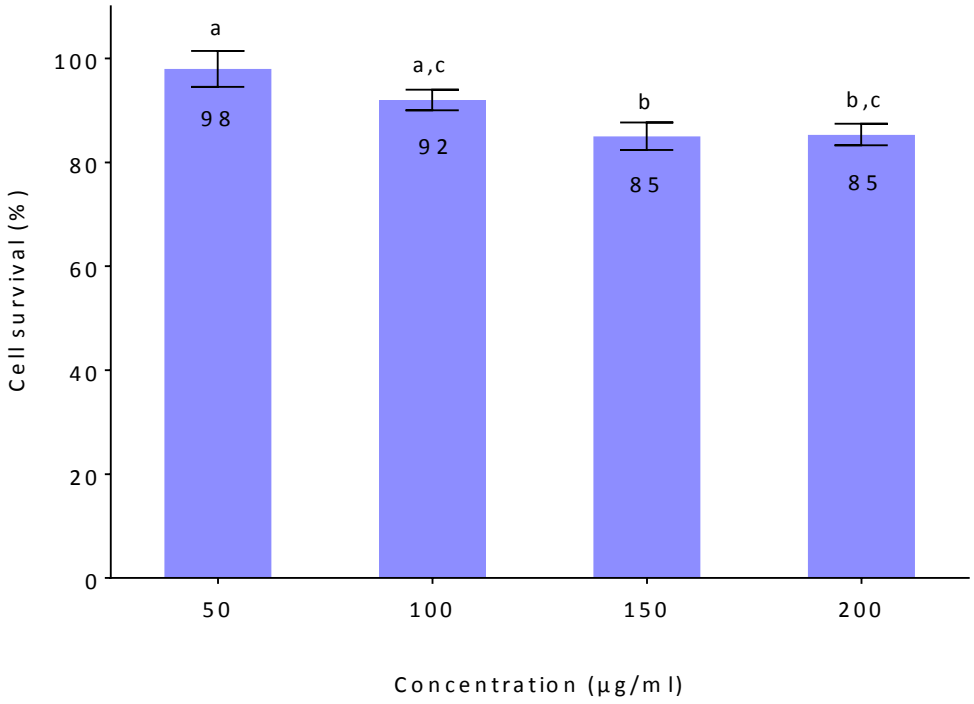

Figure 4.2.11: *In-vitro* cytotoxicity of different concentrations of TST^{-1}-g-PAM 3 on HEK 293. Values with different letters (a, b and c) on the graph are significantly ($p < 0.05$) different

4.2.3.8 Antimicrobial activity of the polyacrylamide grafted bioflocculants (TMT^{-1}-g-PAM 2 and TST^{-1}-g-PAM 3)

The removal of microorganisms during water treatment and purification is important in order to prevent waterborne disease transmission (Willey *et al*., 2011). Flocculation, alone, removes some of the microorganisms (Lin and Harichund, 2012). Thus, water treatment and purification processes usually require the usage of both flocculants and disinfectants (Goncharuk, 2014). However, these agents may inhibit each other, decreasing the remediation efficiency. Therefore, employing a flocculant possessing dual function – flocculation and inhibitory capability – would simplify water treatment process and reduce costs (Liu *et al*., 2017).

Tables 4.2.5 and 4.2.6 show the results of screening antibacterial activities of TMT^{-1}-g-PAM 2 and TST^{-1}-g-PAM 3, respectively. Neither MIC nor MBC was detected for the grafted

bioflocculants. The polyacrylamide grafted bioflocculants did not reveal any antibacterial activity against the tested bacterial strains.

These results differ from those obtained by Huang *et al*. (2016). They found carboxymethyl-starch-graft aminomethylated-polyacrylamide (CMS-g-APAM) to possess a dual function, flocculation and antibacterial activity. The difference in chemical and structural composition between flocculants may account for the observed contrast in results.

Table 4.2.5: Minimum inhibitory concentration of TMT^{-1}-g-PAM 2 on certain bacterial strains

Bacterial strain	TMT^{-1}-g-PAM 2	Ciprofloxacin
	MIC (mg/ml)	MIC (mg/ml)
S. aureus (ATCC 25925)	–	3.13
B. cereus (ATCC 101022)	–	3.13
E. coli (ATCC 25922)	–	3.13
K. *pneumoniae* (ATCC 4352)	–	3.13

MIC (Minimum inhibitory concentration), – = absence

Table 4.2.6: Minimum inhibitory concentration of TST^{-1}-g-PAM 3 on certain bacterial strains

Bacterial strain	TST^{-1}-g-PAM 3	Ciprofloxacin
	MIC (mg/ml)	MIC (mg/ml)
S. aureus (ATCC 25925)	–	3.13
B. cereus (ATCC 101022)	–	3.13
E. coli (ATCC 25922)	–	3.13
K. *pneumoniae* (ATCC 4352)	–	3.13

MIC (Minimum inhibitory concentration), – = absence

4.2.3.9 Biodegradation studies

Biodegradation studies results of polyacrylamide grafted bioflocculants (TMT^{-1}-g-PAM 2 and TST^{-1}-g-PAM 3) and their respective native bioflocculants are presented in Tables 4.2.7 and

4.2.8, correspondingly. The grafted bioflocculants took longer time to be biodegraded than their respective native bioflocculants. It took 4 weeks for 0.5 g of TMT^{-1} to be completely biodegraded (Table 4.2.7); whereas, the graft copolymer TMT^{-1}-g-PAM 2 took 5 weeks. TST^{-1} required only 2 weeks for it to be totally biodegraded. Its graft copolymer (TST^{-1}-g-PAM 3) needed 4 weeks. Thus, the presence of acrylamide chains in the graft copolymers has slightly reduced their biodegradability.

A decrease in biodegradability occurs because graft copolymerization leads to changes in structure of the biopolymers, thus reducing their suitability as substrates for enzymatic degradation (Singh *et al*., 2000). This means an increased shelf life for the graft copolymers (Lee *et al*., 2014). Therefore, they can remain functional and efficient longer than their native bioflocculants.

These results agree with those obtained by some researchers. For instance, the polyacrylamide grafted amylopectin (AP-g-PAM) showed a slower enzymatic degradation rate than amylopectin (Kayla and Tripathy, 2014).

Table 4.2.7: Biodegradation studies of TMT^{-1}-g-PAM 2 in soil

Sample	Initial weight (g)	Weight of sample remaining per week (g) ± SD				
		1	2	3	4	5
TMT^{-1}	0.5 ± 0.01^{a}	0.5 ± 0.01^{a}	0.2 ± 0.01^{a}	0.1 ± 0.04^{a}	0.0 ± 0.00^{a}	0.0 ± 0.00^{a}
TMT^{-1}-g-PAM 2	0.5 ± 0.00^{a}	0.5 ± 0.00^{a}	0.4 ± 0.03^{b}	0.3 ± 0.01^{b}	0.1 ± 0.00^{b}	0.0 ± 0.01^{a}
Control (soil)	0.5 ± 0.00^{a}	0.5 ± 0.00^{a}	0.5 ± 0.00^{c}	0.5 ± 0.01^{c}	0.5 ± 0.01^{c}	0.5 ± 0.00^{b}

Values with different letters (a, b and c) on the same column are significantly ($p < 0.05$) different

Table 4.2.8: Biodegradation studies of TST^{-1}-g-PAM 3 in soil

Sample	Initial weight (g)	Weight of sample remaining per week (g) ± SD		
		1	2	3
TST^{-1}	0.5±0.00[a]	0.4±0.01[a]	0.0±0.00[a]	0.0±0.00[a]
TST^{-1}-g-PAM 3	0.5±0.00[a]	0.4±0.02[a]	0.1±0.02[b]	0.0±0.00[a]
Control (soil)	0.5±0.01[a]	0.5±0.00[b]	0.5±0.00[c]	0.5±0.01[b]

Values with different letters (a, b and c) on the same column are significantly ($p < 0.05$) different

4.2.4 Flocculation properties

4.2.4.1 Effect of dosage size on flocculating activity

There is an optimal dosage size at which flocculation activity is maximal. Beyond this dosage size, flocculation activity declines as a result of excess polymers which destabilise the flocs. On the other hand, below the optimal dosage size, there is no significant bridging that occurs between colloids and polymeric flocculants (Prieto *et al*., 2012).

Figures 4.2.12 and 4.2.13 illustrate the comparative studies of the influence of dosage size on the flocculating activities of the grafted bioflocculants, pure bioflocculants and some conventional flocculants (PAM and $FeCl_3$). The optimum dosage sizes for TMT^{-1}-g-PAM 2 and TST-1-g-PAM 3 were 0.2 mg/ml and 0.1 mg/ml, respectively. These dosage sizes were chosen because even though they were low, they gave high flocculating activities (81% for 0.2 mg/ml and 82% for 0.1 mg/ml) that were comparable with those of higher dosage sizes. The use of relatively lower dosage sizes aids in lowering wastewater treatment costs (Zulkeflee *et al*., 2012). These results were analogous to those of Mishra *et al*. (2011) whereby polyacrylamide grafted agar (Ag-g-PAM2) performed well at low dosage size.

When compared to their respective pure bioflocculants (TMT^{-1} and TST^{-1}), the graft copolymers maintained a relatively higher flocculating activity throughout the dosage size range of 0.1–2 mg/ml (Figures 4.2.12 and 4.2.13). These results can be explained by the easy approachability model that was proposed by Singh *et al*. (2000). The authors proposed

that the branched nature of the graft copolymers enables them to better interact with colloids in water, thus, leading to improved flocculation characteristics in graft copolymers.

In addition to the Singh *et al*. (2000) easy approachability hypothesis, the other contributing factor to the improved flocculation performance of the grafted bioflocculants may be the increased contents of the functional groups in the grafted bioflocculants. According to Tang *et al*. (2014), high contents of functional groups in a biopolymer are associated with high flocculation capability, since functional groups help a biopolymer to perform the flocculation process. The increase in the contents of functional groups is verified, in Figures 4.2.4 and 4.2.5 (pp. 38–39), by two factors. The first factor is the appearance of new and additional functional groups in the grafted bioflocculants. The second factor is the relatively higher absorption peaks intensities and wavenumbers in the FTIR spectra of the grafted bioflocculants than those of their respective pure bioflocculants.

The flocculation efficiency of TMT^{-1}-g-PAM 2 and TST^{-1}-g-PAM 3 is further improved by their higher intrinsic viscosities compared to their respective pure bioflocculants (Tables 4.2.1 and 4.2.2, pp. 33–34). The higher the intrinsic viscosity, the higher will be the hydrodynamic volume; thus, leading to higher flocculation efficiency (Brostow *et al*., 2007). In a study by Sinha *et al*. (2013), they found the graft copolymer (polyacrylamide grafted casein) to have higher flocculation efficiency than the natural biopolymer (casein).

When paralleled with some of the conventional flocculants ($FeCl_3$ and PAM), TMT^{-1}-g-PAM 2 and TST^{-1}-g-PAM 3 displayed better flocculation efficiency than $FeCl_3$. As can be seen in Figures 4.2.12 and 4.2.13, the graft copolymers required low dosage sizes (0.2 mg/ml for TMT^{-1}-g-PAM 2 and 0.1 mg/ml for TST^{-1}-g-PAM 3) to achieve their optimum flocculating activities. In contrast, $FeCl_3$ required a higher dosage size (0.8 mg/ml) in order to reach a flocculating activity that is comparable to those of TMT^{-1}-g-PAM 2 and TST^{-1}-g-PAM 3. The graft copolymers were less efficient than polyacrylamide, which achieved a flocculating activity of 96% at a low dosage size of 0.1 mg/ml (Figures 4.2.12 and 4.2.13). These findings differ from those of Liu *et al*. (2014). The authors found that polyacrylamide grafted bamboo pulp cellulose (BPC-g-PAM) was slightly more efficient in turbidity removal of kaolin suspension than the commercial flocculant, polyacrylamide.

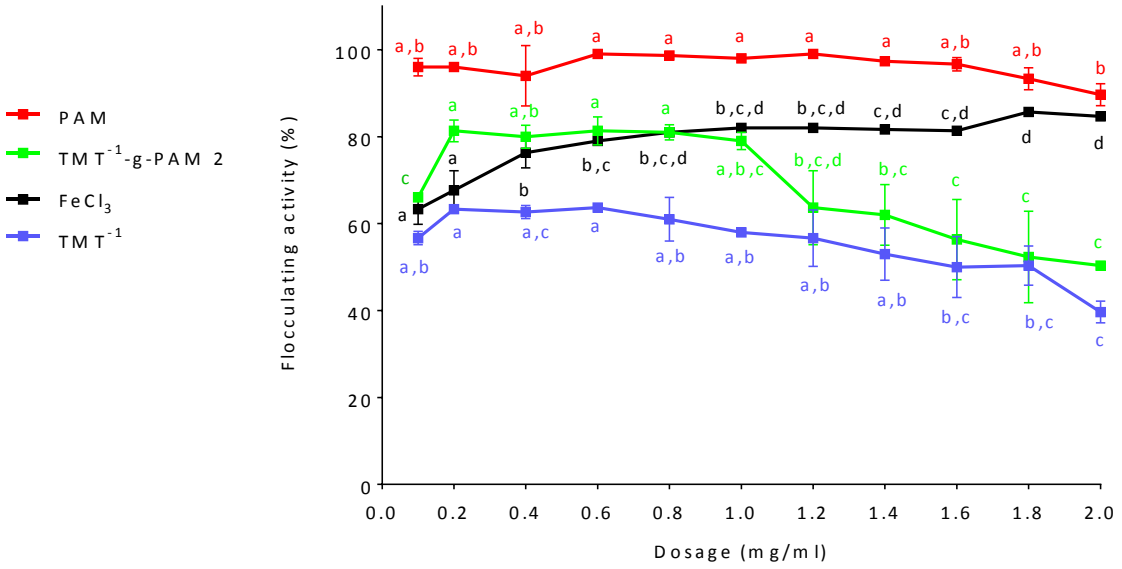

Figure 4.2.12: A comparative study of the effect of dosage size (mg/ml) on TMT^{-1}-g-PAM 2 and other flocculants' flocculating activities. Values with different letters (a, b, c and d) on the same graph are significantly ($p < 0.05$) different

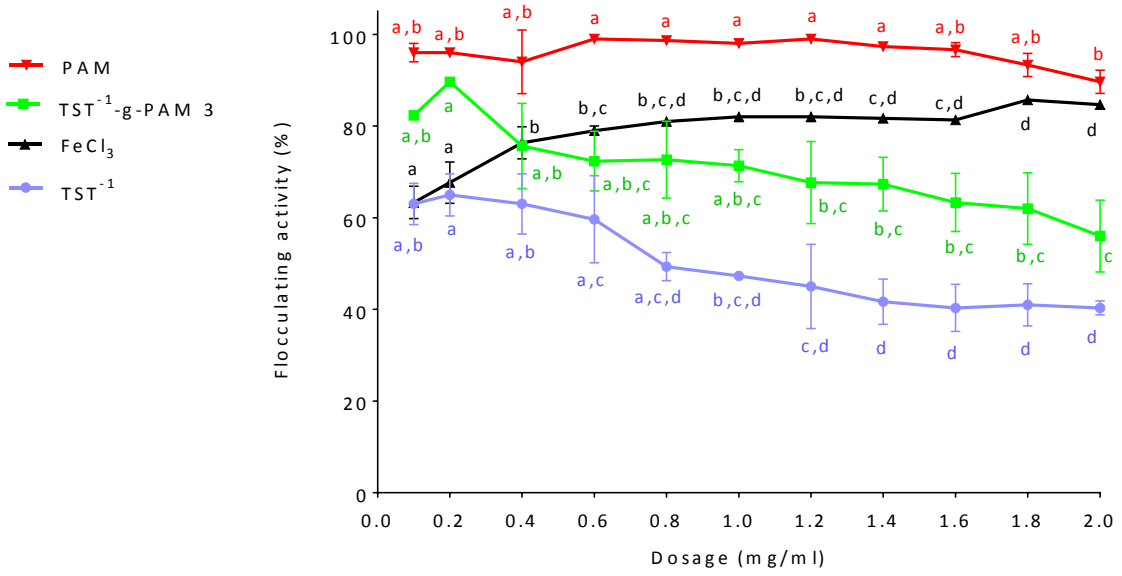

Figure 4.2.13: A comparative study of the effect of dosage size (mg/ml) on TST^{-1}-g-PAM 3 and other flocculants' flocculating activities. Values with different letters (a, b, c and d) on the same graph are significantly ($p < 0.05$) different

4.2.4.2 Effect of cations on flocculating activity

The cations are used to enhance flocculation activity by neutralizing the negatively charged functional groups of the polymeric flocculants and colloidal particles; thereby increasing the adsorption of flocculants to the colloidal particles (He *et al*., 2010). The synergistic effect of different metal cations on flocculation by TMT^{-1}-g-PAM 2 and TST^{-1}-g-PAM 3 is shown in Figures 4.2.14 and 4.2.15, respectively. Generally, all the cations promoted flocculation by TMT^{-1}-g-PAM 2, without any statistically significant differences between flocculating activities (Figure 4.2.14). Nevertheless, Ca^{2+} was the most preferred metal cation. It effectively neutralized the negatively charged functional groups of TMT^{-1}-g-PAM 2 and kaolin clay particles thereby increasing the adsorption of the flocculant to the kaolin particles yielding 87% of flocculating activity. This was significantly higher than the 60% flocculating activity obtained when cations were not used (negative control) (Figure 4.2.14).

For TST^{-1}-g-PAM 3, the cation $BaCl_2$ improved flocculation, with 90% flocculating activity (Figure 4.2.15). However, this was not significantly higher than the flocculating activity of the negative control with a flocculating activity of 75%. Therefore, this graft copolymer can be used without the use of cations, which provide a costs saving in wastewater treatment.

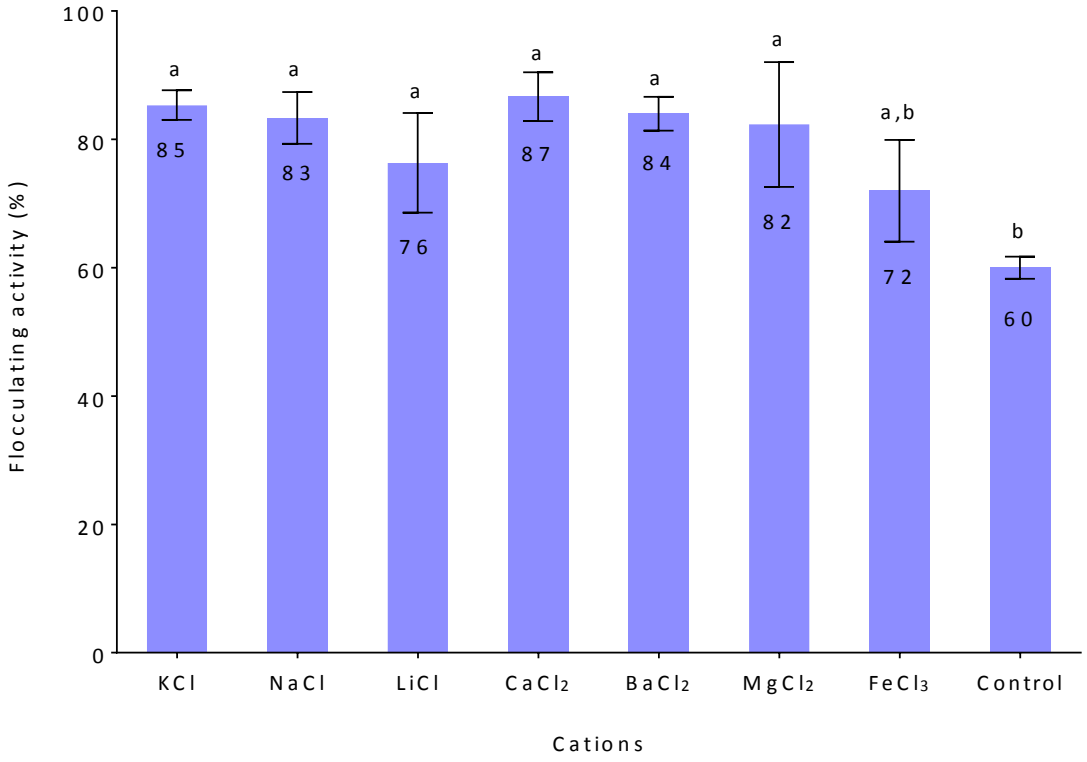

Figure 4.2.14: Influence of cations on flocculating activity of TMT^{-1}-g-PAM 2. Values with different letters (a and b) on the graph are significantly ($p < 0.05$) different

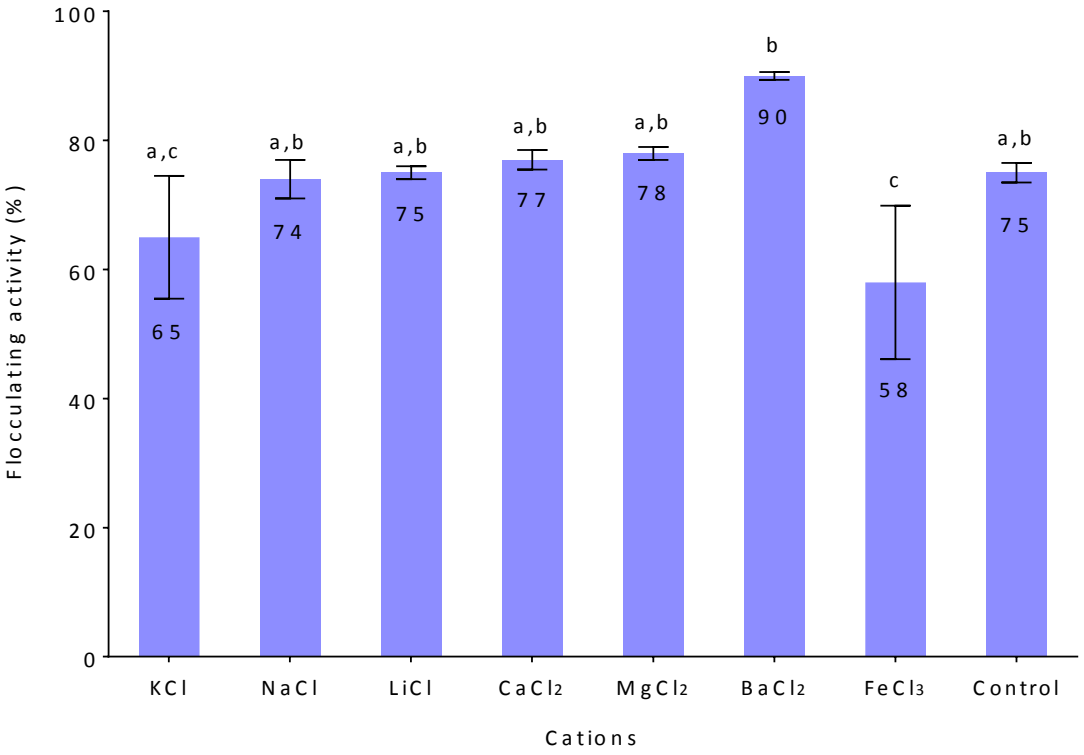

Figure 4.2.15: Effect of cations on flocculating activity of TST^{-1}-g-PAM 3. Values with different letters (a, b and c) on the graph are significantly ($p < 0.05$) different

The flocculating activities of the grafted bioflocculants (without cations) were compared to those of their respective pure bioflocculants and to that of a commercial flocculant PAM (Figures 4.2.16 and 4.2.17). The polyacrylamide grafted bioflocculants showed significantly higher flocculation efficiency than pure bioflocculants. This is due to the integration of polyacrylamide chains in their structures. But their flocculating activities were still significantly lower than that of PAM.

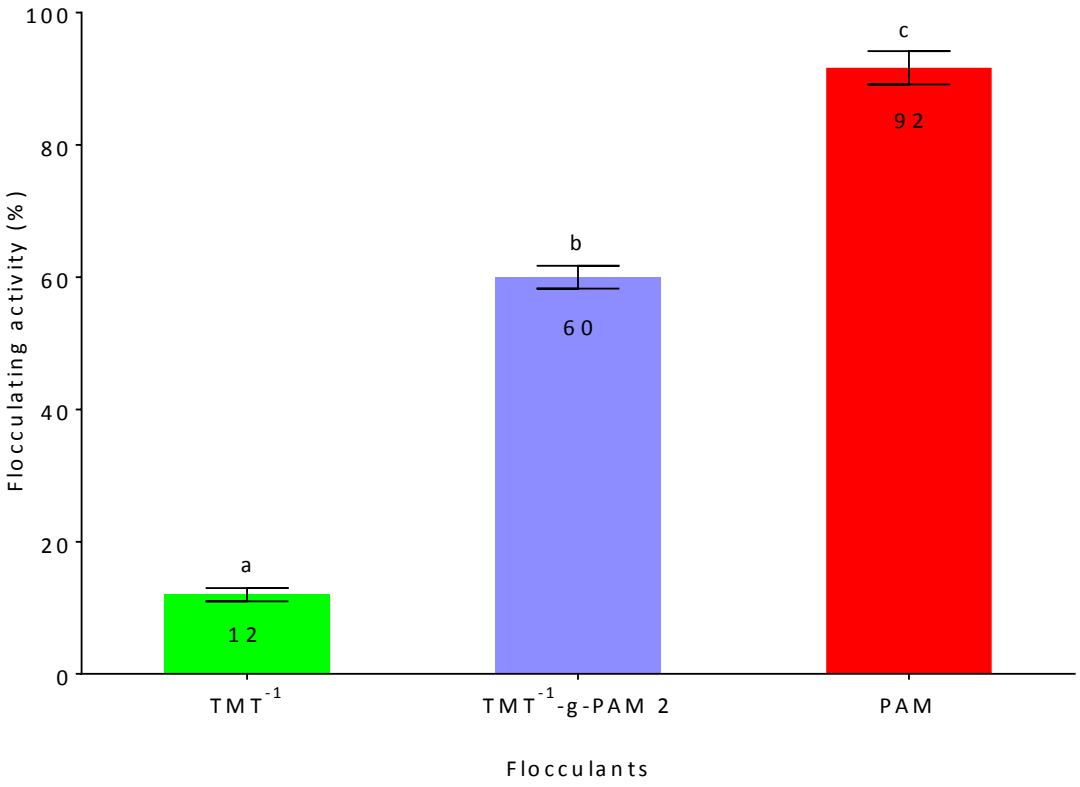

Figure 4.2.16: Flocculating activity of TMT^{-1}-g-PAM 2 in the absence of cations. Values with different letters (a, b and c) on the graph are significantly ($p < 0.05$) different

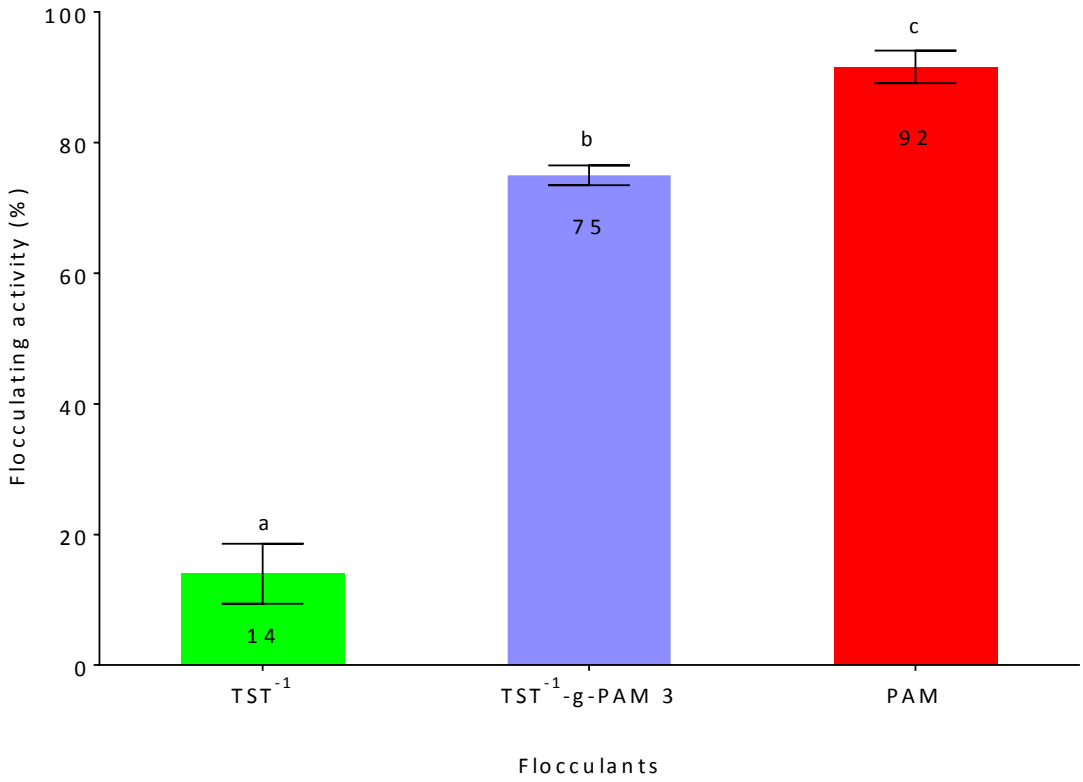

Figure 4.2.17: Flocculating activity of TST^{-1}-g-PAM 3 in the absence of cations. Values with different letters (a, b and c) on the graph are significantly ($p < 0.05$) different

4.2.4.3 Influence of pH on flocculating activity

The pH of aqueous mixtures is one of the main features that have an influence on the flocculating activities of flocculants. It may change the electric state of a flocculant and therefore affect its flocculation efficiency (Okaiyeto *et al*., 2016). Figures 4.2.18 and 4.2.19 respectively exhibit the influence of pH on the flocculating activities of TMT^{-1}-g-PAM 2 and TST^{-1}-g-PAM 3; compared to flocculants TMT^{-1}, TST^{-1}, $FeCl_3$ and PAM.

Both TMT^{-1}-g-PAM 2 and TST^{-1}-g-PAM 3 were stable in a wide range of pH (3–11), giving flocculating activities above 75%. For the flocculant TMT^{-1}-g-PAM 2, the maximal flocculating activity of 91% was obtained at an acidic pH of 3 and the lowest flocculating activity of 76% was obtained at a pH of 9. The slight decrease in flocculating activities in alkaline conditions might be due to the fact that hydroxide ions (OH^-) may have interfered with the bond formation between TMT^{-1}-g-PAM 2 and kaolin particles (Lin and Harichund, 2012).

In the case of TST^{-1}-g-PAM 3, changes in pH did not result in any statistically significant change in flocculating activity. The highest flocculating activity (90%) was attained at pH 9 (Figure 4.2.19). The ability of TMT^{-1}-g-PAM 2 and TST^{-1}-g-PAM 3 to flocculate colloidal particles within a wide range of pH implies a wide potential usage in different biotechnological fields (pH of the medium treated would not have to be adjusted with costly chemicals). Similarly, a graft copolymer named carboxymethyl chitosan-graft-polyacrylamide (CMC-g-PAM) was able to flocculate water under acidic, neutral and basic pH conditions (Yang *et al*., 2013).

It can also be seen in Figures 4.2.18 and 4.2.19 that the polyacrylamide grafted bioflocculants performed better than the pure bioflocculants (TMT^{-1} and TST^{-1}) and the commercial flocculant $FeCl_3$. Each grafted bioflocculant efficiently flocculated kaolin clay solution over a wide pH range of 3 to 11; TMT^{-1}, TST^{-1} and $FeCl_3$ were only able to flocculate the synthetic wastewater at certain pH conditions. $FeCl_3$ only efficiently flocculated kaolin clay solution under acidic, neutral and weakly basic pH (i.e. pH < or = 9). The high OH^- concentration at strongly basic conditions may have interrupted colloids' surface charge neutralization by $FeCl_3$, thus decreasing its flocculating activity.

TMT^{-1} and TST^{-1} only managed to effectively flocculate water at strongly acidic and strongly basic pH environments. The reason for this may be that the functional groups of the native bioflocculants – which attach colloidal particles during the flocculation process – only totally ionize at strongly acidic and basic aqueous pH states (Yong *et al*., 2009).

It is also worth noting that flocculation properties of TMT^{-1}-g-PAM 2 and TST^{-1}-g-PAM 3 closely resemble those of PAM (Figures 4.2.18 and 4.2.19). Since graft copolymerization transfers some of the good attributes of the synthetic polymers onto the natural biopolymer (Lee *et al*., 2014). It may be concluded that the good flocculation efficiency of the polyacrylamide grafted bioflocculants (observed in Figures 4.2.18 and 4.2.19) is due to the incorporation of PAM chains in their chemical structures.

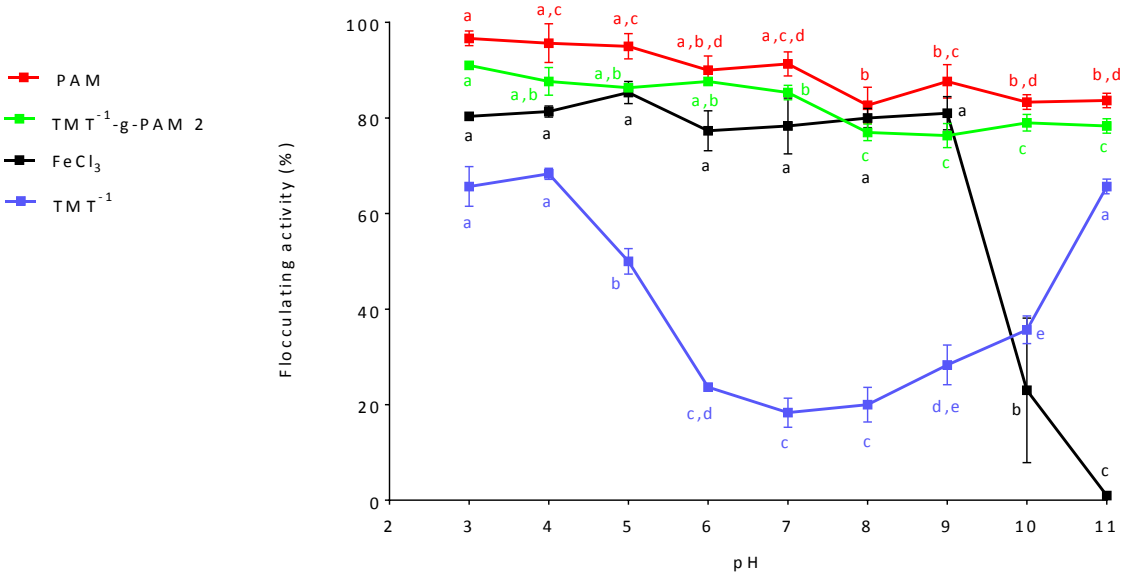

Figure 4.2.18: Comparative analysis of the influence of pH on flocculating activity of TMT^{-1}-g- PAM 2 and other flocculants. Values with different letters (a, b, c, d and e) on the same graph are significantly ($p < 0.05$) different

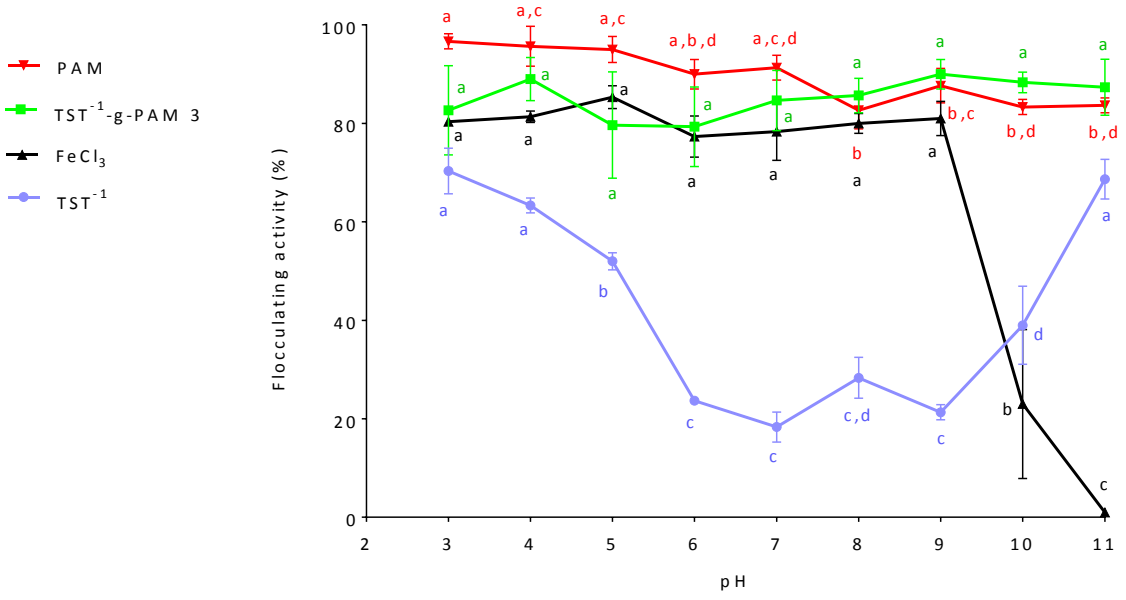

Figure 4.2.19: Comparative analysis of the influence of pH on flocculating activity of TST^{-1}-g- PAM 3 and other flocculants. Values with different letters (a, b, c and d) on the same graph are significantly ($p < 0.05$) different

4.2.4.4 Effect of temperature on flocculating activity

Figures 4.2.20 and 4.2.21 correspondingly depict the effect of temperature on flocculating activities of polyacrylamide grafted bioflocculants (TMT^{-1}-g-PAM 2 and TST^{-1}-g-PAM 3). It was observed that for each polyacrylamide grafted bioflocculant, increase in temperature (in the range of 50–100 °C) did not result in any statistically significant change in flocculating activity. Both of the grafted bioflocculants still maintained high flocculating activities (81%) even after 60 min. of heating at 100 °C**.** Meanwhile, at the aforesaid temperature, the natural bioflocculants retained relatively lower flocculating activities compared to their respective graft copolymers (74% for TMT^{-1} and 64% for TST^{-1}).

The resistance to high temperatures in the graft copolymers is probably caused by the incorporation of PAM chains on their chemical structure during graft copolymerization. This is supported by the observation in Figures 4.2.20 and 4.2.21 that PAM has excellent tolerance at high temperatures, giving a flocculating activity of 94% at 100 °C.

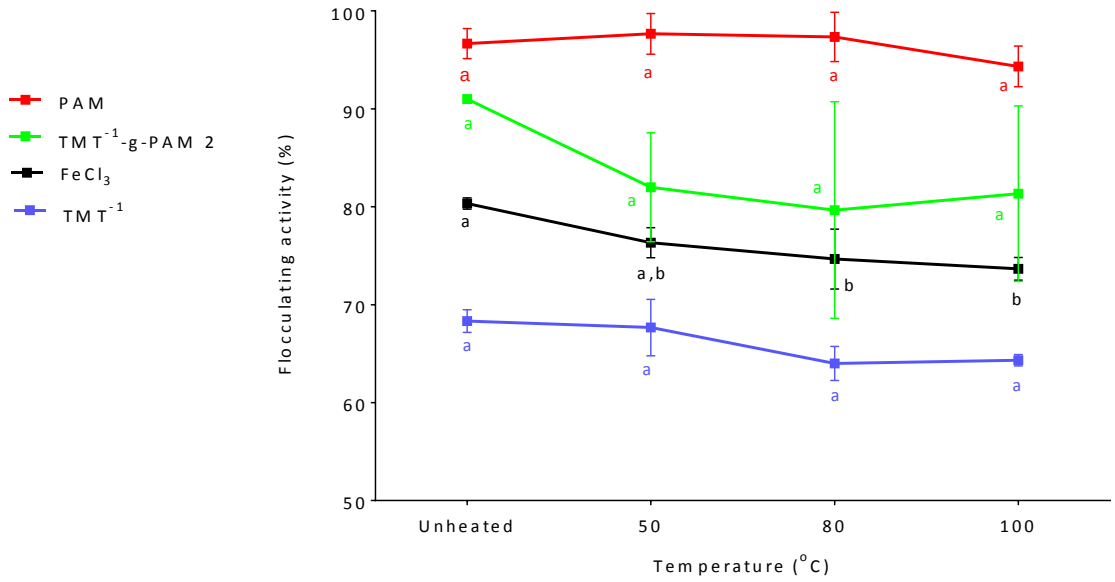

Figure 4.2.20: Influence of temperature on the flocculating activity of TMT^{-1}-g-PAM 2 and comparison to other flocculants. Values with different letters (a and b) on the same graph are significantly ($p < 0.05$) different

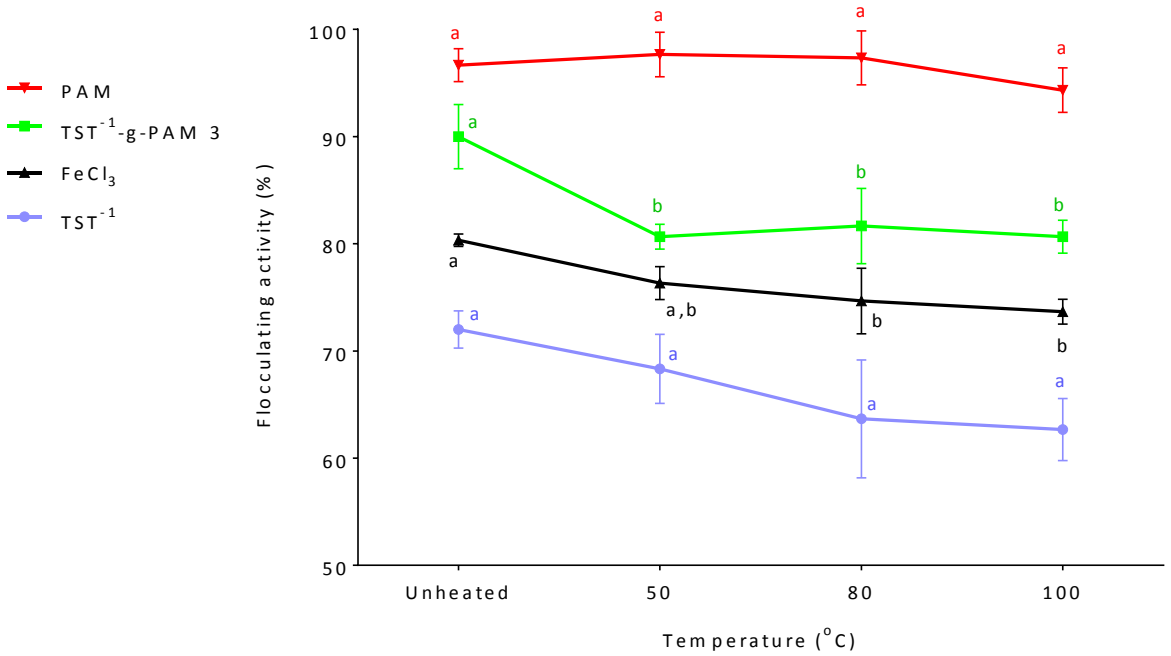

Figure 4.2.21: Influence of temperature on the flocculating activity of TST^{-1}-g-PAM 3 and comparison to other flocculants. Values with different letters (a and b) on the same graph are significantly ($p < 0.05$) different

4.2.4.5 Effect of salinity on flocculating activity

According to Dlamini (2017, 48), high salinity concentrations tend to denature bioflocculants, thus, decreasing their flocculation efficiency. Figures 4.2.22 and 4.2.23 portray the influence of sodium chloride concentration on flocculation by TMT^{-1}-g-PAM 2 and TST^{-1}-g-PAM 3, respectively. There was a proportionate decrease in flocculating activity as NaCl concentration increased. Nevertheless, the polyacrylamide grafted bioflocculants still maintained relatively high flocculating activities (63% for TMT^{-1}-g-PAM 2 and 64% for TST^{-1}-g-PAM 3) at a high salinity (35 g/l).

The results are in contrast to those of the pure bioflocculants (TMT^{-1} and TST^{-1}) and the conventional flocculant $FeCl_3$ which had poor flocculating activities for saline conditions (Figures 4.2.22 and 4.2.23). Therefore, the relatively good flocculation efficiency of the polyacrylamide grafted bioflocculants may be attributed to the presence of the polyacrylamide chains in the grafted product. This conclusion is reinforced by noting that

PAM showed saline stability, giving a flocculating activity of 91% at a high salinity (35 g/l) (Figures 4.2.22 and 4.2.23).

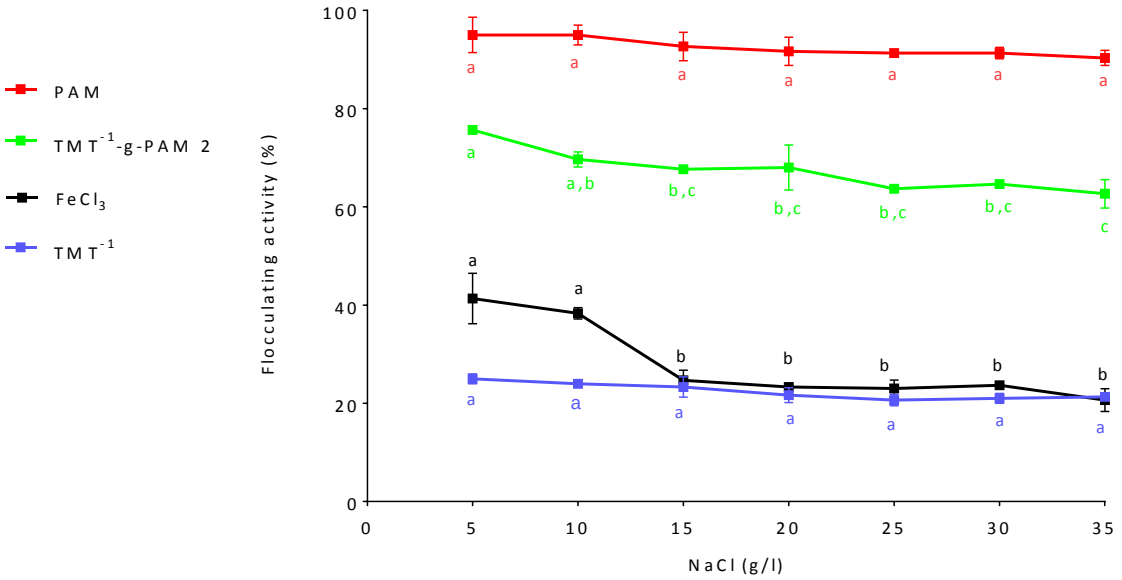

Figure 4.2.22: Effect of salinity on flocculation by TMT^{-1}-g-PAM 2 and comparison to other flocculants (TMT^{-1}, $FeCl_3$ and PAM). Values with different letters (a, b and c) on the same graph are significantly ($p < 0.05$) different

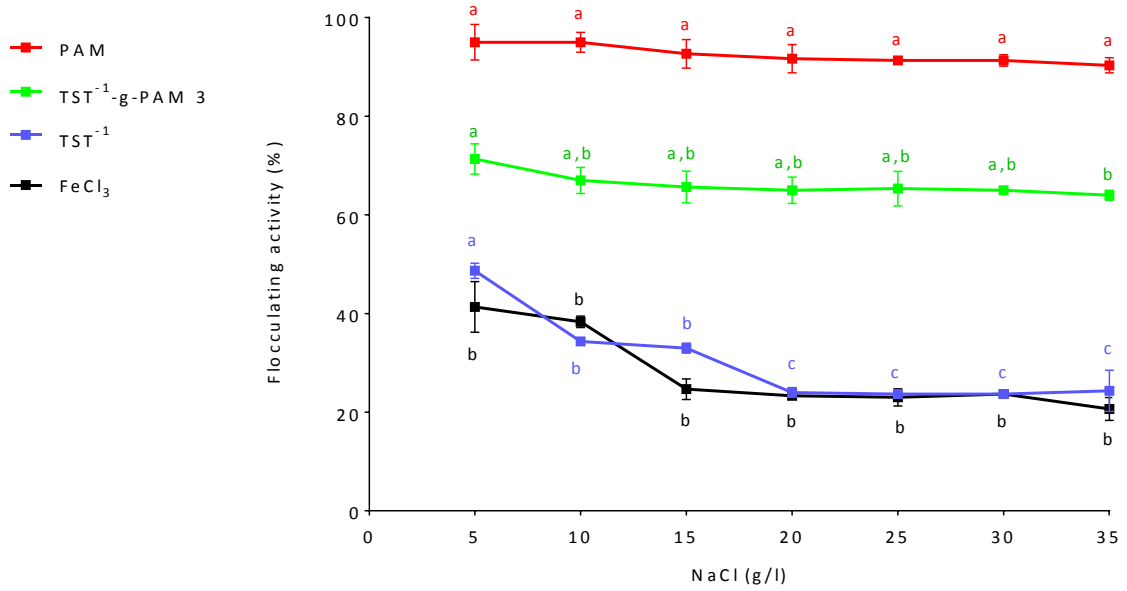

Figure 4.2.23: Effect of salinity on flocculation by TST^{-1}-g-PAM 3 and comparison to other flocculants (TST^{-1}, $FeCl_3$ and PAM). Values with different letters (a, b and c) on the same graph are significantly ($p < 0.05$) different

4.2.4.6 Proposed flocculation mechanisms of TMT^{-1}-g-PAM 2 and TST^{-1}-g-PAM 3

Grafted bioflocculants cause flocculation of particles mostly by two mechanisms namely: charge neutralization and bridging. Charge neutralization occurs when the particle and flocculants are charged oppositely (Wang *et al*., 2011). The bridging mechanism occurs when segments of the flocculant's functional groups are absorbed onto the colloids, thus binding the colloidal particles together (Hendricks, 2006).

The zeta potentials of the grafted bioflocculants (TMT^{-1}-g-PAM 2 and TST^{-1}-g-PAM 3), kaolin suspension, kaolin suspension with cations and kaolin suspension flocculated by the grafted bioflocculants in the presence of cations were all negative (Tables 4.2.9 and 4.2.10). Addition of cations into kaolin clay suspension containing the respective grafted bioflocculants (Ca^{2+} for TMT^{-1}-g-PAM 2 and Ba^{2+} for TST^{-1}-g-PAM 3) resulted in reduction of zeta potentials (Tables 4.2.9 and 4.2.10).

When the negative charge is reduced or totally abolished, the repulsion force becomes terminated and particles easily agglomerate (Freese *et al*., 2004). Thus, Ca^{2+} and Ba^{2+}

increased the adsorption of the respective grafted bioflocculants on the surface of colloidal kaolin particles by decreasing the negative charge on the grafted bioflocculants and kaolin particles. This permits the grafted bioflocculants and kaolin particles in suspension to draw nearer to each other and chemically bind. Ca^{2+} and Ba^{2+} compressed the double layer of colloidal kaolin particles, weakened the static repulsive force and enhanced the grafted bioflocculants to form aggregates with colloidal kaolin particles in suspension.

The presence of hydroxyl and carboxyl groups in the grafted bioflocculants suggests that the chemical interactions might have included the formation of the ionic and hydrogen bonds. The flocculation process for both grafted bioflocculants could be as a result of double layer compression by the cations, chemical reactions and bridging mechanisms.

Table 4.2.9: Zeta potential of samples

Samples	Zeta potential (mV)
TMT^{-1}-g-PAM 2	-13.6±5.90
Kaolin particles	-6.59±3.00
Kaolin particles with Ca^{2+}	-7.01±0.99
Kaolin particles flocculated by TMT^{-1}-g-PAM 2 in the presence of Ca^{2+}	-11.9±7.35

Table 4.2.10: Zeta potential of samples

Samples	Zeta potential (mV)
TST^{-1}-g-PAM 3	-13.2±5.95
Kaolin particles	-6.59±3.00
Kaolin particles with Ba^{2+}	-7.01±0.99
Kaolin particles flocculated by TST-g-PAM 3 in the presence of Ba^{2+}	-5.46±5.05

4.2.5 Application of the grafted bioflocculants in domestic and industrial wastewater treatment

Water that is highly concentrated with COD and BOD results in over-growth of chemo-organotrophs (Willey *et al*., 2011). These microbes use the available oxygen. This then causes the formation of anoxic zones in water which lead to the death of most macroscopic organisms in water. Anoxic zones may also result from high levels of N, S and P; because high concentration of such parameters in water may generate eutrophication (Willey *et al*., 2011). Therefore, the removal of water pollutants is very important.

4.2.5.1 Removal of pollutants in domestic wastewater

Tables 4.2.11 and 4.2.12 respectively display efficiencies of TMT^{-1}-g-PAM 2 and TST^{-1}-g-PAM 3 in removing BOD, COD, N, P and suspended particles (or turbidity) in wastewater obtained from Vulindlela Domestic Wastewater Treatment Works, KwaDlangezwa, RSA. The efficiencies of TMT^{-1}-g-PAM 2 and TST^{-1}-g-PAM 3 were then compared to those of the natural bioflocculants (TMT^{-1} and TST^{-1}) and commercial flocculants (polyacrylamide and ferric chloride). The grafted bioflocculants had significantly higher removal efficiencies of COD and turbidity than both their respective natural bioflocculants and the commercial flocculants.

These findings share some similarities with those obtained by Pal *et al*. (2012). They found that the polyacrylamide grafted tamarind kernel polysaccharide (TKP-g-PAM) had higher COD and turbidity removal rates than its original biopolymer (tamarind kernel polysaccharide, TKP) and the commercial flocculant (Rishfloc 226 LV).

Furthermore, the grafted bioflocculants had slightly higher removal rates of BOD, N and P than the natural bioflocculants (Tables 4.2.11 and 4.2.12). In addition, TMT^{-1}-g-PAM 2 had a significantly higher removal rate of the said parameters than $FeCl_3$; whereas TST^{-1}-g-PAM 3 showed higher efficiency than $FeCl_3$ in removing BOD and N (but not P) from the wastewater. Both the grafted bioflocculants had significantly lower removal efficiency of BOD, N and P than that of the commercial flocculant polyacrylamide (Tables 4.2.11 and 4.2.12).

Table 4.2.11: Removal efficiency (RE) and flocculating activity (FA) of TMT^{-1}-g-PAM 2 in domestic wastewater

Flocculant	RE(%) ± SD				FA(%) ± SD
	COD	BOD	N	P	
TMT^{-1}	97±0.6[a]	53±0.6[a]	53±0.6[a]	54±2.1[a]	74±1.2[a]
TMT^{-1}-g-PAM 2	**98±2.3[b]**	**54±2.0[a]**	**53±0.7[a]**	**57±19.5[a]**	**90±3.1[b]**
$FeCl_3$	97±1.0[a]	53±1.0[a]	43±1.0[b]	39±1.9[b]	67±3.1[c]
Polyacrylamide	97±0.2[a]	88±0.2[b]	100±0.1[c]	100±0.0[c]	3±1.8[d]

Values with different letters (a, b, c and d) on the same column are significantly ($p < 0.05$) different

Table 4.2.12: Removal efficiency (RE) and flocculating activity (FA) of TST^{-1}-g-PAM 3 in domestic wastewater

Flocculant	RE(%) ± SD				FA(%) ± SD
	COD	BOD	N	P	
TST^{-1}	97±0.1[a]	55±0.6[a]	31±1.0[a]	4±0.2[a]	100±0.0[a]
TST^{-1}-g-PAM 3	**98±1.2[b]**	**73±1.1[b]**	**74±0.3[b]**	**17±0.4[b]**	**100±0.0[a]**
$FeCl_3$	97±1.0[a]	53±1.0[a]	43±1.0[c]	39±1.9[c]	67±3.1[b]
Polyacrylamide	97±4.0[a]	88±0.2[c]	100±0.1[d]	100±0.0[d]	3±1.8[c]

Values with different letters (a, b, c and d) on the same column are significantly ($p < 0.05$) different

4.2.5.2 Removal of pollutants in coal mine wastewater

Tables 4.2.13 and 4.2.14 correspondingly exhibit efficiencies of TMT^{-1}-PAM 2 and TST^{-1}-g-PAM 3 in removing COD, BOD, N, S and suspended particles in wastewater collected from Tendele Coal Mine, Mtubatuba, RSA. The effectiveness of the polyacrylamide grafted bioflocculants was then compared with that of the natural bioflocculants and the commercial flocculants.

The grafted bioflocculants showed good removal efficiencies of the tested parameters. For instance, TMT^{-1}-PAM 2 revealed a significantly higher effectiveness in removing BOD, N and suspended particles compared to flocculants TMT^{-1} and $FeCl_3$ (Table 4.2.13).

However, with the exception of BOD, its removal efficiency of the aforementioned parameters was still significantly lower than the removal efficiency by the polyacrylamide flocculant. COD removal by TMT^{-1}-PAM 2 was comparable to that displayed by all the investigated flocculants (Table 4.2.13).

On the other hand, TST^{-1}-PAM 3 was also highly effective in removing the examined parameters (Table 4.2.14). This flocculant's COD, N, S and suspended particles removal was similar to that by TST^{-1}. The removal efficiency of BOD was significantly higher than that of TST^{-1}. It also had a significantly higher ability than $FeCl_3$ to remove suspended particles and N in the mine wastewater. But it had a relatively lower COD and BOD removal than the conventional flocculants, $FeCl_3$ and polyacrylamide (Table 4.2.14).

In general, it can be summarized that the polyacrylamide grafted bioflocculants had efficient removal rates of both the suspended solids and the dissolved solids, in the domestic and industrial effluents. This may be attributed to the following factors: (i) the flocculants' branched nature which ensures easy approachability of pollutants in water, (ii) functional groups, (iii) intrinsic viscosities and (iv) the surface morphologies of the flocculants (Brostow *et al*., 2007; Maliehe, 2017; Singh *et al*., 2000). These findings had similarities to those obtained in other studies (Liu *et al*., 2014; Mishra *et al*., 2011; Pal *et al*., 2012; Sinha *et al*., 2013). Thus, the polyacrylamide grafted bioflocculants show a potential to replace the non-biodegradable and harmful conventional flocculants.

Table 4.2.13: Removal efficiency (RE) and flocculating activity (FA) of TMT^{-1}-PAM 2 in coal mine wastewater

Flocculant	RE (%) ± SD				FA(%) ± SD
	COD	BOD	N	S	
TMT^{-1}	98±0.6[a]	86±1.3[b]	38±8.9[a]	79±12.1[a]	60±1.7[a]
TMT^{-1}-g-PAM 2	**99±0.0[a]**	**93±0.1[a]**	**59±3.5[b]**	**83±0.0[a]**	**71±5.5[b]**
$FeCl_3$	98±0.0[a]	84±0.0[b]	31±2.3[a]	48±2.3[b]	69±1.2[c]
Polyacrylamide	99±0.0[a]	95±0.0[a]	100±0.2[c]	88±0.1[c]	99±1.0[d]

Values with different letters (a, b, c and d) on the same column are significantly ($p < 0.05$) different

Table 4.2.14: Removal efficiency (RE) and flocculating activity (FA) of TST^{-1}-PAM 3 in coal mine wastewater

Flocculant	RE (%) ± SD				FA(%) ± SD
	COD	BOD	N	S	
TST^{-1}	95±0.6[a]	44±2[a]	89±2.3[a]	57±1.7[a,b]	85±9.5[a]
TST^{-1}-g-PAM 3	**95±0.6[a]**	**62±0.5[b]**	**89±2.3[a]**	**57±2.1[a,b]**	**90±6.7[a]**
$FeCl_3$	98±0.0[b]	84±0.4[c]	31±2.3[b]	48±2.3[b]	69±1.2[b]
Polyacrylamide	99±0.0[b]	95±0.0[d]	100±0.2[c]	88±0.1[c]	99±1.0[a]

Values with different letters (a, b, c and d) on the same column are significantly ($p < 0.05$) different

Chapter 5

5.1 Conclusion

The polyacrylamide grafted bioflocculants (TMT^{-1}-g-PAM 2 and TST^{-1}-g-PAM 3) were successfully synthesized using the microwave initiated synthesis method. This synthesis was verified through grafting percentage, intrinsic viscosity, elemental analysis, SEM, FTIR, XRD and TGA.

The polyacrylamide grafted bioflocculants were found to be non-cytotoxic, lack antibacterial activity and possessed a longer shelf life than their respective natural bioflocculants. They exhibited pH, thermal and saline stabilities. They showed better flocculation characteristics on kaolin clay suspension than their respective natural bioflocculants and the conventional flocculant $FeCl_3$. When tested on domestic and industrial wastewater, the grafted bioflocculants exhibited good removal capabilities of pollutants; particularly in domestic wastewater, wherein, the grafted bioflocculants showed a significantly higher removal efficiency of suspended particles and COD than the commercial flocculants (polyacrylamide and $FeCl_3$). These findings were attributed to Singh's easy approachability hypothesis for the grafted bioflocculants and also confirmed our hypothesis. Their good flocculation properties suggest that they have a potential role in bioremediation processes and may be used as alternatives to conventional flocculants.

5.2 Recommendations

For bioflocculant production, inexpensive substrates should be investigated in order to decrease microbial bioflocculant production costs. Moreover, molecular techniques such as gene overexpression should be used on bacterial strains in an attempt to improve their bioflocculant production capacity.

For the graft copolymers, more characterization should be done. This may include molecular weight and shear stability analyses. The properties of the graft copolymers may be enhanced further through etherification, a polymer modification method.

The flocculation efficacy of the graft copolymers should be tested directly at a wastewater treatment plant.

References

AKPOR, O.B. and MUCHIE, M. (2011) Environmental and public health implications of wastewater quality. *African Journal of Biotechnology*. 10(13): 2379 – 2387.

ALJUBOORI, A.H., IDRIS, A., AL-JOUBORY, H.H., UEMURA, Y. and IBN ABUBAKAR, B.S. (2015) Flocculation behavior and mechanism of bioflocculant produced by *Aspergillus flavus*. *J. Environ. Manage*. 150: 466 – 471.

AREZOO, C. (2002) The potential role of aluminum in Alzheimer's disease. *Nephrol. Dialys. Transplant.* 17: 17 – 20.

BALA, S. S., YAN, S., TYAGI, R.D. and SURAMPALLI, R.Y. (2010) Extracellular polymeric substances (EPS) producing bacterial strains of municipal wastewater sludge: Isolation, molecular identification, EPS characterization and performance for sludge settling and dewatering. *Water Res*. 44: 2253 – 2266.

BATZING, B.L. (2002) *Microbiology: an introduction*. USA: Brooks/Cole Thomson Learning.

BELL, F.G., HÄLBICH, T.F.J. and BULLOCK, S.E.T. (2002) The effects of acid mine drainage from an old mine in the Witbank Coalfield, South Africa. *Quarterly Journal of Engineering Geology and Hydrogeology*. 35: 265 – 278.

BHATTACHARYA, A., DAS, A. and DE, A. (1998) Structural influence on grafting of acrylamide based monomers on cellulose acetate. *Ind. J. Chem. Tech*. 5: 135 – 8.

BHATTACHARYA, A. and MISRA, B.N. (2004) Grafting: a versatile means to modify polymers: Techniques, factors and applications. *Prog. Polym. Sci.* 29: 767 – 814.

BISWAL, D.R. and SINGH, R.P. (2004) Characterization of carboxymethyl cellulose and polyacrylamide graft copolymer. *Carbohydrate Polymers*. 57: 379 – 387.

BOLTO, B. and GREGORY, J. (2007) Organic polyelectrolytes in water treatment. *Water Res*. 41: 2301 – 2324.

BONADONNA, L., BRIANCESCO, R., OTTAVIANI, M. and VESCHETTI, E. (2002) Occurrence of Cryptosporidium oocysts in sewage effluents and correlation with microbial, chemical and physical water variables. *Environmental Management and Assessment*. 75: 241 – 252.

BUTHELEZI, S.P., OLANIRAN, A.O. and PILLAY, B. (2010) Production and characterization of bioflocculants from bacteria isolated from wastewater treatment plant in South Africa. *Biotechnol. Bioproc. Eng.* 15: 874 – 881.

BRADY, J.E. and SENESE, F. (2004) *Chemistry: matter and its changes*. 4th Ed. USA: Willey.

BROSTOW, W., PAL, S. and SINGH, R.P. (2007) A model of flocculation. *Materials letters*. 61(22): 4381 – 4384.

CARRAHER, C.E. (2003) *Seymour/Carraher's Polymer Chemistry*. 6th Ed. USA: Marcel Dekker.

CHANG, W.C., SOON, A.Y., IN, H.O. and SANG, H.P. (1998) Characterization of an extracellular flocculating substance produced by a planktonic cyanobacterium, *Anabaena sp*. *Biotechnol. Lett.* 20 (12): 643 – 646.

CONG-LIANG, Z., YA-NAN, C. and YAN, W. (2012) Bioflocculant produced from bacteria for decolorization, Cr removal and swine wastewater application. *Sustain. Environ. Res*. 22(2): 129 – 134.

CONVERTI, A., ALIAKBARIAN, B., DOMINGUEZ, J.M. VAZQUEZ, G.B. and PEREGO, P. (2010) Microbial production of biovanillin. *Braz. J. Microbiol.* 41 (3): 519 – 530.

CORCORAN, E., NELLEMANN, C., BAKER, E., BOS, R., OSBORN, D. and SAVELLI, H. (eds.) (2010) *Sick Water? The Central Role of Wastewater Management in Sustainable*

Development. [Online] Norway: Birkenland Trykkeri. Available from: www.grida.no. [Accessed: 17th May 2018].

COSA, S. and OKOH, A. (2014) Bioflocculant production by a consortium of two bacterial species and its potential application in industrial wastewater and river water treatment. *Pol. J. Environ*. *Stud*. 23(3): 689 – 696.

COSA, S., UGBENYEN, M.A., MABINYA, L.V. and OKOH, I.A. (2013) Characterization of a thermostable polysaccharide bioflocculant produced by *Virgibacillus species* isolated from Algoa Bay. *Afr*. *J*. *Microbiol*. *Res*. 7 (23): 2925 – 2938.

DEARFIELD, K.L., ABERNATHY, C.O., OTTLEY, M.S., BRANTNER, J.H. and HAYES, P.F. (1988) Acrylamide: Its metabolism, developmental and reproductive effects, genotoxicity, and carcinogenicity. *Mutat. Res*. 195: 45 – 77.

DEY, K.P., MISHRA, S. and SEN, G. (2017) Synthesis and characterization of polymethylmethacrylate grafted barley for treatment of industrial and municipal wastewater. *Journal of Water Process Engineering*. 18: 113 – 125.

DILLI, S., GARNETT, J.L. (1967) Radiation induced reactions with cellulose. III. Kinetics of styrene copolymerisation in methanol. *J. Appl. Polym. Sci.* 11(6): 859 – 70.

DLAMINI, N.G. (2017) *Biosynthesis of copper nanoparticles using a bioflocculant from Alcaligenis faecalis, characterization and its application*. MSc. University of Zululand.

EDWARD, J.K. (2011) *Water quality and treatment-a handbook of drinking water*. 6th Ed. American Water Works Association. McGraw-Hill.

ELOFF, J.N. (1998) A Sensitive and quick microplate method to determine the minimum inhibitory concentration of plant extracts for bacteria. *Plant Medica*. 64: 711 – 713.

ESKOM. (2018) *Understanding electricity*. [Online] Available from:

http://www.eskom.co.za/AboutElectricity/ElectricityTechnologies/Pages/Understanding_Electricity.aspx
[Accessed: 25th August 2018].

FANTA, G.F. (1973) Synthesis of graft and block copolymers of starch. New York: Willey & Sons.

FLEMMING, H.C. and WINGENDER, J. (2010) The biofilm matrix. *Nat. Rev. Microbiol*. 8: 623 – 633.

FREESE, S.D., HODGSON, K.G., NOZAIC, D.J. and BORAIN, G. (2004) Quantification of factors affecting coagulation of water with cationic polymers and laboratory methods for determining these effects. [Online] South Africa: Water Research Commission (WRC). Available from: http://www.wrc.org.za/Knowledge%20Hub%20Documents/Research%20Reports/1225-1-04.pdf. [Accessed: 18th May 2018].

GIRI, T.K., PURE, S. and TRIPATHI D.K. (2015) Synthesis of graft copolymers of acrylamide for locust bean gum using microwave energy: swelling behavior, flocculation characteristics and acute toxicity study. *Polímeros*. 25(2): 168 – 174.

GONCHARUK, V.V. (2014) *Drinking water: physics, chemistry and biology*. Springer International Publishing: Switzerland.

GOUIN, T., ROCHE, N., LOHMANN, R. and HODGES, G. (2011) A thermodynamic approach for assessing the environmental exposure of chemicals absorbed to microplastic. *Environmental Science & Technology*. 45: 1466 – 1472.

GROENEWALD, Y. (2012) *Coal's hidden water cost to South Africa.* [Online] Available from: https://www.greenpeace.org/africa/Global/africa/publications/coal/CoalsHiddenWaterCost.pdf
[Accessed: 05th September 2018].

HANNA, S. H. S., OSBORNE-LEE, I. W., CESARETTI, G. P., MISSO, R. and KHALIL, M. T. (2016) Ecological agro-ecosystem sustainable development in relationship to other sectors in the economic system, and human ecological footprint and imprint. *Agriculture and Agricultural Science Procedia*. 8: 17 – 30.

HANDTKE, S., SCHROETER, R., JÜRGEN, B., METHLING, K., SCHLÜTER, R., ALBRECHT, D., VAN HIJUM, A.F.T., BONGAERTS, J., MAURER, K., LALK, M., SCHWEDER, T., HECKER, M. and VOIGT, B. (2014) *Bacillus pumilus* reveals a remarkably high resistance to hydrogen peroxide provoked oxidative stress. *PLoS ONE*. 9(1).

HE, J., ZOU, J., SHAO, Z. and ZHANG, J. (2010) Characteristics and flocculating mechanism of a novel bioflocculant HBF-3 produced by deep-sea bacterium mutant *Halomona* sp. V3a. *World J*. *Microbiol*. *Biotechnol*. 26: 1135 – 1141.

HENDRICKS, D. (2006) *Water treatment unit process-Physical and chemical*. New York, USA: CRS Press.

HU, C., LIU, H., OU, J., WANG, D. and RU, J. (2006) Coagulation behaviour of aluminium salts in eutrophic water: significance of All3 species and pH control. *Environ. Sci. Technol*. 40: 325 – 331.

HUANG, M., WANG, Y.W., CAI, J., BAI, J.F., YANG, H. and LI, A.M. (2016) Preparation of dual function starch-based flocculants for the simultaneous removal of turbidity and inhibition of *Escherichia coli* in water. *Water Res*. 98: 128 – 137.

INTER MINISTERIAL COMMITTEE ON ACID MINE DRAINAGE (IMC). (2010) Mine water management in the Witwatersrand gold fields with special emphasis on acid mine drainage. South Africa. Available from: www.dmr.gov.za/Portals/0/Resource%20Center/Reports%20and%20Other%20Documents/2010_Report_Interministerial%20Committee_Acid%20Mine%20Drainage.pdf?ver=2018-03-13-020432-273
[Accessed: 17th September 2018].

KALEA, G., AURASA, R., SINGHA, S.P. and NARAYAN, R. (2007) Biodegradability of polylactide bottles in real and simulated composting conditions. *Polymer Testing*. 26: 1049 – 1061.

KALIA, S. and SABAA, M.W. (eds) (2013) *Polysaccharide Based Graft Copolymers.* Berlin Heidelberg: Springer-Verlag.

KARTHIGA, D. and NATARAJAN, K.A. (2015) Production and characterization of bioflocculants for mineral processing applications. *Int*. *J*. *Miner*. *Process*. 137: 15 – 25.

KAYLA, H. and TRIPATHY, T. (2014) Biodegradable flocculants based on polyacrylamide and poly (N,N-dimethylacrylamide) grafted amylopectin. *Int. J. Biol. Macromolecules*. 70: 26 – 36.

KEMPF, M.J., CHEN, F., KERN, R. (2005) Recurrent isolation of hydrogen peroxide-resistant spores of *Bacillus pumilus* from a spacecraft assembly facility. *Astrobiology*. 5: 319 – 405.

KOKTA, B.V., VALADE, J.L. and DANEAULT, C. (1981) Modification of mechanical and thermomechanical pulps by grafting with synthetic polymers. II. Effect of ozonation on polymerization parameters and pulp properties. *Transactions*. 7: TR5 – TR10.

KOJIMA, K., IGUCHI, S., KAJIMA, Y. and YOSHIKUNI, M. (1983) Grafting of methylmethacrylate onto collagen initiated by tributylborane. *J. Appl. Polym Sci*. 28: 87 – 95.

KURANE, R., HATAMOCHI, K., KAKUNO, T., KIYOHARA, M., HIRONO, M., TANIGUCHI, T. (1994) Production of a bioflocculant by *Rhodococcus erythropolis* S-1 grown on alcohols. *Biosci. Biotechnol. Biochem*. 58: 428 – 429.

LARSDOTTER, K. (2006) *Microalgae for phosphorus removal from wastewater in a Nordic climate.* PHD. School of Biotechnology, Royal Institute of Technology, Stockholm, Sweden. [Online] Available from:

http://www.diva-portal.org/smash/get/diva2:9924/FULLTEXT01.pdf
[Accessed: 17th September 2018].

LEE, C.S., ROBINSON, J. and CHONG, M.F. (2014) A review on application of flocculants in wastewater treatment. *Process Safety and Environmental Protection.* 92(6): 489 – 568.

LEE, K.E., MORAD, N., TENG, T.T. and POH, B.T. (2012) Development, characterization and the application of hybrid materials in coagulation/flocculation of wastewater: a review. *Chem. Eng. J*. 203: 370 – 386.

LEE, S.H., SHIN, W.S., SHIN, M.C., CHOI, S.J. and PARK, L.S. (2001) Improvement of water treatment performance by using polyamine flocculants. *Environ*. *Technol*. 22: 653.

LI, W.W., ZHOU, W.Z., ZHANG, Y.Z., WANG, J. and ZHU, X.B. (2008) Flocculation behavior and mechanism of an exopolysaccharide from the deep-sea psychrophilic bacterium *Pseudoalteromonas* sp. SM9913. *Bioresource Technology*. 99: 6893 – 6899.

LIN, J. and HARICHUND, C. (2012) Production and characterization of heavy metal removing bacterial bioflocculants. *Afr*. *J*. *Biotech*. 11(40): 9619 – 9629.

LIN, X.Y., FAN, H.S., LI, X.D., TANG, M. and ZHANG, X.D. (2005) Evaluation of bioactivity and cytocompatibility of nano-hydroxyapatite/collagen composite in vitro. *Key Eng. Mater*. 284: 553 – 556.

LIU, H., YANG, X., ZHANG, Y., ZHU, H. and YAO, J. (2014) Flocculation characteristics of polyacrylamide grafted cellulose from *Phyllostachys heterocycla*: an efficient and eco-friendly flocculant. *Water Research*. 59: 165 – 171.

LIU, Z., HUANG, M., LI, A. and Yang, H. (2017) Flocculation and antimicrobial properties of a cationized starch. *Water Research*. 119(4): 57 – 66.

MABINYA, L.V., COSA, S., NWODO, U. and OKOH, A.I. (2012) Studies on bioflocculant production by *Arthrobacte*r sp. Raats, freshwater bacteria isolated from Tyume River, South Africa. *Int. J. Mol. Sci*. 13: 1054 – 1065.

MADIGAN, M.T., MARTINKO, J.M., STAHL, D.A. and CLARK, D.P. (2012) *Brock biology of microorganism.* San Francisco: Pearson.

MALIEHE, T.S. (2017) *Characterization, biosafety and effectiveness of bioflocculants by bacterial strains isolated from Sodwana Bay sediment*. PHD. University of Zululand.

MALIEHE, T.S., SHANDU, J.S. and BASSON, A.K. (2015) Evaluation of the antibacterial activity of *Syzygium cordatum* fruit-pulp and seed extracts against bacterial strains implicated in gastrointestinal tract infections. *African Journal of Biotechnology.* 14(16): 1387 – 1392.

MALIEHE, T. S., SIMONIS, J., BASSON, A. K., REVE, M., NGEMA, S. and XABA, P. S. (2016) Production, characterisation and flocculation mechanism of bioflocculant TMT^{-1} from marine *Bacillus pumilus* JX860616. *African Journal of Biotechnology*. 15(41): 2352 – 2367.

MARVASI, M., VISSCHER, P.T., CASILLAS MARTINEZ, L. (2010) Exopolymeric substances (EPS) from *Bacillus subtilis*: polymers and genes encoding their synthesis. *FEMS Microbiol. Lett.* 313: 1 – 9.

MASINDI, V., CHATZISYMEON, E., KORTIDIS, I. and FOTEINIS, S. (2018) Assessing the sustainability of acid mine drainage (AMD) treatment in South Africa. *Science of the Total Environment*. 635: 793 – 802.

MEKONNEN, M.M. and HOEKSTRA, A.Y. (2016) Four billion people facing severe water scarcity. *Science Advances*. 2(2): 1 – 6. [Online] Available from: http://advances.sciencemag.org/content/advances/2/2/e1500323.full.pdf [Accessed: 10th September 2018].

MISHRA, A., YADAV, A., PAL, A. and SINGH, A. (2006) Biodegradable graft copolymers of fenugreek mucilage and polyacrylamide: A renewable reservoir to biomaterials. *Carbohydrate Polymers*. 65: 58 – 63.

MISHRA, R.K., SUTAR, P.B., SINGHAL, J.P. and BANTHIA, A.K. (2007) Graft copolymerization of pectin with polyacrylamide. *Polymer-Plastics Technology and Engineering*. 46: 1079 – 1085.

MISHRA, S. and SEN, G. (2011) Microwave initiated synthesis of polymethylmethacrylate grafted guar (GG-g-PMMA), characterizations and applications. *International Journal of Biological Macromolecules*. 48: 688 – 694.

MISHRA, S., SINHA, S., DEY, K.P. and SEN, G. (2014) Synthesis, characterization and applications of polymethylmethacrylate grafted psyllium as flocculant. *Carbohydr. Polym*. 99: 462 – 468.

MORE, T.T., YADAVA, J.S.S., YAN, S., TYAGI, R.D. and SURAMPALLI, R.Y. (2014) Extracellular polymeric substances of bacteria and their potential environmental applications. *Journal of Environmental Management*. 144: 1 – 25.

MORIKAWA, M. (2006) Beneficial Biofilm Formation by Industrial Bacteria *Bacillus subtilis* and Related Species. *Journal of Bioscience and Bioengineering*. 101(1): 1 – 8.

MOSMAN, T. (1983) Rapid colorimetric assay for cellular growth and survival: application to proliferation and cytotoxicity assays. *J. Immunol. Methods*. 65: 55 – 63.

NAIDOO, D. (2018) *Gauteng water contaminated*. [Interview] eNCA. Interviewed by Uveka Rangappa, *The eNCA Morning News Today*, 12 August.

NAKATA, K. and KURANE, R. (1999) Production of an extracellular polysaccharide bioflocculant by *Klebsiella pneumoniae*. *Biosci. Biotechnol. Biochem.* 63(12): 2064 – 2068.

NAYAK, B.R., BISWAL, D.R., KARMAKAR, N.C. and SINGH, R.P. (2002) Grafted hydroxypropyl guargum: development, characterization and application as flocculating agent. *Bull. Mater. Sci*. 25(6): 537 – 540.

NICHOLSON, W.L., MUNAKATA, N., HORNECK, G., MELOSH, H.J. and SETLOW, P. (2000) Resistance of *Bacillus* endospores to extreme terrestrial and extraterrestrial environments. *Microbiol. Mol. Biol. Rev.* 64 (3): 548 – 572.

NIE, M., YIN, X., JIA, J., WANG, Y., LIU, S., SHEN, Q., LI, P. and WANG, Z. (2011) Production of a novel bioflocculant MNXY1 by *Klebsiella pneumoniae* strain NY1 and application in precipitation of cyanobacteria and municipal wastewater treatment. *J. Appl. Microbial*. 111: 547 – 558.

OKAIYETO, K., NWODO, U.U. and MABINYA, L.V. (2013) Characterization of a bioflocculant produced by a consortium of *Halomonas* sp. Okoh and *Micrococcus* sp. Leo. *Int. J. Environ. Res. Public Health*. 10(10): 5097 – 5110.

OKAIYETO, K., NWODO, U.U., MABINYA, L.V. and OKOH, A.I. (2014) Evaluation of the flocculation potential and characterization of bioflocculant produced by *Micrococcus* sp. Leo. *Applied Biochemistry and Microbiology*. 50(6): 601 – 608.

OKAIYETO, K., NWODO, U.U., MABINYA, L.V., OKOLI, A.S. and OKOH, A.I. (2015) Characterization of a bioflocculant (MBF-UFH) produced by *Bacillus* sp. AEMREG7. *Int. J. Mol. Sci*. 6: 12986 – 13003.

OKAIYETO, K., NWODO, U.U., MABINYA, L.V., OKOLI, A.S. and OKOH, A.I. (2016) Evaluation of flocculating performance of a thermostable bioflocculant produced by marine *Bacillus* sp. *Environmental technology*. 37(14): 1829 – 1842.

PAL, S., GHORAI, S., DASH, M.K., GHOSH, S. and UDAYABHANU, G. (2011) Flocculation properties of polyacrylamide grafted carboxymethyl guar gum (CMG-g-PAM) synthesised by conventional and microwave assisted method. *J. Hazard. Mater.* 192: 1580 – 1588.

PAL, S., SEN, G., GHOSH, S. and SINGH, R.P. (2012) High performance polymeric flocculants based on modified polysaccharides – microwave assisted synthesis. *Carbohydrate Polymers*. 87: 336 – 342.

PATIL, D.R. and FANTA, G.F. (1993) Graft copolymerization of starch with methylacrylate: an examination of reaction variables. *J. Appl. Polym. Sci*. 47: 1765 – 72.

PEREZ, A.R., ABANES-DE MELLO, A. and POGLIANO, K. (2000) "SpoIIB Localizes to Active Sites of Septal Biogenesis and Spatially Regulates Septal Thinning during Engulfment in *Bacillus subtilis*". *Journal of Bacteriology*. 182(4): 1096 – 1108.

PRIETO, E.M., RIVAS, B. and SANCHEZ, J. (2012) Natural polymer grafted with synthetic monomer by microwave for water treatment-a review. *Ciencia en Desarrollo*. 4(1): 219 – 240.

QARALLEH, H., SITI, A.K., OTHMAN, A.S., MUHAMMAD, T. and DENY, S. (2012) Antimicrobial activity and essential oils of *Curcuma aeruginosa*, *Curcuma mangga*, and *Zingiber cassumunar* from Malaysia. *Asian Pac. J. Trop. Med*. 5(3): 202 – 209.

RANJBAR-MOHAMMADI, M., ARAMIA, M., BAHRAMIA, H., MAZAHERI, F. and MAHMOODI, N.M. (2010) Grafting of chitosan as a biopolymer on to wool fabric using anhydride bridge and its antibacterial property. *Colloids and Surfaces B: Biointerfaces.* 76(2): 397 – 403.

RAJPUT, R. and GUPTA, R. (2014) Expression of *Bacillus pumilus* keratinase Rk (27) in *Bacillus subtilis*: enzyme application for developing renewable flocculants from bone meal. *Ann. Microbiol.* 64: 1257 – 1266.

REDDY, D.H.K. (2017) Water pollution control technologies. *Encyclopedia of Sustainable Technologies*. 3 – 22.

REZANIA, S., TAIB, S. M., MD DIN, M.F., DAHALAN, F. A. and KAMYAB, H. (2016) Comprehensive review on phytotechnology: heavy metals removal by diverse aquatic plants species from wastewater. *Journal of Hazardous Materials*. 318: 587 – 599.

RHEOSENSE. (2016) *Application note: measuring intrinsic viscosity with miroVISC.* [Online] Available from: www.rheosense.com. [Accessed: 19th November 2017].

ROCHMAN, C. M., KROSS, S. M., ARMSTRONG, J. B., BOGAN, M. T., DARLING, E. S., GREEN, S. J., SMYTH, A. R. and VERÍSSIMO, D. (2015) Scientific evidence supports a ban on microbeads. *Environmental Science & Technology*. 49: 10759 – 10761.

SALEHIZADEH, H. and SHOJAOSADATI, S.A. (2001) Extracellular biopolymeric flocculants: Recent trends and biotechnological importance. *Biotechnol. Adv.* 19: 371 – 385.

SAMAL, S., SAHU, G., LENKA, S. and NAYAK, P.L. (1987) Photo-induced graft copolymerization. XI. Graft copolymerization of methylmethacrylate onto silk using isoquinoline-sulphur dioxide charge transfer complex as the initiator. *J. Appl. Polym. Sci*. 33(5): 1853 – 8.

SANLI, O. AND PULET, E. (1993) Solvent assisted graft copolymerization of acrylamide on poly (ethylene terephthalate) films using benzoyl peroxide initiator. *J. Appl. Polym. Sci*. 47: 1 – 6.

SCHWEITZER, L. and NOBLET, J. (2017) Water contamination and pollution. In TÖRÖK, B. and DRANSFIELD, T. (eds). *Green chemistry: an inclusive approach.* USA: Elsevier.

SEN, G., KUMAR,S., GHOSH, S. and PAL, S. (2009) A novel polymeric flocculant based on polyacrylamide grafted carboxymethyl starch. *Carbohydrate Polymers*. 77: 822 – 831.

SEN, G., MISHRA, S., RANI, G.U., RANI, P. and PRASAD, R. (2012) Microwave initiated synthesis of polyacrylamide grafted psyllium and its application as a flocculant. *International Journal of Biological Macromolecules*. 50: 369 – 375.

SEN, G. and PAL, S. (2009) Microwave initiated synthesis of polyacrylamide grafted carboxymethyl starch (CMS-g-PAM): Application as a novel matrix for sustained drug release. *International Journal of Biological Macromolecules*. 45: 48 – 55.

SEN, G., SINGH, R.P. and PAL, S. (2010) Microwave-initiated synthesis of polyacrylamide grafted sodium alginate: Synthesis and characterization. *Journal of Appl. Sci.* 115(1): 63 – 71.

SHAHID, M., BUKHARI, S.A., GUL, Y., MUNIR, H., ANJUM, F., ZUBER, M., JAMIL, T. and ZIA, K.M. (2013) Graft polymerization of guar gum with acryl amide irradiated by microwaves for colonic drug delivery. *International Journal of Biological Macromolecules*. 62: 172 – 179.

SHARMA, B.R., DHULDHOYA, N.C. and MERCHANT, U.C. (2006) Flocculants – an ecofriendly approach. *J. Polym. Environ.* 14: 195 – 202.

SHARMA, S. and CHATTERJEE, S. (2017) Microplastic pollution, a threat to marine ecosystem and human health: a short review. *Environ*. *Sci*. *Pollut*. *Res*. 24: 21530 – 21547.

SHENG, G.P., YU, H.Q. and LI, X.Y. (2010) Extracellular polymeric substances (EPS) of microbial aggregates in biological wastewater treatment systems: a review. *Biotechnol. Adv*. 28: 882 – 894.

SINGH, R.P., KARMAKAR, G.P., RATH, S.K., KARMAKAR, N.C., PANDEY, S.R., TRIPATHY, T., PANDA, J., KANAN, K., JAIN, S.K. and LAN, N.T. (2000) Biodegradable drag reducing agents and flocculants based on polysaccharides: materials and applications. *Polym. Eng. Sci*. 40: 46 – 60.

SINGH, V., KUMAR, P. and SANGHI, R. (2012) Use of microwave irradiation in the grafting modification of the polysaccharides – a review. *Progress in Polymer Science*. 37: 340 – 364.

SINGH, V., TIWARI, A., TRIPATHI, D.N. and SANGHI, R. (2006) Microwave enhanced synthesis of chitosan-graft-polyacrylamide. *Polymer*. 47: 254 – 260.

SINHA, S., MISHRA, S. and SEN, G. (2013) Microwave initiated synthesis of polyacrylamide grafted Casein (CAS-g-PAM) – Its application as a flocculant. *Inter. Biolog. Macromol*. 60: 141 – 147.

SMITH, J.C. (2009) *Biotechnology*. 5th Ed. Cambridge, UK: Cambridge University press.

SOMMER, S.G., CHRISTENSEN, M.L., SCHMIDT, T. and JENSEN, L.S. (eds.) (2013) *Animal Manure Recycling: Treatment and Management*. United Kingdom: Willey & Sons.

SPELLMAN, F.R. (2014) *Handbook of water and wastewater treatment plant operation.* 3rd Ed. CRC Press–Taylor and Francis.

STANNETT, V. (1981) Grafting. *Radiat. Phys. Chem*. 18: 215 – 222.

SUN, T., XU, P., LIU, Q., XUE, J. AND XIE, W. (2003) Graft copolymerization of methacrylic acid onto carboxymethyl chitosan. *Eur. Polym. J*. 39: 189 – 92.

TANG, J., QI, S., LI, Z., AN, Q., XIE, M. and YANG, B. (2014) Production, purification and application of polysaccharide-based bioflocculant by *Paenibacillus mucilaginosus. Carbohydrate Polymers*. 113: 463 – 470.

TCHOUNWOU, P.B., YEDJOU, C.G., PATLOLLA, A.K. and SUTTON, D.J. (2012) Heavy metals toxicity and the environment. *EXS*. 101: 133 – 164.

THOMAS, L., USHASREE, M.V. and PANDEY, A. (2014) An alkali-thermostable xylanase from *Bacillus pumilus* functionally expressed in *Kluyveromyces lactis* and evaluation of its deinking efficiency. *Bioresource Technol.* 165: 309 – 313.

TRIPATHY, T. and DE, B.R. (2006) Flocculation: a new way to treat the waste water. *Journal of Physical Sciences*. 10: 93 – 127.

TYUGANOVA, M.A., GALBRAIKH, L.S., ULMASOVE, A.A., TSAREVSKAYA, I.Y. and KHIDOYATOR, A.A. (1985) Use of rice straw as cellulosic raw material for ion exchanger production. *Cell Chem. Technol.* 19(5): 557 – 568.

UNITED NATIONS INTERNATIONAL CHILDREN'S EMERGENCY FUND (UNICEF) and WORLD HEALTH ORGANIZATION (WHO). (2015) *Progress on sanitation and drinking water–2015 update and MDG assessment.* Switzerland: WHO Press. [Online] Available from: https://europa.eu/capacity4dev/public-water_and_sanitation/document/whounicef-progress-sanitation-and-drinking-water-–-2015-update-and-mdg-assessment [Accessed: 30 September 2018].

WANG, L., MA, F., QU, Y., SUN, D., LI, A and GUO, J. (2011) Characterization of a compound bioflocculant produced by mixed culture of *Rhizobium radiobacter* F2 and *Bacillus sphaeicus* F6. *World*. *J*. *Microbiol*. *Biotechnol*. 27: 2559 – 2565.

WANG, Y., GAO, B.Y., YUE, Q.T., WIE, J.C., ZHOU, W.Z. and GU, R. (2010) Color removal from textile industry wastewater using composite flocculants. *Environ*. *Technol*. 28: 629 – 637.

WINGENDER, J., NEU, T.R. and FLEMMING, H.C. (1999) *Microbial Extracellular Polymeric Substances: Characterization, Structure and Function*. Berlin: Springer-Verlag.

WILLEY, J.M., SHERWOOD, L.M. and WOOLVERTON, C.J. (2011) *Prescott's microbiology.* 8th Edn. New York: McGraw-Hill.

WORLD HEALTH ORGANISATION (WHO). (2017) *Global Health Observatory (GHO) data*. [Online] Available from: http://www.who.int/gho/publications/worldhealthstatistics/2017/en/. [Accessed: 18th May 2018].

WORLD HEALTH ORGANIZATION (WHO). (2006) *Guidelines for the safe use of wastewater, excreta and greywater—volume 3: wastewater and excreta use in aquaculture*. France: World Health Organization Press. [Online] Available from: http://www.who.int/water_sanitation_health/publications/gsuweg3/en/ [Accessed: 20th August 2018].

WORLD WIDE FUND FOR NATURE (WWF). (2011) Coal and water futures in South Africa: the case for protecting headwaters in the Enkangala grasslands. [Online] Available from: http://awsassets.wwf.org.za/downloads/wwf_coal_water_report_2011_web.pdf [Accessed: 25th August 2018].

XIONG, Y., WANG, Y., YU, Y., LI, Q., WANG, H., CHEN, R. and HE, N. (2010) Production and characterization of a novel bioflocculant from *Bacillus licheniformis*. *Appl. Environ. Microbiol.* 76: 2778 – 2782.

YAHYA, N.Y., NGADI, N., MUHAMAD, I.I. and ALIAS, H. (2015) Application of cellulose from pandan leaves a grafted flocculant for dyes treatment. *Journal of Engineering Science and Technology*. 19 – 28.

YANG, Z., YANG, H., JIANG, Z., CAI, T., LI, H., LI, H., LI, A. and CHENG, R. (2013) Flocculation of both anionic and cationic dyes inaqueous solutions by the amphoteric grafting flocculant carboxymethyl chitosan-graft-polyacrylamide. *J. Hazard. Mater.* 254 – 255(6): 36 – 45.

YONG, P., BO, S. and YU, Z. (2009) Research on flocculation property of bioflocculant PGa21 Ca. *Modern Appl*. *Sci*. 3: 106 – 112.

ZHANG, Z.Q., LIN, B., XIA, S.Q., WANG, X.J. and YANG, A.M. (2007) Production and application of a novel bioflocculant by multiple-microorganism consortia using brewery wastewater as carbon source. *J*. *Environ*. *Sci*. 19(6): 667 – 673.

ZHENG, Y., YE, Z., FANG, X., LI, Y. and CIA, W. (2008) Production and characteristics of a bioflocculant produced by *Bacillus* sp. F19. *Bioresour. Technol*. 99: 7686 – 7691.

ZULKEFLEE, Z., ARIS, A.Z., SHAMSUDDIN, Z.H. and YUSOFF, M.K. (2012) Cation dependence, pH tolerance, and dosage requirement of a bioflocculant produced by *Bacillus* spp. UPMB13: flocculation performance optimization through kaolin assays. *Sci. World J*. 2012.

Appendix

Data showing synthetic details of different polymer grades of the polyacrylamide grafted bioflocculants

Table A1: Synthetic details for TMT^{-1}-g-PAM

Polymer grade	Weight of graft copolymer (g)	Absolute viscosity of graft copolymer		
		Reading 1	Reading 2	Reading 3
TMT^{-1}-g-PAM 1	0.55	11.00	10.23	10.27
TMT^{-1}-g-PAM 2	0.97	12.05	12.05	12.31
TMT^{-1}-g-PAM 3	0.51	9.96	9.96	9.17
TMT^{-1}-g-PAM 4	0.76	12.31	11.28	11.78
TMT^{-1}-g-PAM 5	0.71	11.27	11.27	10.74

Table A2: Synthetic details for TST^{-1}-g-PAM

Polymer grade	Weight of graft copolymer (g)	Absolute viscosity of graft copolymer		
		Reading 1	Reading 2	Reading 3
TST^{-1}-g-PAM 1	0.81	11.27	11.80	10.73
TST^{-1}-g-PAM 2	0.87	11.27	11.79	11.27
TST^{-1}-g-PAM 3	0.91	12.58	11.79	11.53
TST^{-1}-g-PAM 4	0.62	10.74	11.26	11.80
TST^{-1}-g-PAM 5	0.65	11.53	10.22	10.48
TST^{-1}-g-PAM 6	0.47	9.44	9.69	9.69

Data for elemental analyses of compounds

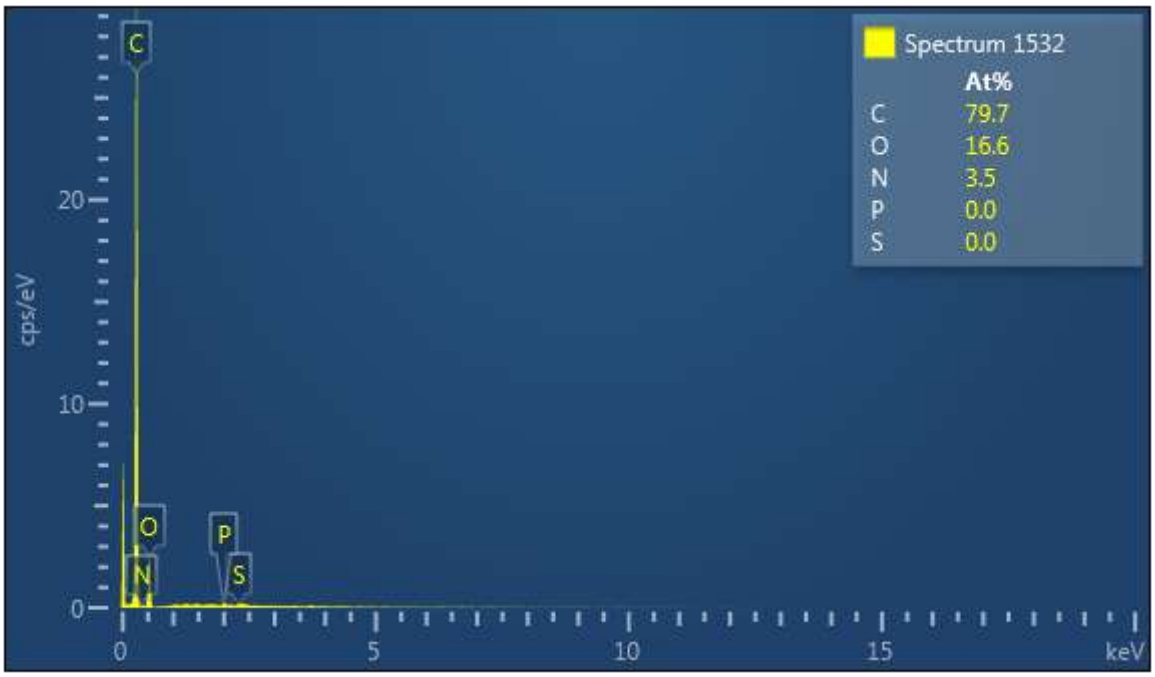

Figure A1: Elemental analysis of acrylamide

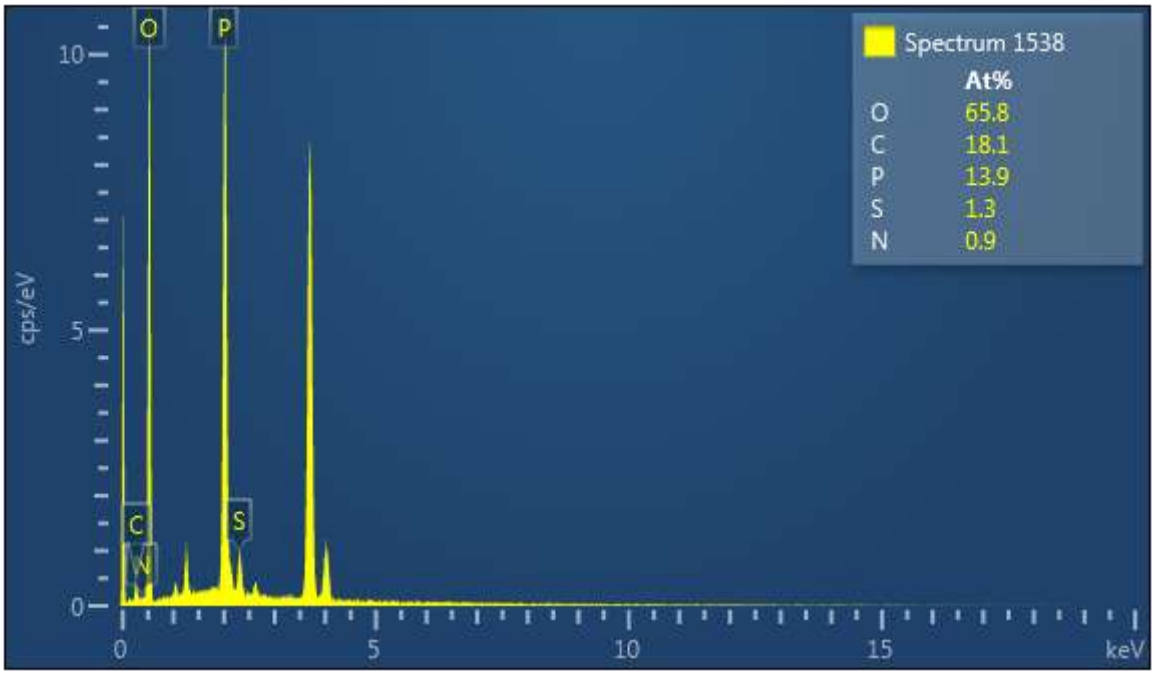

Figure A2: Elemental analysis of bioflocculant TMT^{-1}

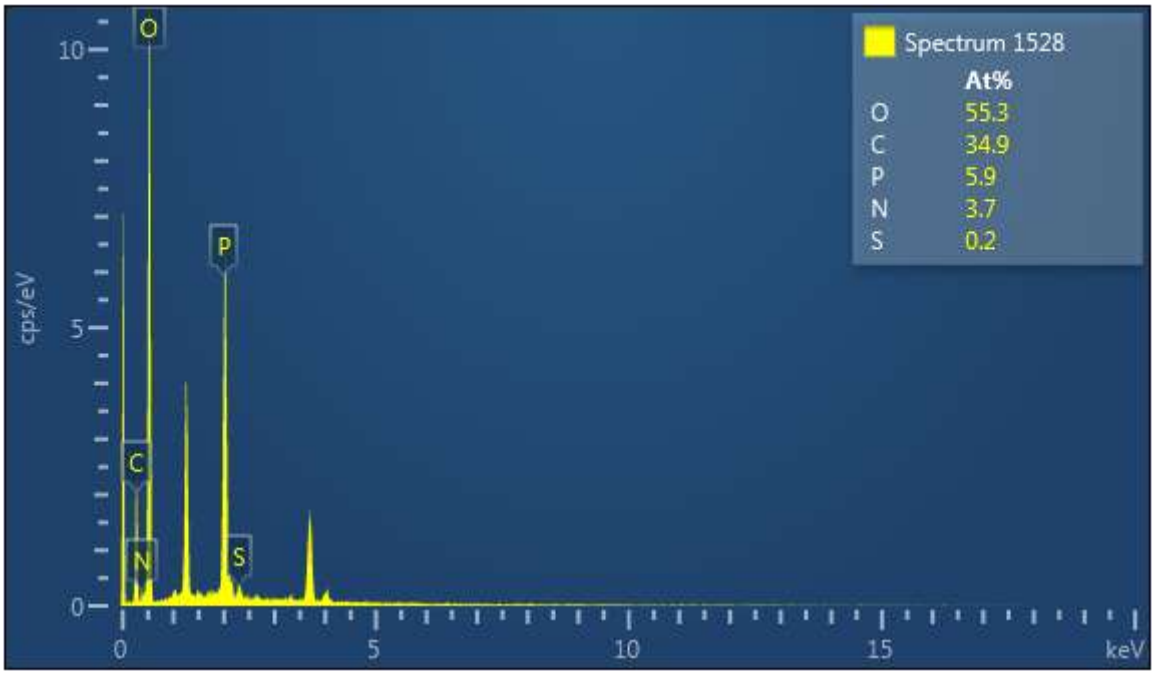

Figure A3: Elemental analysis of TMT^{-1}-g-PAM 2

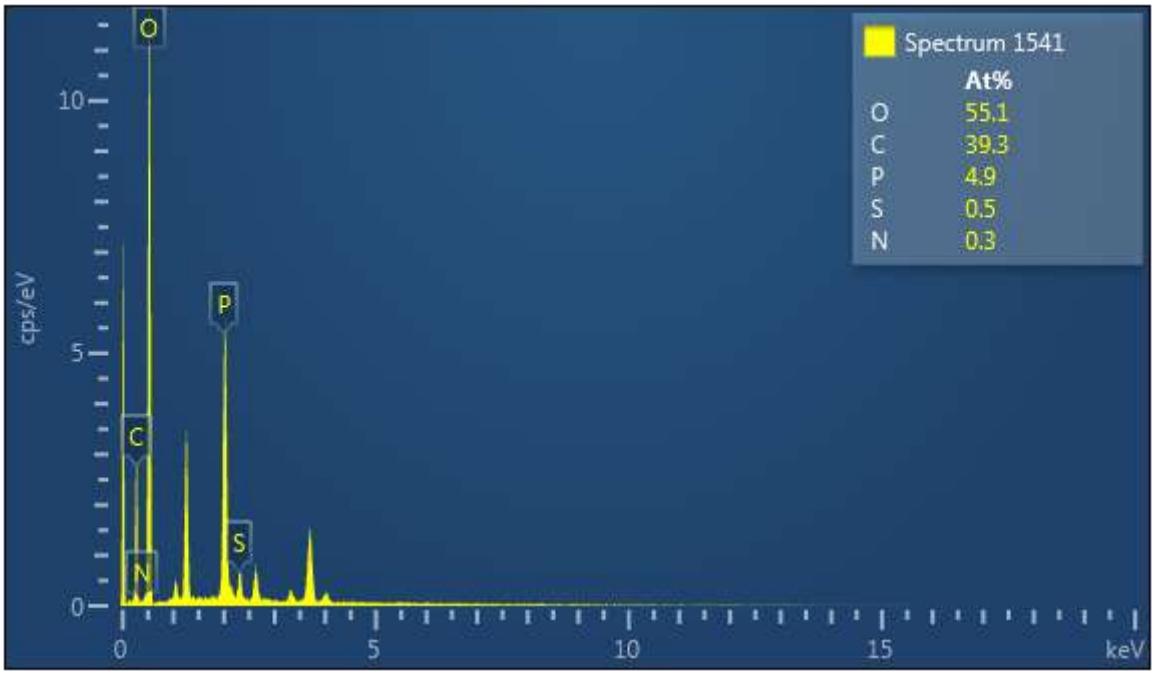

Figure A4: Elemental analysis of bioflocculant TST^{-1}

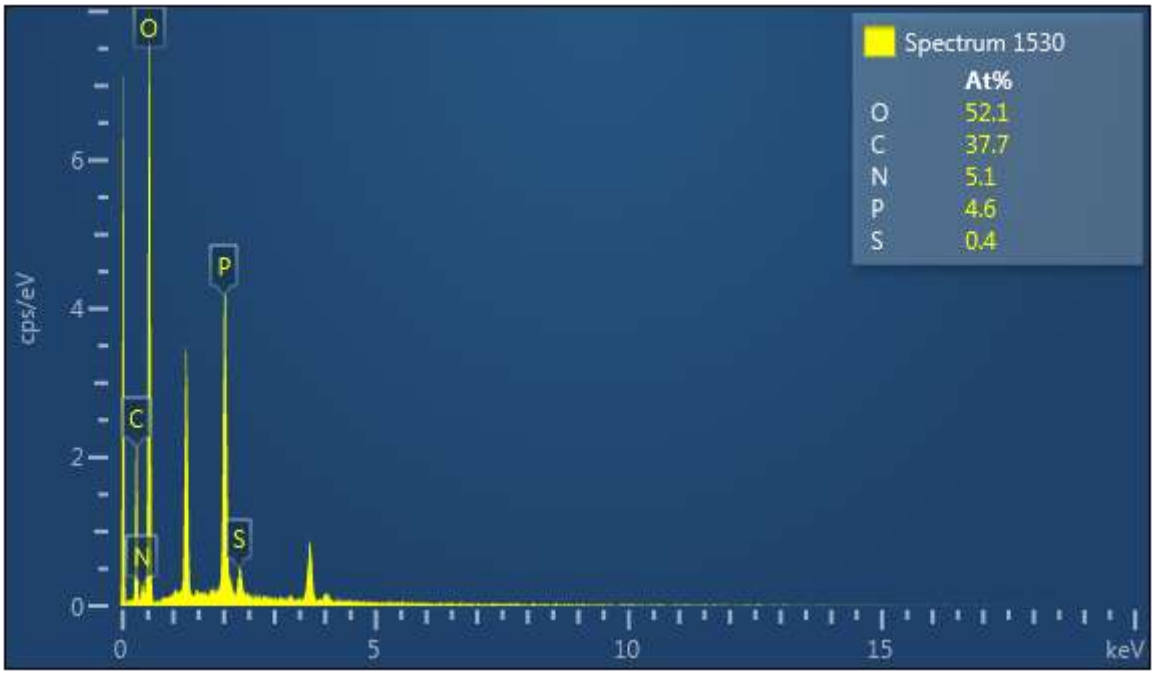

Figure A5: Elemental analysis of TST^{-1}-g-PAM 3

Data for acrylamide

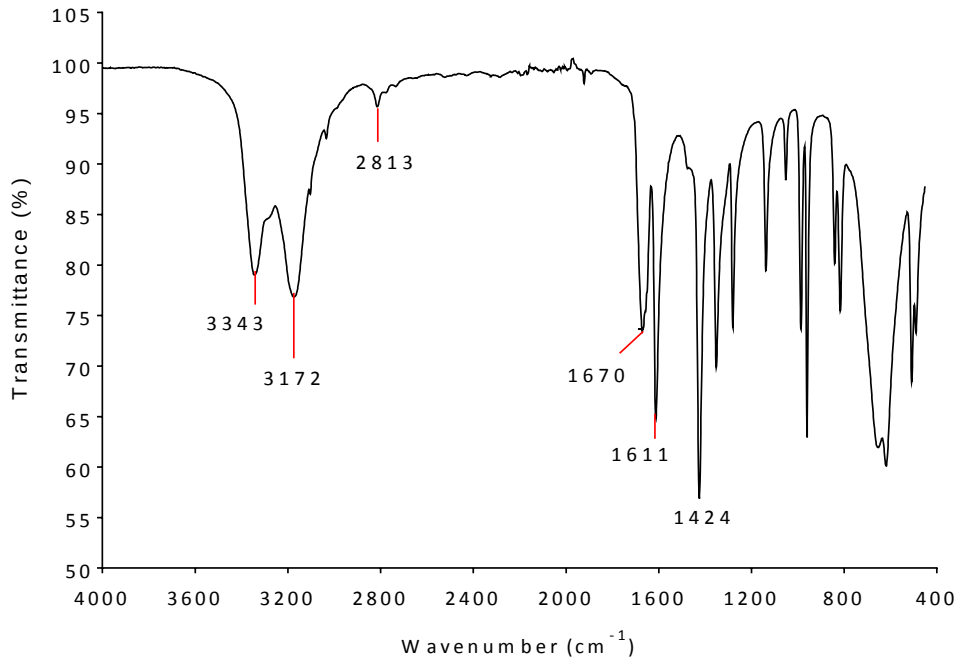

Figure A6: FTIR of acrylamide. Wavenumbers (cm^{-1}): 3343 & 3172 = NH_2; 2813 = C-H; 1670 = C=O; 1611 = N-H and 1424 = C-N.

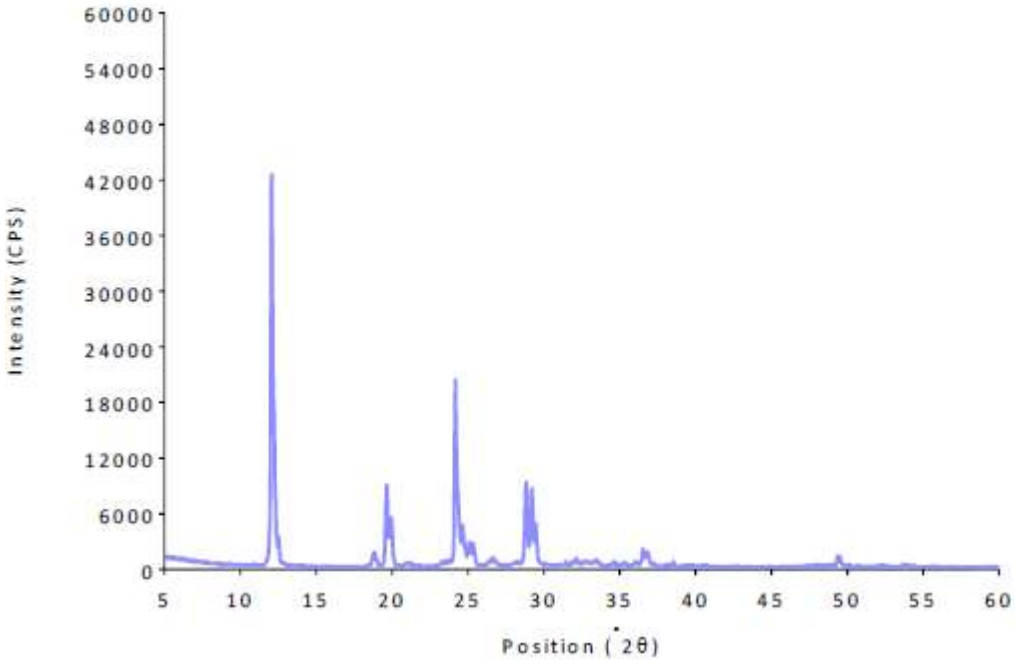

Figure A7: XRD of acrylamide

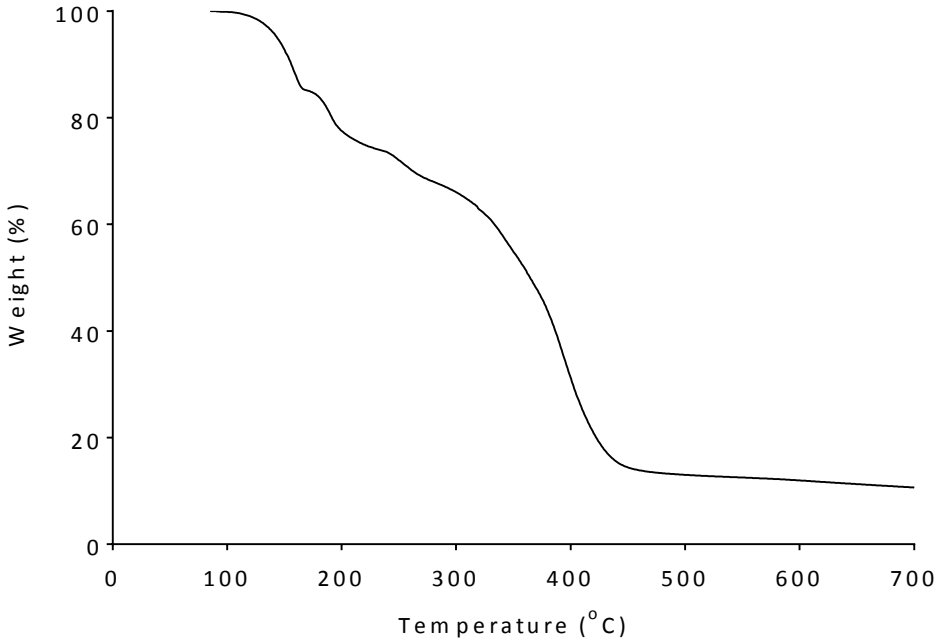

Figure A8: TGA of acrylamide

Data for the cytotoxicity assay of grafted bioflocculants (TMT^{-1}-g-PAM 2 & TST^{-1}-g-PAM 3)

Table A3: *In-vitro* cytotoxicity

TMT^{-1}-g-PAM 2 (µg/ml)	HEK 293		
	Reading 1	Reading 2	Reading 3
50	1.15	1.15	1.12
100	0.98	1.06	1.01
150	0.95	0.88	0.96
200	0.952	0.84	0.99
Control	1.16	1.23	1.32

Table A4: *In-vitro* cytotoxicity

TST^{-1}-g-PAM 3 (µg/ml)	HEK 293		
	Reading 1	Reading 2	Reading 3
50	1.17	1.26	1.26
100	1.12	1.16	1.14
150	1.09	1.03	1.04
200	1.08	1.03	1.06
Control	1.16	1.23	1.32

Data for the biodegradation studies of flocculants

Table A5: Biodegradation studies for TMT^{-1}-g-PAM 2

Sample	Weight (g)								
	Week 1			Week 2			Week 3		
	Reading 1	Reading 2	Reading 3	Reading 1	Reading 2	Reading 3	Reading 1	Reading 2	Reading 3
Soil + TMT^{-1}	4.50	4.51	4.49	4.30	4.29	4.31	4.20	4.06	4.14
Soil + TMT^{-1}-g-PAM 2	4.50	4.50	4.50	4.40	4.37	4.43	4.30	4.31	4.29
Control (soil)	4.50	4.50	4.50	4.50	4.50	4.50	4.50	4.50	4.50

Table A6: Biodegradation studies for TMT^{-1}-g-PAM 2

Sample	Weight (g)					
	Week 4			Week 5		
	Reading 1	Reading 2	Reading 3	Reading 1	Reading 2	Reading 3
Soil + TMT^{-1}	4.00	4.00	4.00	4.00	4.00	4.00
Soil + TMT^{-1}-g-PAM 2	4.10	4.10	4.10	4.00	4.01	3.99
Control (soil)	4.50	4.50	4.50	4.50	4.50	4.50

Table A7: Biodegradation studies for TST^{-1}-g-PAM 3

Sample	Weight (g)								
	Week 1			Week 2			Week 3		
	Reading 1	Reading 2	Reading 3	Reading 1	Reading 2	Reading 3	Reading 1	Reading 2	Reading 3
Soil + TST^{-1}	4.40	4.41	4.39	4.00	4.00	4.00	4.00	4.00	4.00
Soil + TST^{-1}-g-PAM 3	4.40	4.38	4.42	4.10	4.98	4.12	4.00	4.00	4.00
Control (soil)	4.50	4.50	4.50	4.50	4.50	4.50	4.50	4.50	4.50

Data for the effect of dosage size on flocculation of kaolin clay suspension

Table A8: TMT^{-1}-g-PAM 2 dosage size. Optical density (OD) of the control (kaolin clay suspension) at 550 nm was 3.09

Dosage size (mg/ml)	OD at 550 nm		
	Reading 1	Reading 2	Reading 3
0.1	1.083	1.015	1.049
0.2	0.513	0.647	0.599
0.4	0.536	0.692	0.662
0.6	0.463	0.625	0.660
0.8	0.516	0.636	0.621
1	0.588	0.724	0.659
1.2	0.955	1.411	1.183
1.4	0.862	1.388	1.125
1.6	1.011	1.522	1.514
1.8	1.516	1.562	1.539
2	1.143	1.815	1.479

Table A9: TMT^{-1} dosage size. OD of the control (kaolin clay suspension) at 550 nm was 3.09

Dosage size (mg/ml)	OD at 550 nm		
	Reading 1	Reading 2	Reading 3
0.1	1.146	1.113	1.130
0.2	1.134	1.121	1.224
0.4	1.121	1.147	1.134
0.6	1.214	1.367	1.061
0.8	1.335	1.262	1.2985
1	1.290	1.383	1.337
1.2	1.139	1.551	1.345
1.4	1.281	1.629	1.455
1.6	1.405	1.669	1.537
1.8	1.346	1.759	1.553
2	1.793	1.949	1.871

Table A10: TST^{-1}-g-PAM 3 dosage size. Optical density (OD) of the control (kaolin clay suspension) at 550 nm was 3.09

Dosage size (mg/ml)	OD at 550 nm		
	Reading 1	Reading 2	Reading 3
0.1	0.506	0.548	0.567
0.2	0.318	0.297	0.336
0.4	0.726	1.155	0.697
0.6	0.883	0.640	1.053
0.8	1.183	1.164	0.692
1	0.756	0.791	0.995
1.2	0.988	0.424	0.822
1.4	0.809	1.144	1.080
1.6	1.014	1.370	1.011
1.8	1.017	1.452	1.041
2	1.533	1.089	1.478

Table A11: TST^{-1} dosage size. OD of the control (kaolin clay suspension) at 550 nm was 3.09

Dosage size (mg/ml)	OD at 550 nm		
	Reading 1	Reading 2	Reading 3
0.1	1.009	1.287	1.148
0.2	0.930	1.225	1.120
0.4	0.926	1.348	1.179
0.6	0.957	1.557	1.257
0.8	1.505	1.667	1.567
1	1.639	1.629	1.630
1.2	1.655	1.946	1.395
1.4	1.748	1.709	1.987
1.6	1.984	1.895	1.667
1.8	1.709	1.810	1.975
2	1.814	1.858	1.906

Table A12: PAM dosage size. OD of the control (kaolin clay suspension) at 550 nm was 3.09

Dosage size (mg/ml)	Optical density at 550 nm		
	Reading 1	Reading 2	Reading 3
0.1	0.202	0.070	0.136
0.2	0.135	0.113	0.124
0.4	0.441	0.069	0.058
0.6	0.032	0.030	0.031
0.8	0.029	0.053	0.041
1	0.053	0.047	0.050
1.2	0.068	0.007	0.0375
1.4	0.110	0.073	0.0915
1.6	0.063	0.149	0.106
1.8	0.263	0.391	0.327
2	0.273	0.207	0.141

Table A13: $FeCl_3$ dosage size. OD of the control (kaolin clay suspension) at 550 nm was 3.09

Dosage size (mg/ml)	OD at 550 nm		
	Reading 1	Reading 2	Reading 3
0.1	1.036	1.236	1.136
0.2	1.138	0.873	1.006
0.4	0.854	0.630	0.742
0.6	0.636	0.688	0.662
0.8	0.585	0.579	0.582
1	0.597	0.517	0.557
1.2	0.527	0.593	0.560
1.4	0.579	0.567	0.573
1.6	0.606	0.563	0.585
1.8	0.423	0.453	0.438
2	0.472	0.490	0.481

Data for the effect of cations on flocculation of kaolin clay suspension

Table A14: Effect of cations on FA of TMT^{-1}-g-PAM 2. OD of the control (kaolin clay suspension) at 550 nm was 3.12

Cations	OD at 550 nm		
	Reading 1	Reading 2	Reading 3
KCl	0.510	0.499	0.365
NaCl	0.365	0.599	0.585
LiCl	0.946	0.472	0.808
$CaCl_2$	0.483	0.456	0.277
$BaCl_2$	0.601	0.430	0.471
$MgCl_2$	0.626	0.794	0.220
$FeCl_3$	0.579	1.065	0.952

Table A15: Flocculation of kaolin suspension in the absence of cations. OD of the control (kaolin clay suspension) at 550 nm was 3.12

Flocculants	OD at 550 nm		
	Reading 1	Reading 2	Reading 3
TMT^{-1}	2.769	2.719	2.689
TMT^{-1}-g-PAM 2	1.184	1.281	1.263
PAM	0.235	0.332	0.191

Table A16: The effect of cations on of FA of TST^{-1}-g-PAM 3. OD of the control (kaolin clay suspension) at 550 nm was 3.12

Cations	OD at 550 nm		
	Reading 1	Reading 2	Reading 3
$BaCl_2$	0.318	0.297	0.336
$CaCl_2$	0.769	0.710	0.688
$MgCl_2$	0.654	0.700	0.689
KCl	0.747	1.177	1.300
$FeCl_3$	1.156	1.730	1.048
LiCl	0.759	0.789	0.726
NaCl	0.626	0.794	0.220
	0.579	1.065	0.952

Table A17: Flocculation of kaolin suspension in the absence of cations. OD of the control (kaolin clay suspension) at 550 nm was 3.12

Flocculants	OD at 550 nm		
	Reading 1	Reading 2	Reading 3
TST^{-1}	2.751	2.812	2.577
TST^{-1}-g-PAM 3	0.799	0.706	0.778
PAM	0.235	0.332	0.191

Data for the effect of pH on flocculation of kaolin clay suspension

Table A18: Effect of pH on the FA of TMT-g-PAM 2. OD of the control (kaolin clay suspension) at 550 nm was 3.12

pH	OD at 550 nm		
	Reading 1	Reading 2	Reading 3
3	0.285	0.275	0.280
4	0.287	0.463	0.421
5	0.423	0.444	0.403
6	0.417	0.366	0.375
7	0.461	0.420	0.487
8	0.735	0.643	0.732
9	0.739	0.797	0.640
10	0.627	0.703	0.635
11	0.635	0.726	0.690

Table A19: Effect of pH on the FA of TMT^{-1}. OD of the control (kaolin clay suspension) at 550 nm was 3.12

pH	OD at 550 nm		
	Reading 1	Reading 2	Reading 3
3	1.032	0.976	1.215
4	0.952	0.959	1.013
5	1.622	1.460	1.594
6	2.446	2.305	2.500
7	2.542	2.508	2.609
8	2.182	2.005	2.159
9	2.382	2.603	2.438
10	1.898	2.058	2.056
11	1.126	1.063	1.04

Table A20: Effect of pH on the FA of TST^{-1}-g-PAM 3. OD of the control (kaolin clay suspension) at 550 nm was 3.12

pH	OD at 550 nm		
	Reading 1	Reading 2	Reading 3
3	0.652	0.748	0.218
4	0.445	0.407	0.187
5	0.864	0.764	0.261
6	0.684	0.875	0.369
7	0.691	0.327	0.424
8	0.426	0.556	0.337
9	0.390	0.230	0.325
10	0.310	0.425	0.332
11	0.586	0.260	0.345

Table A21: Effect of pH on the FA of TST^{-1}. OD of the control (kaolin clay suspension) at 550 nm was 3.12

pH	OD at 550 nm		
	Reading 1	Reading 2	Reading 3
3	0.850	0.828	1.087
4	1.094	1.184	1.151
5	1.507	1.521	1.425
6	2.364	2.350	2.381
7	2.453	2.502	2.650
8	2.270	2.076	2.335
9	2.400	2.458	2.471
10	1.785	2.176	1.700
11	1.129	0.886	0.900

Table A22: Effect of pH on the FA of PAM. OD of the control (kaolin clay suspension) at 550 nm was 3.12

pH	OD at 550 nm		
	Reading 1	Reading 2	Reading 3
3	0.079	0.083	0.156
4	0.276	0.075	0.075
5	0.179	0.069	0.204
6	0.410	0.301	0.205
7	0.183	0.275	0.336
8	0.761	0.411	0.946
9	0.484	0.284	0.384
10	0.549	0.480	0.518
11	0.470	0.510	0.550

Table A23: Effect of pH on the FA of $FeCl_3$. OD of the control (kaolin clay suspension) at 550 nm was 3.12

pH	OD at 550 nm		
	Reading 1	Reading 2	Reading 3
3	0.619	0.602	0.627
4	0.623	0.563	0.550
5	0.486	0.380	0.488
6	0.818	0.732	0.558
7	0.482	0.820	0.753
8	0.561	0.635	0.691
9	0.466	0.657	0.653
10	2.810	2.460	1.906
11	3.242	3.174	3.211

Data for the effect of temperature on flocculation of kaolin clay suspension

Table A24: Effect of temperature on the FA of TMT^{-1}-g-PAM 2. OD of the control (kaolin clay suspension) at 550 nm was 3.12

Temperature (°C)	OD at 550 nm		
	Reading 1	Reading 2	Reading 3
Unheated	0.483	0.456	0.277
50	0.712	0.603	0.389
80	1.003	0.297	0.598
100	0.411	0.440	0.902

Table A25: Effect of temperature on the FA of TMT^{-1}. OD of the control (kaolin clay suspension) at 550 nm was 3.12

Temperature (°C)	OD at 550 nm		
	Reading 1	Reading 2	Reading 3
Unheated	1.023	0.961	1.209
50	1.065	0.892	1.050
80	1.390	1.177	1.272
100	1.078	1.122	1.107

Table A26: Effect of temperature on the FA of TST^{-1}-g-PAM 3. OD of the control (kaolin clay suspension) at 550 nm was 3.12

Temperature (°C)	OD at 550 nm		
	Reading 1	Reading 2	Reading 3
Unheated	0.318	0.297	0.336
50	0.547	0.615	0.616
80	0.453	0.575	0.693
100	0.578	0.560	0.667

Table A27: Effect of temperature on the FA of TST^{-1}. OD of the control (kaolin clay suspension) at 550 nm was 3.12

Temperature (°C)	OD at 550 nm		
	Reading 1	Reading 2	Reading 3
Unheated	0.850	0.828	1.087
50	1.294	0.963	1.114
80	1.217	1.043	1.205
100	0.863	1.056	1.012

Table A28: Effect of temperature on the FA of PAM. OD of the control (kaolin clay suspension) at 550 nm was 3.12

Temperature (°C)	OD at 550 nm		
	Reading 1	Reading 2	Reading 3
Unheated	0.093	0.062	0.155
50	0.120	0.005	0.082
80	0.159	0.017	0.106
100	0.123	0.257	0.155

Table A29: Effect of temperature on the FA of $FeCl_3$. OD of the control (kaolin clay suspension) at 550 nm was 3.12

Temperature (°C)	OD at 550 nm		
	Reading 1	Reading 2	Reading 3
Unheated	0.620	0.620	0.589
50	0.744	0.693	0.782
80	0.696	0.793	0.870
100	0.840	0.824	0.774

Data for the effect of salinity on flocculation of kaolin clay suspension

Table A30: Effect of salinity on the FA of TMT^{-1}-g-PAM 2. OD of the control (kaolin clay suspension) at 550 nm was 3.11

Salinity (g/l)	OD at 550 nm		
	Reading 1	Reading 2	Reading 3
5	0.755	0.750	0.731
10	0.918	0.986	0.916
15	1.001	1.002	1.026
20	0.836	1.130	1.027
25	1.161	1.109	1.112
30	1.073	1.123	1.077
35	1.207	1.219	1.045

Table A31: Effect of salinity on the FA of TMT^{-1}. OD of the control (kaolin clay suspension) at 550 nm was 3.11

Salinity (g/l)	OD at 550 nm		
	Reading 1	Reading 2	Reading 3
5	2.395	2.481	2.406
10	2.458	2.418	2.447
15	2.345	2.357	2.351
20	2.329	2.345	2.459
25	2.471	2.432	2.496
30	2.303	2.348	2.331
35	2.422	2.466	2.477

Table A32: Effect of salinity on the FA of TST^{-1}-g-PAM 3. OD of the control (kaolin clay suspension) at 550 nm was 3.11

Salinity (g/l)	OD at 550 nm		
	Reading 1	Reading 2	Reading 3
5	0.793	0.980	0.870
10	1.122	0.984	0.966
15	1.182	1.016	0.993
20	1.140	1.114	0.989
25	1.180	1.091	0.952
30	1.086	1.091	1.080
35	1.159	1.098	1.116

Table A33: Effect of salinity on the FA of TST^{-1}. OD of the control (kaolin clay suspension) at 550 nm was 3.11

Salinity (g/l)	OD at 550 nm		
	Reading 1	Reading 2	Reading 3
5	1.583	1.642	1.559
10	2.040	2.006	2.035
15	2.086	2.041	2.097
20	2.327	2.365	2.385
25	2.349	2.384	2.368
30	2.375	2.350	2.347
35	2.446	2.393	2.209

Table A34: Effect of salinity on the FA of PAM. OD of the control (kaolin clay suspension) at 550 nm was 3.11

Salinity (g/l)	OD at 550 nm		
	Reading 1	Reading 2	Reading 3
5	0.205	0.099	0.171
10	0.183	0.255	0.032
15	0.135	0.291	0.275
20	0.205	0.099	0.171
25	0.307	0.237	0.237
30	0.287	0.237	0.295
35	0.265	0.301	0.340

Table A35: Effect of salinity on the FA of $FeCl_3$. OD of the control (kaolin clay suspension) at 550 nm was 3.11

Salinity (g/l)	OD at 550 nm		
	Reading 1	Reading 2	Reading 3
5	1.630	1.964	1.863
10	1.900	1.890	1.961
15	2.355	2.272	2.396
20	2.374	2.388	2.346
25	2.416	2.327	2.419
30	2.361	2.399	2.366
35	2.545	2.429	2.420

Data for zeta potential

Results

			Mean (mV)	Area (%)	St Dev (mV)
Zeta Potential (mV):	-13.6	**Peak 1:**	-13.6	100.0	5.90
Zeta Deviation (mV):	5.90	**Peak 2:**	0.00	0.0	0.00
Conductivity (mS/cm):	0.332	**Peak 3:**	0.00	0.0	0.00
Result quality :	Good				

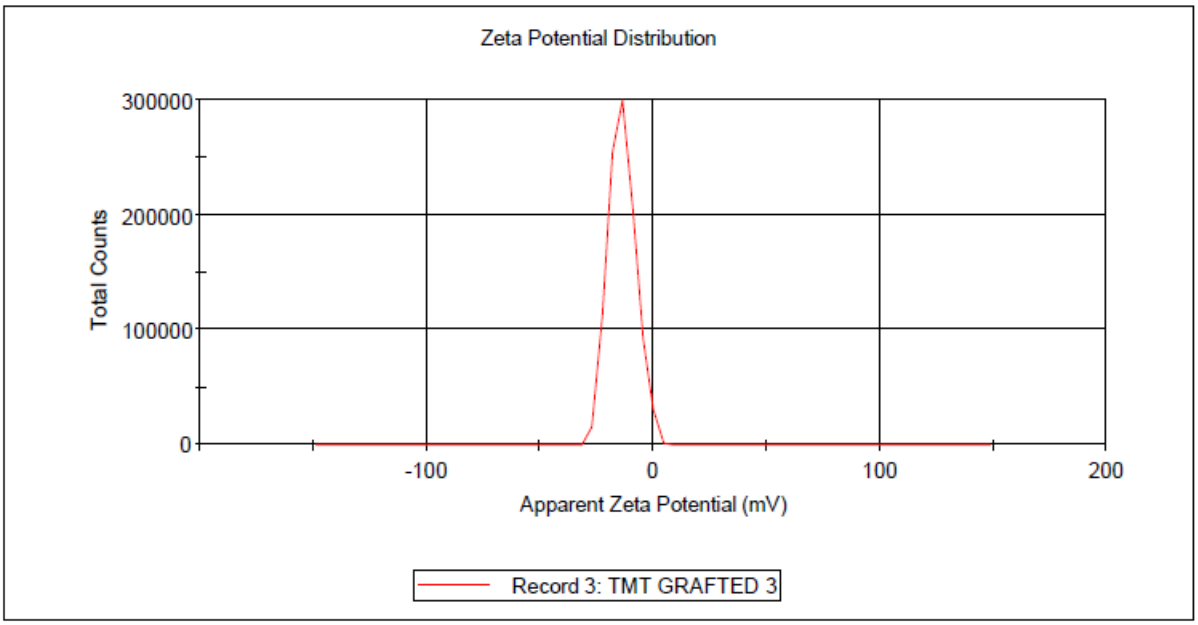

Figure A9: Zeta potential for TMT^{-1}-g-PAM 2

Results

		Mean (mV)	Area (%)	St Dev (mV)
Zeta Potential (mV):	-11.9	**Peak 1:** -11.9	100.0	7.35
Zeta Deviation (mV):	7.35	**Peak 2:** 0.00	0.0	0.00
Conductivity (mS/cm):	0.537	**Peak 3:** 0.00	0.0	0.00
Result quality :	Good			

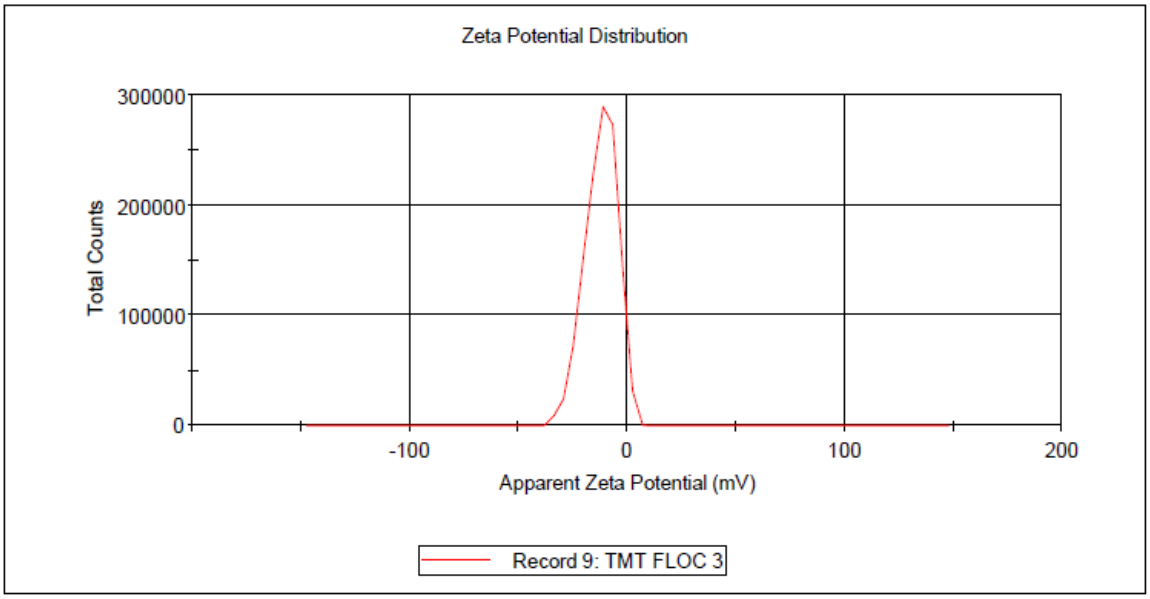

Figure A10: Zeta potential of kaolin particles flocculated by TMT^{-1}-g-PAM 2 in the presence of Ca^{2+}

Results

			Mean (mV)	Area (%)	St Dev (mV)
Zeta Potential (mV):	-13.2	**Peak 1:**	-13.2	100.0	5.95
Zeta Deviation (mV):	5.95	**Peak 2:**	0.00	0.0	0.00
Conductivity (mS/cm):	0.244	**Peak 3:**	0.00	0.0	0.00
Result quality :	Good				

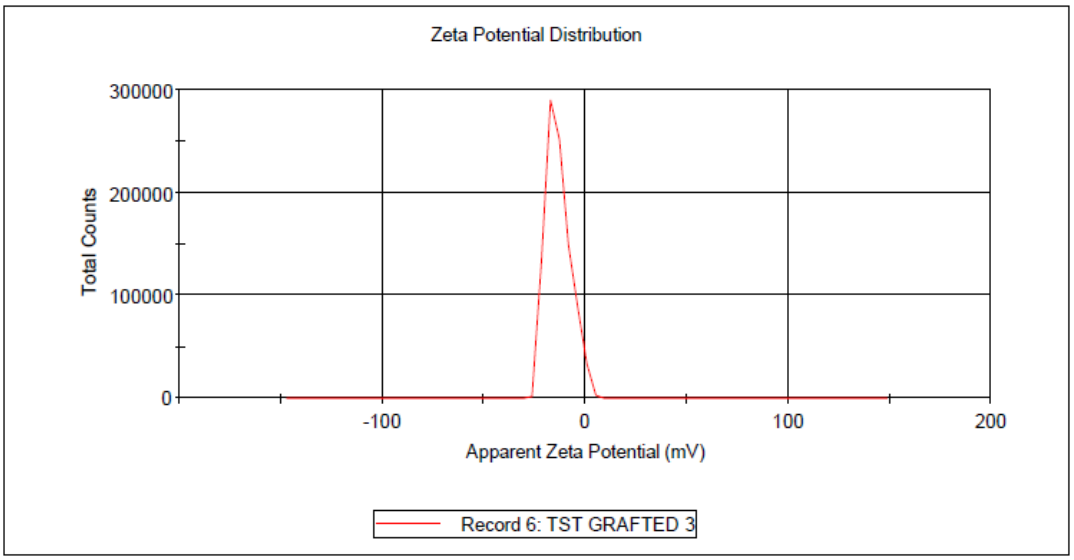

Figure A11: Zeta potential of TST^{-1}-g-PAM 3

Results

		Mean (mV)	Area (%)	St Dev (mV)
Zeta Potential (mV):	-5.46	**Peak 1:** -5.46	100.0	5.05
Zeta Deviation (mV):	5.05	**Peak 2:** 0.00	0.0	0.00
Conductivity (mS/cm):	0.498	**Peak 3:** 0.00	0.0	0.00
Result quality :	Good			

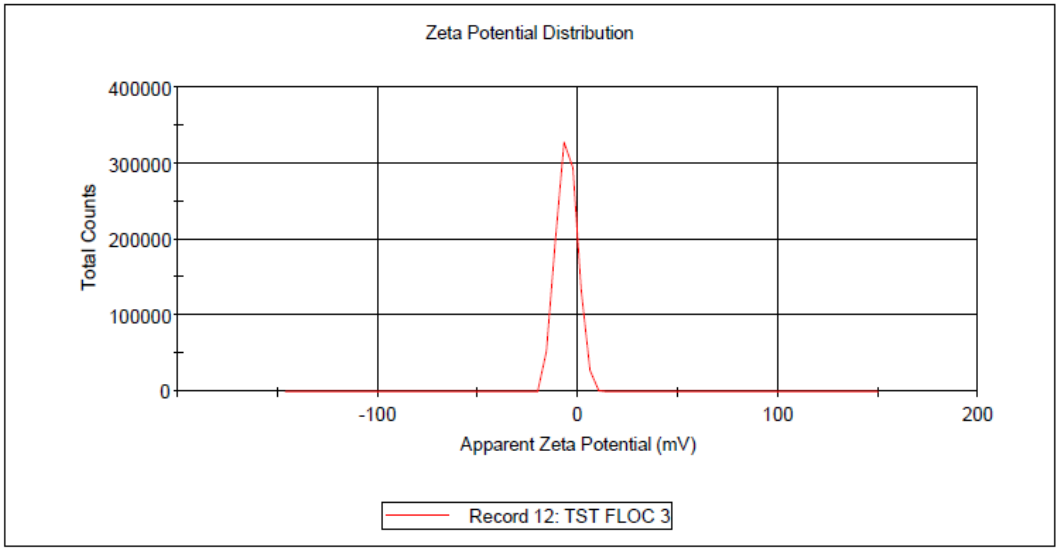

Figure A12: Zeta potential of kaolin particles flocculated by TST^{-1}-g-PAM 3 in the presence of Ba^{2+}

Data used to calculate removal efficiency of pollutants in domestic wastewater

Table A36: Water quality before treatment (W_i) and water quality after treatment (W_f)

Flocculants	Parameters	W_i			W_f		
		Reading 1	Reading 2	Reading 3	Reading 1	Reading 2	Reading 3
TMT^{-1}	COD (mg/l)	1600	1600	1600	44	44	45
TMT^{-1}-g-PAM 2	COD (mg/l)	1600	1600	1600	40	37	37
$FeCl_3$	COD (mg/l)	1600	1600	1600	50	51	49
PAM	COD (mg/l)	1600	1600	1600	42	48	48
TMT^{-1}	BOD (mg/l)	183	183	183	86.0	85.4	86.6
TMT^{-1}-g-PAM 2	BOD (mg/l)	183	183	183	86.0	84.0	84.0
$FeCl_3$	BOD (mg/l)	183	183	183	88.0	86.0	87.0
PAM	BOD (mg/l)	183	183	183	21.8	21.9	22.2
TMT^{-1}	N (mg/l)	13.1	13.1	13.1	6.2	6.2	6.0
TMT^{-1}-g-PAM 2	N (mg/l)	13.1	13.1	13.1	6.0	6.1	6.1
$FeCl_3$	N (mg/l)	13.1	13.1	13.1	7.5	7.4	7.6
PAM	N (mg/l)	13.1	13.1	13.1	0.1	0.0	0.0
TMT^{-1}	P (mg/l)	20.7	20.7	20.7	9.6	9.0	9.8
TMT^{-1}-g-PAM 2	P (mg/l)	20.7	20.7	20.7	5.0	13.0	9.0
$FeCl_3$	P (mg/l)	20.7	20.7	20.7	12.6	14.5	10.7
PAM	P (mg/l)	20.7	20.7	20.7	0.0	0.0	0.0
TMT^{-1}	OD_{550nm}	2.8	2.8	2.8	0.73	0.73	0.75
TMT^{-1}-g-PAM 2	OD_{550nm}	2.8	2.8	2.8	0.28	0.26	0.31
$FeCl_3$	OD_{550nm}	2.8	2.8	2.8	0.89	0.93	0.96
PAM	OD_{550nm}	2.8	2.8	2.8	2.71	2.73	2.70

Table A37: Water quality before treatment (W_i) and water quality after treatment (W_f)

Flocculants	Parameters	W_i			W_f		
		Reading 1	Reading 2	Reading 3	Reading 1	Reading 2	Reading 3
TST^{-1}	COD (mg/l)	1600	1600	1600	43.8	43.9	44.2
TST^{-1}-g-PAM 3	COD (mg/l)	1600	1600	1600	33.2	30.8	30.8
$FeCl_3$	COD (mg/l)	1600	1600	1600	50.0	51.0	49.0
PAM	COD (mg/l)	1600	1600	1600	42.0	48.0	48.0
TST^{-1}	BOD (mg/l)	183	183	183	82.0	82.1	81.6
TST^{-1}-g-PAM 3	BOD (mg/l)	183	183	183	50.1	50.1	47.9
$FeCl_3$	BOD (mg/l)	183	183	183	88.0	86.0	87.0
PAM	BOD (mg/l)	183	183	183	21.8	21.9	22.2
TST^{-1}	N (mg/l)	13.1	13.1	13.1	10.0	8.2	9.0
TST^{-1}-g-PAM 3	N (mg/l)	13.1	13.1	13.1	3.7	3.2	3.6
$FeCl_3$	N (mg/l)	13.1	13.1	13.1	7.5	7.4	7.6
PAM	N (mg/l)	13.1	13.1	13.1	0.1	0.0	0.0
TST^{-1}	P (mg/l)	20.7	20.7	20.7	19.7	19.1	20.0
TST^{-1}-g-PAM 3	P (mg/l)	20.7	20.7	20.7	16.5	17.4	17.1
$FeCl_3$	P (mg/l)	20.7	20.7	20.7	12.6	14.5	10.7
PAM	P (mg/l)	20.7	20.7	20.7	0.0	0.0	0.0
TST^{-1}	OD_{550nm}	2.8	2.8	2.8	0.0	0.0	0.0
TST^{-1}-g-PAM 3	OD_{550nm}	2.8	2.8	2.8	0.0	0.0	0.0
$FeCl_3$	OD_{550nm}	2.8	2.8	2.8	0.89	0.93	0.96
PAM	OD_{550nm}	2.8	2.8	2.8	2.71	2.73	2.70

Data used to calculate removal efficiency of pollutants in coal mine wastewater

Table A38: Water quality before treatment (W_i) and water quality after treatment (W_f)

Flocculants	Parameters	W_i			W_f		
		Reading 1	Reading 2	Reading 3	Reading 1	Reading 2	Reading 3
TMT^{-1}	COD (mg/l)	1557	1557	1557	21	26	25
TMT^{-1}-g-PAM 2	COD (mg/l)	1557	1557	1557	22	22	22
$FeCl_3$	COD (mg/l)	1557	1557	1557	27	27	26
PAM	COD (mg/l)	1557	1557	1557	22	23	22
TMT^{-1}	BOD (mg/l)	73	73	73	10.0	10.0	9.9
TMT^{-1}-g-PAM 2	BOD (mg/l)	73	73	73	4.8	5.1	5.2
$FeCl_3$	BOD (mg/l)	73	73	73	12.0	12.0	12.0
PAM	BOD (mg/l)	73	73	73	4.0	4.0	4.0
TMT^{-1}	N (mg/l)	2.9	2.9	2.9	1.7	1.7	2.0
TMT^{-1}-g-PAM 2	N (mg/l)	2.9	2.9	2.9	1.2	1.2	1.1
$FeCl_3$	N (mg/l)	2.9	2.9	2.9	1.8	2.1	2.2
PAM	N (mg/l)	2.9	2.9	2.9	0.1	0.1	0.0
TMT^{-1}	S (mg/l)	0.3	0.3	0.3	0.07	0.05	0.07
TMT^{-1}-g-PAM 2	S (mg/l)	0.3	0.3	0.3	0.05	0.05	0.05
$FeCl_3$	S (mg/l)	0.3	0.3	0.3	0.18	0.21	0.21
PAM	S (mg/l)	0.3	0.3	0.3	0.03	0.03	0.06
TMT^{-1}	OD_{550nm}	2.2	2.2	2.2	0.43	0.24	0.27
TMT^{-1}-g-PAM 2	OD_{550nm}	2.2	2.2	2.2	0.29	0.18	0.16
$FeCl_3$	OD_{550nm}	2.2	2.2	2.2	0.69	0.69	0.67
PAM	OD_{550nm}	2.2	2.2	2.2	0.01	0.03	0.01

Table A39: Water quality before treatment (W_i) and water quality after treatment (W_f)

Flocculants	Parameters	W_i			W_f		
		Reading 1	Reading 2	Reading 3	Reading 1	Reading 2	Reading 3
TST^{-1}	COD (mg/l)	1557	1557	1557	87.5	84.1	84.0
TST^{-1}-g-PAM 3	COD (mg/l)	1557	1557	1557	86.0	82.0	87.4
$FeCl_3$	COD (mg/l)	1557	1557	1557	27	27	26
PAM	COD (mg/l)	1557	1557	1557	22	23	22
TST^{-1}	BOD (mg/l)	73	73	73	40.9	41.0	41.0
TST^{-1}-g-PAM 3	BOD (mg/l)	73	73	73	28.6	27.5	27.0
$FeCl_3$	BOD (mg/l)	73	73	73	12.0	12.0	12.0
PAM	BOD (mg/l)	73	73	73	4.0	4.0	4.0
TST^{-1}	N (mg/l)	2.9	2.9	2.9	0.3	0.3	0.4
TST^{-1}-g-PAM 3	N (mg/l)	2.9	2.9	2.9	0.3	0.3	0.4
$FeCl_3$	N (mg/l)	2.9	2.9	2.9	1.8	2.1	2.2
PAM	N (mg/l)	2.9	2.9	2.9	0.1	0.1	0.0
TST^{-1}	S (mg/l)	0.3	0.3	0.3	0.13	0.14	0.13
TST^{-1}-g-PAM 3	S (mg/l)	0.3	0.3	0.3	0.14	0.13	0.13
$FeCl_3$	S (mg/l)	0.3	0.3	0.3	0.18	0.21	0.21
PAM	S (mg/l)	0.3	0.3	0.3	0.03	0.03	0.06
TST^{-1}	OD_{550nm}	2.2	2.2	2.2	0.33	0.22	0.42
TST^{-1}-g-PAM 2	OD_{550nm}	2.2	2.2	2.2	0.21	0.23	0.21
$FeCl_3$	OD_{550nm}	2.2	2.2	2.2	0.69	0.69	0.67
PAM	OD_{550nm}	2.2	2.2	2.2	0.01	0.03	0.01